arXiv:0803.1488v2 [astro-ph] 22 Sep 2008

Deep MMT[1]Transit Survey of the Open Cluster M37 III: Stellar Rotation at 550 Myr

J. D. Hartman[2], B. S. Gaudi[3], M. H. Pinsonneault[3], K. Z. Stanek[3], M. J. Holman[2], B. A. McLeod[2], S. Meibom[2], J. A. Barranco[4], and J. S. Kalirai[5,6]

ABSTRACT

In the course of conducting a deep ($14.5 \lesssim r \lesssim 23$), 20 night survey for transiting planets in the rich ~ 550 Myr old open cluster M37 we have measured the rotation periods of 575 stars which lie near the cluster main sequence, with masses $0.2M_{\odot} \lesssim M \lesssim 1.3M_{\odot}$. This is the largest sample of rotation periods for a cluster older than 500 Myr. Using this rich sample we investigate a number of relations between rotation period, color and the amplitude of photometric variability. Stars with $M \gtrsim 0.8M_{\odot}$ show a tight correlation between period and mass with heavier stars rotating more rapidly. There is a group of 4 stars with $P > 15$ days that fall well above this relation, which, if real, would present a significant challenge to theories of stellar angular momentum evolution. Below $0.8M_{\odot}$ the stars continue to follow the period-mass correlation but with a broad tail of rapid rotators that expands to shorter periods with decreasing mass. We combine these results with observations of other open clusters to test the standard theory of lower-main sequence stellar angular momentum evolution. We find that the model reproduces the observations for solar mass stars, but discrepancies are apparent for stars with $0.6 \lesssim M \lesssim 1.0M_{\odot}$. We also find that for late-K through early-M dwarf stars in this cluster rapid rotators tend to be bluer than slow rotators in $B - V$ but redder than slow rotators in $V - I_C$. This result supports the hypothesis that the significant discrepancy between the observed

[2]Harvard-Smithsonian Center for Astrophysics, 60 Garden St., Cambridge, MA 02138, USA; jhartman@cfa.harvard.edu, mholman@cfa.harvard.edu, bmcleod@cfa.harvard.edu, smeibom@cfa.harvard.edu

[3]Department of Astronomy, The Ohio State University, Columbus, OH 43210, USA; gaudi@astronomy.ohio-state.edu, pinsono@astronomy.ohio-state.edu, kstanek@astronomy.ohio-state.edu

[4]Department of Physics and Astronomy, San Francisco State University, 1600 Holloway Ave., San Francisco, CA 94132, USA; barranco@stars.sfsu.edu

[5]University of California Observatories/Lick Observatory, University of California at Santa Cruz, Santa Cruz CA, 95060; jkalirai@ucolick.org

[6]Hubble Fellow

and predicted temperatures and radii of low-mass main sequence stars is due to stellar activity.

Subject headings: open clusters and associations:individual (M37) — stars:rotation — stars:low-mass — stars:spots — stars:variables:other

1. Introduction

This paper is the third in a series of papers on a deep survey for transiting planets in the open cluster M37 (NGC 2099) using the MMT. In the first paper (Hartman et al. 2008a, Paper I) we introduced the survey, described the spectroscopic and photometric observations and the data reduction, determined the fundamental parameters (age, metallicity, distance and reddening) of the cluster, and obtained its mass and luminosity functions and radial density profile. In the second paper (Hartman et al. 2008b, Paper II) we identified 1445 variable stars in the field of the cluster, of which 99% were new discoveries. We found that $\gtrsim 500$ of these variables lie near the cluster main sequence on photometric color-magnitude diagrams (CMDs) and show a correlation between period and magnitude. In this paper we investigate this population of variables arguing that the photometric variations are due to spotted star rotation. We use these variables to study the rotation of F-M main sequence stars at the age of the cluster (550 ± 30 Myr, Paper I; note that for the rest of this paper we adopt this age which was derived by comparison to models with convective overshooting).

Rotation plays an important role in the life of a star. Empirically there is a strong relation between the rotation rate and the activity and age of low-mass stars (Skumanich 1972), with older stars being slower rotators and less active than younger stars. Rotation affects the structure of a star (see Sills, Pinsonneault, & Terndrup 2000) and its evolution may have important consequences for mixing at the base of a star's convection zone (see the review by Pinsonneault 1997). Rotation also affects the spectral energy distribution of low-mass stars (Stauffer et al. 2003). It has even been suggested that rotation may be used as a tool to determine the ages of field stars older than a few hundred million years, and that ages determined in this fashion may be significantly more accurate than ages determined using other methods (Barnes 2007). However, the usefulness of these "gyrochronology" ages is predicated on an accurate understanding and calibration of the age-rotation rate relation. As we discuss next, there are relatively few constraints on this relation for ages $\gtrsim 200$ Myr.

---

[1]Observations reported here were obtained at the MMT Observatory, a joint facility of the Smithsonian Institution and the University of Arizona.

The surface rotation period of a star can be measured directly from photometric variations if it has substantial surface brightness inhomogeneities, from variations in the strength of spectroscopic features such as the cores of the Ca II H and K lines, or it can be constrained by measuring the projected equatorial rotation velocity $v \sin i$ from the Doppler broadening of spectral absorption lines. The latter method suffers from the inclination axis ambiguity and thus requires a substantial ensemble of stars, as well as an assumption on the inclination axis distribution, to determine the underlying velocity, and hence rotation period, distribution. While it is more desirable for the study of stellar rotation to directly measure the rotation period of a star than $v \sin i$, a consequence of the activity-age relation is that older stars show lower amplitude photometric variations. For example, at 100 Myr a typical solar-like star will have a photometric amplitude of $\sim 7\%$ in r, at 500 Myr its photometric amplitude will have fallen to $\sim 1\%$, and at 2 Gyr the typical amplitude is only $\sim 0.1\%$. Moreover, longer rotation periods are more difficult to measure as they require observations spanning a longer baseline. As a result it becomes increasingly difficult to directly measure the rotation periods of stars at greater ages. Our understanding of the angular momentum evolution of stars older than a few hundred million years has been gleaned primarily from $v \sin i$ measurements (See for example the review by Bouvier (1997)).

Most photometric studies of stellar rotation have focused on young (< 100 Myr) open clusters whose stars show relatively large amplitude photometric variations (See Stassun & Terndrup (2003) for a review). These studies have given great insight into the evolution of angular momentum for pre-main sequence stars (PMS). As a star contracts on to the main sequence the expectation is that it will spin up. Observations of the youngest clusters, however, have revealed that not all PMS achieve these short rotation periods (See for example Herbst et al. (2002) for observations of the ~ 1 Myr Orion Nebula Cluster, Cieza & Baliber (2006) for observations of $\sim 2-3$ Myr IC 348, Lamm et al. (2005) for observations of $\sim 2-4$ Myr NGC 2264, Irwin et al. (2008b) for observations of ~ 5 Myr NGC 2362, and Irwin et al. (2008a) for observations of ~ 40 Myr NGC 2547). Possible explanations for the presence of slow rotators in these clusters include magnetic locking of the star's rotation to the inner accretion disk (Königl 1991; Shu et al. 1994) or the presence of an accretion-driven wind which carries angular momentum away from the star (Shu et al. 2000).

Photometric determinations of rotation periods have been obtained for stars in a number of clusters in the age range $50-200$ Myr; at these ages solar-like stars have settled on to the main sequence. Clusters that have been studied include IC 2391 (~ 50 Myr; Patten & Simon 1996), IC 2602 (~ 50 Myr; Barnes et al. 1999), α Persei (~ 80 Myr; Stauffer et al. 1985; Stauffer, Hartmann & Jones 1989; Prosser 1991; Prosser et al. 1993a,b; O'Dell & Collier Cameron 1993; O'Dell, Hendry & Collier Cameron 1994; Prosser et al. 1995; O'Dell et al. 1997; Allain et al. 1996; Martín & Zapatero Osorio 1997; Prosser & Randich

1998; Prosser, Randich & Simon 1998; Barnes et al. 1998), the Pleiades ($\sim$ 125 Myr; Magnitskii 1987; Stauffer et al. 1987; Van Leeuwan, Alphenaar & Meys 1987; Prosser et al. 1993a,b, 1995; Krishnamurthi et al. 1998; Terndrup et al. 1999; Scholz & Eislöffel 2004), NGC 2516 ($\sim$ 150 Myr; Irwin et al. 2007), and M34 ($\sim$ 200 Myr; Barnes 2003; Irwin et al. 2006).

The data for older clusters is scarcer. Periods have been determined for 87 stars in NGC 3532 ($\sim$ 300 Myr; Barnes 1998), 4 stars in Coma ($\sim$ 600 Myr; Radick, Skiff & Lockwood 1990), 35 stars in the Hyades ($\sim$ 625 Myr; Radick et al. 1987, 1995; Prosser et al. 1995), and 5 stars in Praesepe ($\sim$ 625 Myr; Scholz & Eislöffel 2007).

The observations discussed above have clearly demonstrated that once a low-mass star (G and later) reaches the main sequence it begins to lose angular momentum; this is understood to be the result of a magnetized stellar wind (Webber & Davis 1967). By comparing the rotation velocities of stars in the Pleiades and the Hyades with the Sun, Skumanich (1972) found the scaling relation $v \propto t^{-1/2}$, where v is the average equatorial velocity and t is the age. This can be explained by a surface angular momentum loss rate that is proportional to ω^3 (Kawaler 1988) and naturally leads to a convergence in the rotation rates of stars at a given mass as seen by Radick et al. (1987) for stars in the Hyades. The presence of solar-mass rapid rotators in the Pleiades (Van Leeuwen & Alphenaar 1982) appears to contradict the Skumanich (1972) law and suggests that the angular momentum loss rate is saturated above some critical rotation rate ω_{crit} so that it scales as $\omega_{crit}^2\omega$ for $\omega > \omega_{crit}$ (Kawaler 1988). The critical rotation rate must be mass dependent to explain the spread in rotation rates for lower mass stars (Krishnamurthi et al. 1997).

The rotation history of a star will depend not only on the rate of angular momentum loss, but also on the efficiency of internal angular momentum transport. Models in which the core and envelope of a star are decoupled lead to a rapid spin-down of the envelope (Soderblom et al. 1993). In these models once the core and envelope become re-coupled the spin-down is much less dramatic. Models in which the internal angular momentum transport is calculated by hydrodynamic mechanisms, and in which some degree of core-envelope decoupling is permitted have been produced (e.g. Sills, Pinsonneault, & Terndrup (2000) show that models that incorporate differential rotation with depth in stars are needed to reproduce the angular momentum evolution of systems younger than the Pleiades). Alternatively, models in which the star is assumed to rotate as a solid body have also been developed (e.g. Bouvier, Forestini, & Allain (1997)).

This paper presents rotation periods for 575 stars in the open cluster M37 (NGC 2099). In Paper I we found that the cluster has an age of 550 ± 30 Myr, a reddening of $E(B-V) = 0.227 \pm 0.038$, a distance modulus of $(m-M)_V = 11.57 \pm 0.13$ and a metallicity of $[M/H] = +0.045 \pm 0.044$ which are in good agreement with previous measurements.

The age of M37 is thus comparable to that of the Hyades (625 Myr with overshooting; Perryman et al. 1998) which at present is the oldest cluster for which a significant number of stellar rotation periods have been measured. M37 is, however, substantially richer than the Hyades and thus has the potential to provide a much larger data-set of rotation periods for older stars.

As we were preparing to submit this manuscript, we became aware of a similar, independent study by Messina et al. (2008), which presents rotation periods for 122 stars in this cluster. Our survey goes more than 2 magnitudes deeper than Messina et al. (2008) with more than an order of magnitude more observations from more than twice as many nights. As a result we are able to study the rotation evolution for late K and early M dwarfs as well as the late F, G and early K dwarfs studied by Messina et al. (2008). On the other hand, the Messina et al. (2008) survey has measured periods for early F stars that are saturated in our survey. We compare the periods measured by both surveys in §3.6.

In the next section we provide a brief summary of the observations and data reduction. In §3 we compile the catalog of candidate cluster members with measured rotation periods. In §4 we fit analytic models to the observed period-color sequence in M37. In §5 we compare the photometric observations to spectroscopic $v \sin i$ measurements for a number of these stars. In §6 we study the amplitude distribution as a function of period and color. In §7 we study the Blue K dwarf phenomenon in M37. In §8 we compare these observations to theories of stellar angular momentum evolution. We discuss the results in §9.

2. Summary of Observations

The observations and data reduction procedure were described in detail in Papers I and II, we provide a brief overview here. The observations consist of both *gri* photometry for ~ 16000 stars, and r time-series photometry for ~ 23000 stars obtained with the Megacam mosaic imager (McLeod et al. 2000) on the 6.5 m MMT. We also obtained high-resolution spectroscopy of 127 stars using the Hectochelle multi-fiber, high-dispersion spectrograph (Szentgyorgyi et al. 1998) on the MMT.

The primary time-series photometric observations were done using the r filter and consist of ~ 4000 high quality images obtained over twenty four nights (including eight half nights) between December 21, 2005 and January 21, 2006. We obtained light curves for stars with $14.5 \lesssim r \lesssim 23$ using a reduction pipeline based on the image subtraction technique and software due to Alard & Lupton (1998) and Alard (2000). We apply two cleaning routines to the data: clipping outlier points and removing individual bad images. We do not decorrelate

against other systematic variations since doing so tends to distort the light curves of large amplitude variables.

The spectra were obtained on four separate nights between February 23, 2007 and March 12, 2007 and were used to measure T_{eff}, $[Fe/H]$, $v \sin i$ and the radial velocity (RV) via cross-correlation against a grid of model stellar spectra computed using ATLAS 9 and SYNTHE (Kurucz 1993). The classification procedure was developed by Meibom et al. (2008, in preparation), and made use of the *xcsao* routine in the IRAF[2] *rvsao* package (Kurtz & Mink 1998) to perform the cross-correlation. In performing the cross-correlation we found that it was necessary to fix $\log(g) = 4.5$, however given that very few of the field stars in our sample are likely to be giants or sub-giants fixing $\log(g)$ should not substantially bias the resulting parameters. We measured the parameters separately for each of the four nights choosing the $v \sin i$ and T_{eff} values that maximize the cross-correlation peak-height value at three $[Fe/H]$ grid points ($[Fe/H] = -0.5$, $[Fe/H] = 0.0$, and $[Fe/H] = +0.5$). For each $[Fe/H]$ grid point we determined the average $v \sin i$ and T_{eff} values over the four nights together with uncertainties on the values for each night estimated using the standard deviation of the measurements. We then fit a quadratic relation between $[Fe/H]$ and the average peak-height values to estimate the value of $[Fe/H]$ that maximizes the cross-correlation and then determined $v \sin i$ and T_{eff} by fitting a quadratic relation between each of these parameters and $[Fe/H]$. The final errors on each parameter are the standard errors from the fit. For a given star the error on $v \sin i$ can be substantially larger than the average value, particularly for fainter targets, when the value of $[Fe/H]$ is not strongly constrained or when $v \sin i$ is small, in these cases the error should be taken as an upper limit on the value. To determine the RV for each star we used *rvsao* to cross-correlate the spectra on each night against the best matching template spectrum from the full grid.

As described in Paper I we also take BV photometry for stars in the field of this cluster from Kalirai et al. (2001), K_S photometry from 2MASS (Skrutskie et al. 2006) and we transform our ri photometry to I_C using a transformation based on the I_C photometry from Nilakshi & Sagar (2002).

---

[2]IRAF is distributed by the National Optical Astronomy Observatories, which is operated by the Association of Universities for Research in Astronomy, Inc., under agreement with the National Science Foundation.

3. Catalog of Candidate Cluster Members with Measured Rotation Periods

3.1. Selection of Rotational Variables

In Paper II we selected 1445 periodic variable stars using the Lomb-Scargle (L-S; Lomb 1976; Scargle 1982; Press & Rybicki 1989; Press et al. 1992), phase-binning analysis of variance (AoV; Schwarzenberg-Czerny 1989; Devor 2005) and box-fitting least squares (BLS; Kovács, Zucker and Mazeh 2002) algorithms. From this catalog we will now select a population of probable cluster member, rotational variables. To do this we follow the procedure for selecting candidate photometric cluster members described in Paper I. For each star we determine the g, r, i, B, V point within the fiducial cluster main sequences, generated by eye, that has a minimum χ^2 deviation from the observed g, r, i, B, V values for the star. We then select as candidate cluster members stars with $\chi^2 < 150$ in g, r, i and $\chi^2 < 250$ in B, V for $B - V < 1.38$ and $V < 20$ or $\chi^2 < 150$ in B, V for other stars. Figure 1 shows the selected variables on $g - r$ and $g - i$ CMDs. After rejecting variables that were classified in Paper II as eclipsing binaries or short period pulsators and rejecting variables without period determinations we are left with 575 variables that are candidate cluster members. A catalog of these 575 variables is given in tables 1-3, we show only the first ten rows of each table for illustration, the full tables are available in the online edition of the journal. Note that only stars with spectroscopy are included in table 3.

3.2. Revised Periods

In Paper II we calculated the periods of the variable stars using the L-S, phase-binning AoV, and BLS algorithms. We then selected, by eye, the most likely period for each star from the values returned by the three algorithms. Here we recalculate the periods using the multi-harmonic AoV algorithm due to Schwarzenberg-Czerny (1996). This method is equivalent to fitting to each light curve a harmonic series of the form:

$$\tilde{r}(t) = a_0 + \sum_{i=1}^{N} a_i \cos(2\pi i t/P + \phi_i) \tag{1}$$

where P is the period, a_i are the amplitudes, and ϕ_i are the phases. This method is more general than the L-S algorithm which is equivalent to fitting a $N = 1$ series without a floating mean, and may give a more accurate period determination for light curves that have multiple minima in a single cycle. We calculate the period for each light curve for $N = 1, 2$ and 3. Figure 2 shows the period-$(B - V)_0$ relation for each value of N while figure 3 shows the period-$< r >$ relation. Here $< r >$ is the average r magnitude of the light curve. The

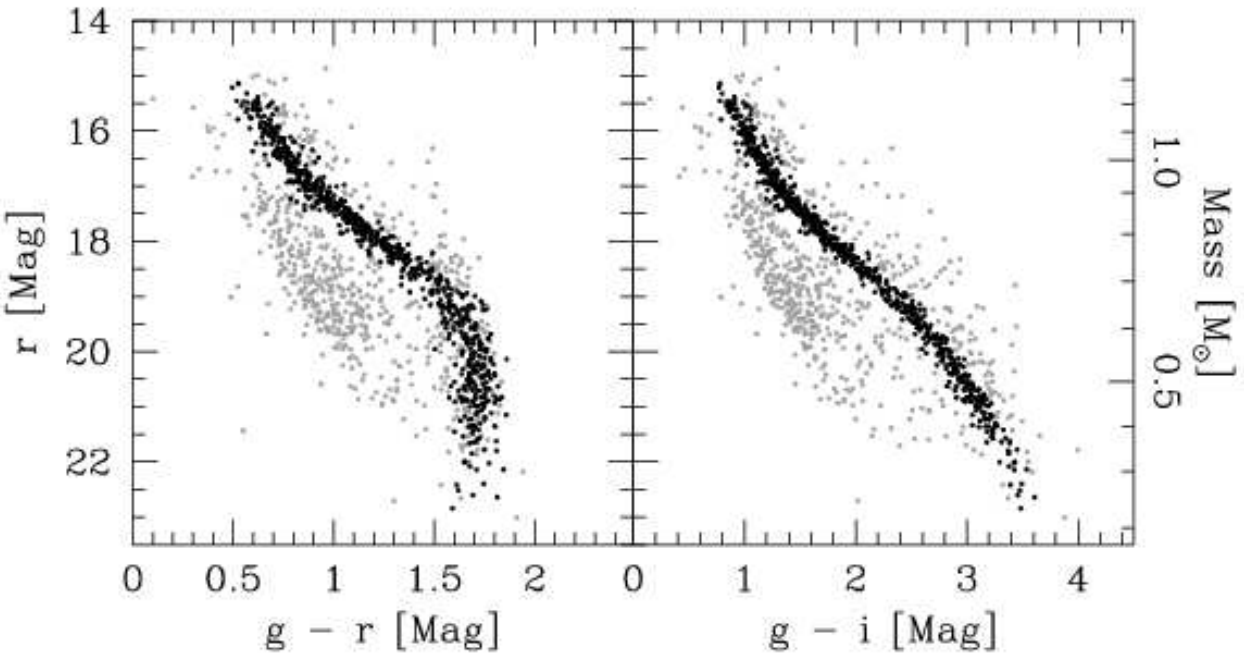

Fig. 1.— $g - r$ vs r (left) and $g - i$ vs r (right) CMDs showing the selection of variable stars that are candidate cluster members; only variable stars are included on this plot. Dark points show the candidate cluster member variables, light points show field variables. Variables classified as pulsators or eclipsing binaries (see Paper II) are not included on this plot. The vertical scale on the right side of the plot shows the masses of cluster members as a function of r magnitude.

magnitudes and colors have been converted to masses using the mass-r and mass-$(B-V)_0$ relations for this cluster that were determined in Paper I.

As seen in figures 2 and 3, there is a clear period-stellar mass sequence running from $P \sim 3$ days, $M \sim 1.2M_\odot$ to $P \sim 17$ days, $M \sim 0.5M_\odot$. There also appears to be a significant number of stars with periods falling below the sequence for $M < 0.8M_\odot$ and a cluster of stars with 15 days $< P <$ 20 days and $0.7M_\odot < M < 1.1M_\odot$. For $N = 1$ there appears to be a second sequence with periods that are half the main-band values, while $N = 2$ and $N = 3$ yield a sequence with periods that are twice the main-band values. Light curves that fall in the long period sequence for $N = 2$ and $N = 3$ show multiple minima in a cycle when phased at the long period. Changing the number of harmonics in the fit can select different harmonics of the true period. Light curves with multiple, unequal, minima in a cycle or light curves that are not perfectly periodic (e.g. due to spot evolution, or uncorrected systematic errors in the photometry) are particularly susceptible to choosing an incorrect harmonic of the true period. For the remainder of the paper it is important to have a sample of stars with unambiguous periods. We therefore select a clean sample of 372 stars for which periods determined with $N = 1, 2$ and 3 do not differ by more than 10%. For this sample we adopt the $N = 2$ periods. As seen in figure 2 and 3, the half-period harmonic sequence is removed from the clean sample. We note that a handful of long-period variables remain in the clean sample, we discuss these further in §9. Tables 1 and 2 include the full sample of stars, the $N = 1$, 2 and 3 periods are provided in table 1.

In figure 4 we show phased light curves for a random sample of stars that fall along the main period-color band (see §4). Figure 5 shows phased light curves for a random sample of rapid rotators ($P < 2$ days). Finally, in figure 6 we show the light curves of 4 of the 5 long-period stars in the clean sample with $P > 15$ days and $r < 18.5$ mag. Note that the fifth star is rejected as a non-cluster member based on its RV.

3.3. Period and Color Uncertainties

As we will discuss in §8.2, the spread in rotation periods for stars of a given mass puts a powerful constraint on theories of stellar angular momentum evolution. To determine whether or not the observed period spread is real it is important to have accurate estimates for both the period and color uncertainties.

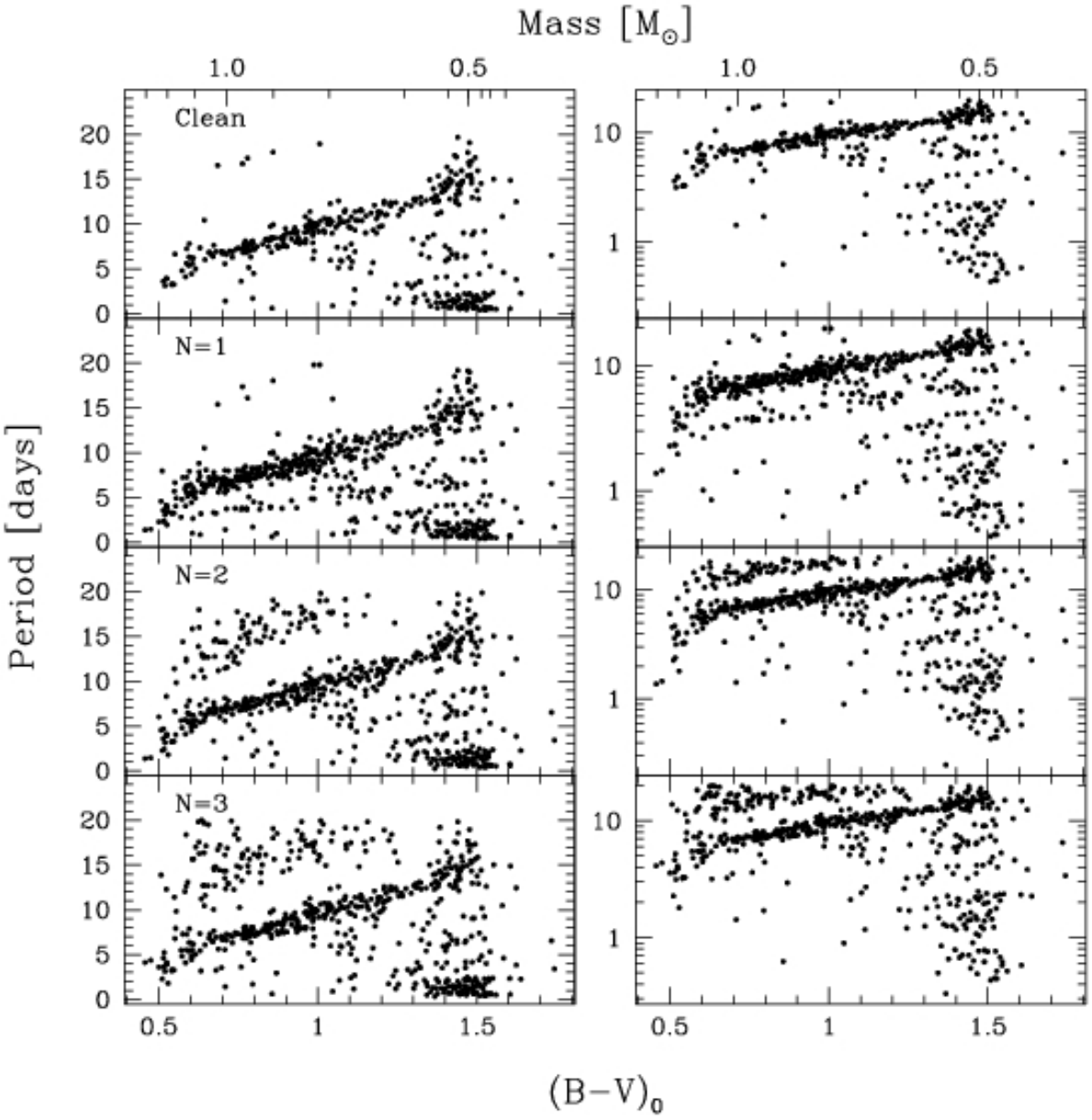

Fig. 2.— Period versus $(B-V)_0$ color (bottom axis) and mass (top axis) for variable stars that are candidate cluster members. The periods are determined with the multi-harmonic AoV method, which is equivalent to fitting equation 1 to the light curves. We show the results for $N = 1, 2$ and 3. In the top panel we show a clean sample of stars for which the $N = 1, 2$ and 3 periods do not differ from each other by more than 10%. In the left panels the period is plotted on a linear scale, in the right panels it is plotted on a logarithmic scale. We adopt the $N = 2$ period for the clean sample of stars.

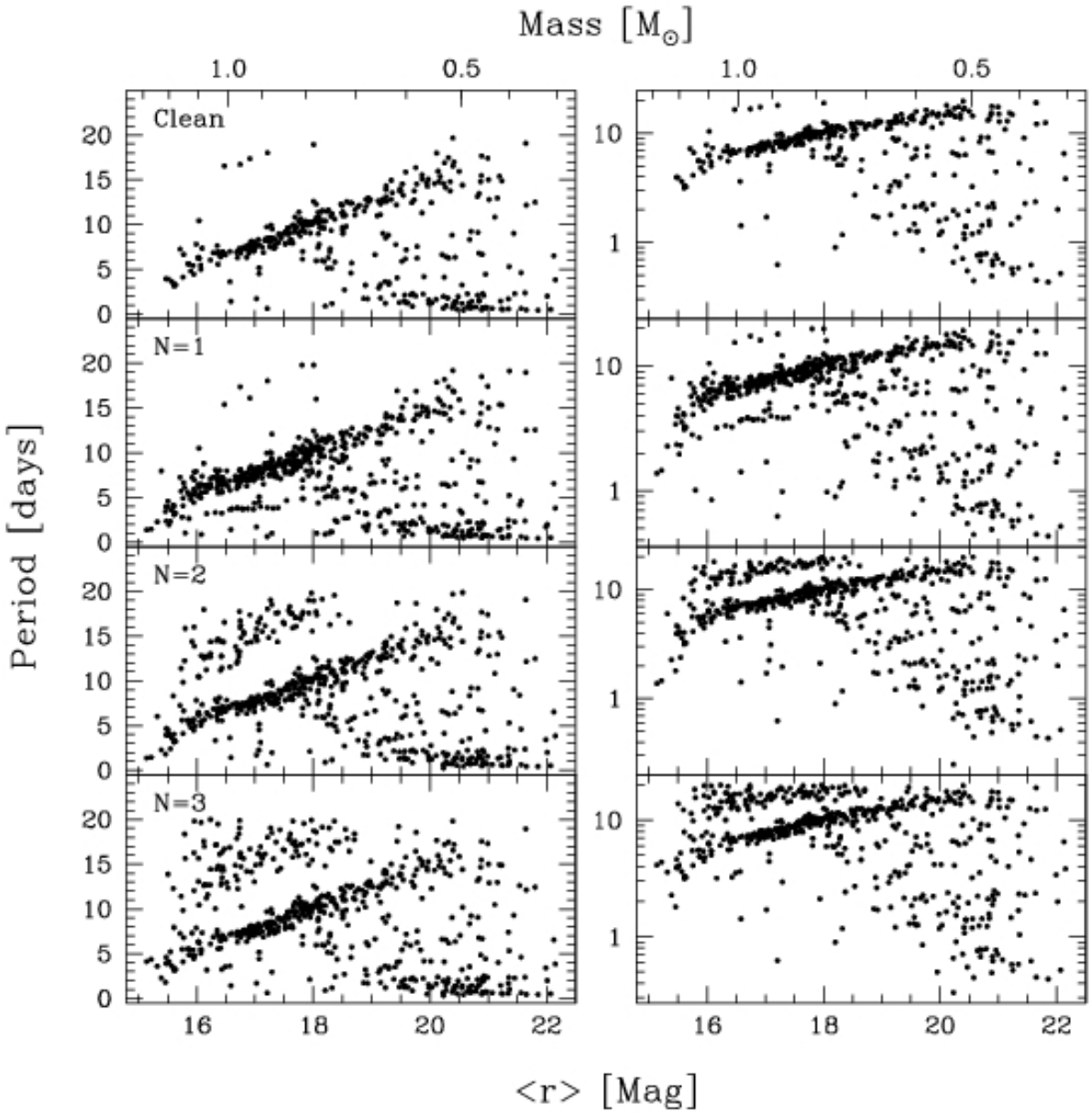

Fig. 3.— Same as figure 2, here we plot period against $< r >$, the average r magnitude of each light curve.

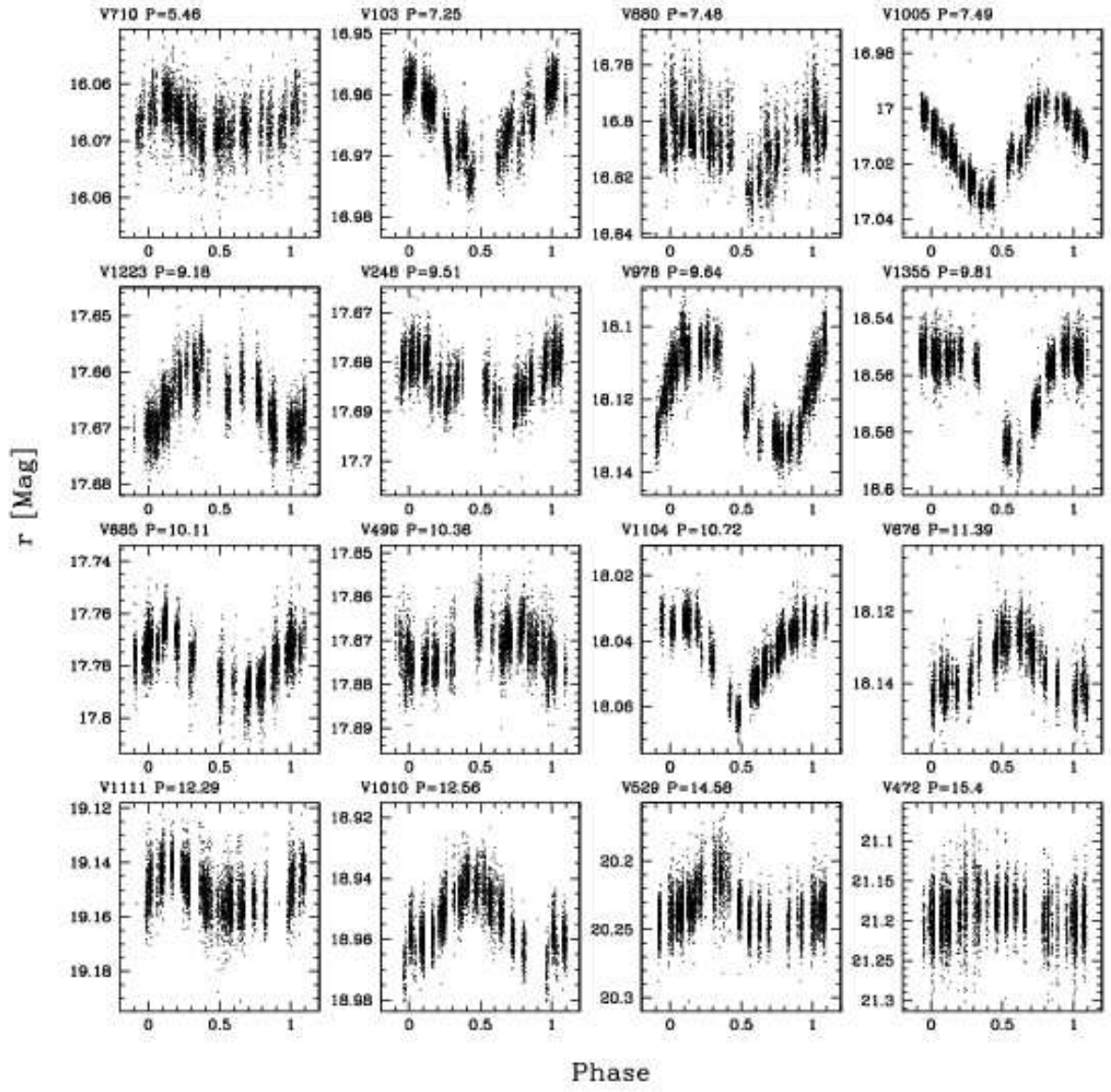

Fig. 4.— Example light curves for 16 randomly selected variable stars that are candidate cluster members and lie along the main period-color band (§4). The period listed for each light curve is in days. The continuous quasi-periodic variations are consistent with spotted star rotation. The light curves are sorted by period.

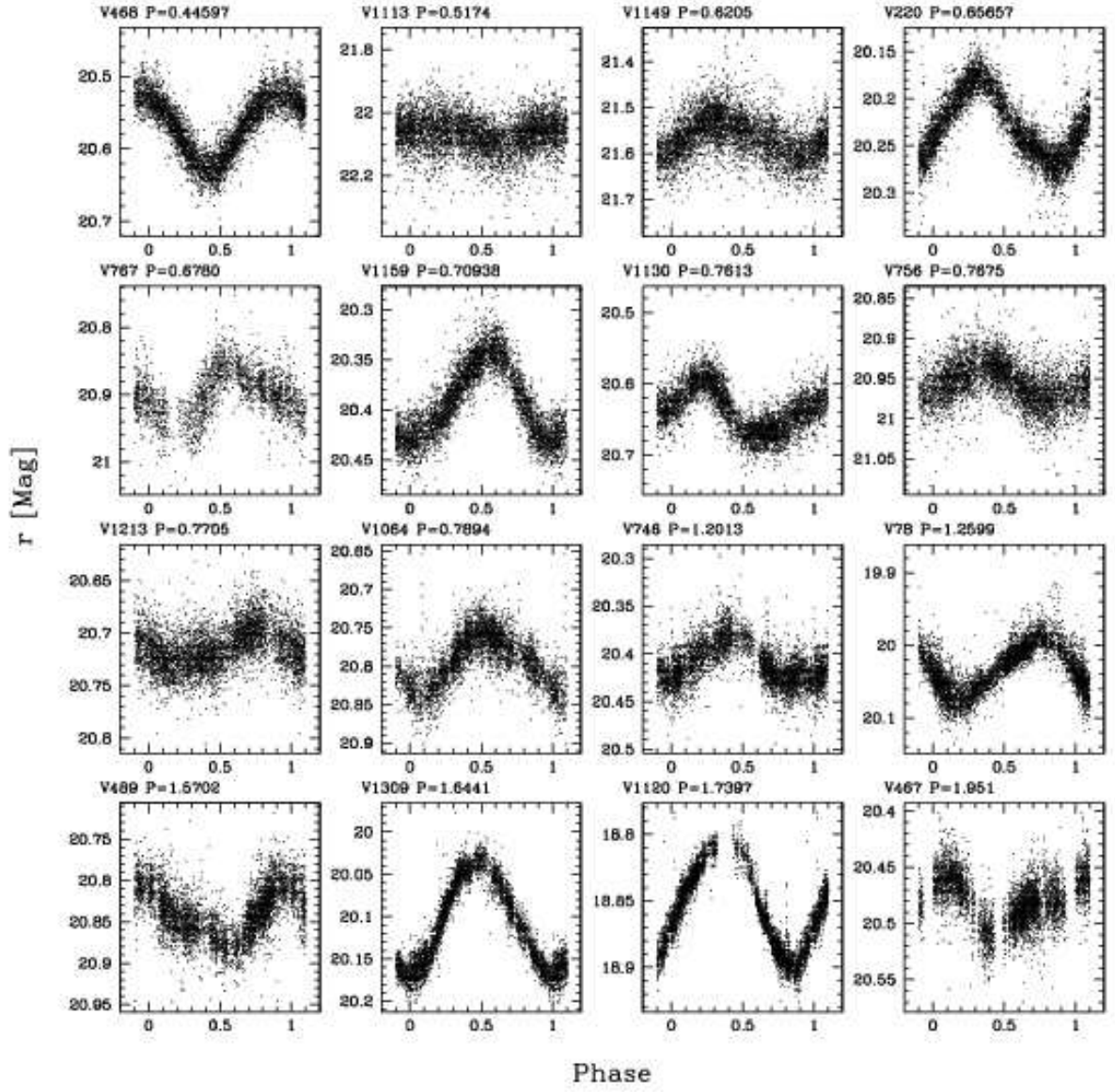

Fig. 5.— Example light curves for 16 randomly selected candidate cluster member variable stars with $P < 2$ days.

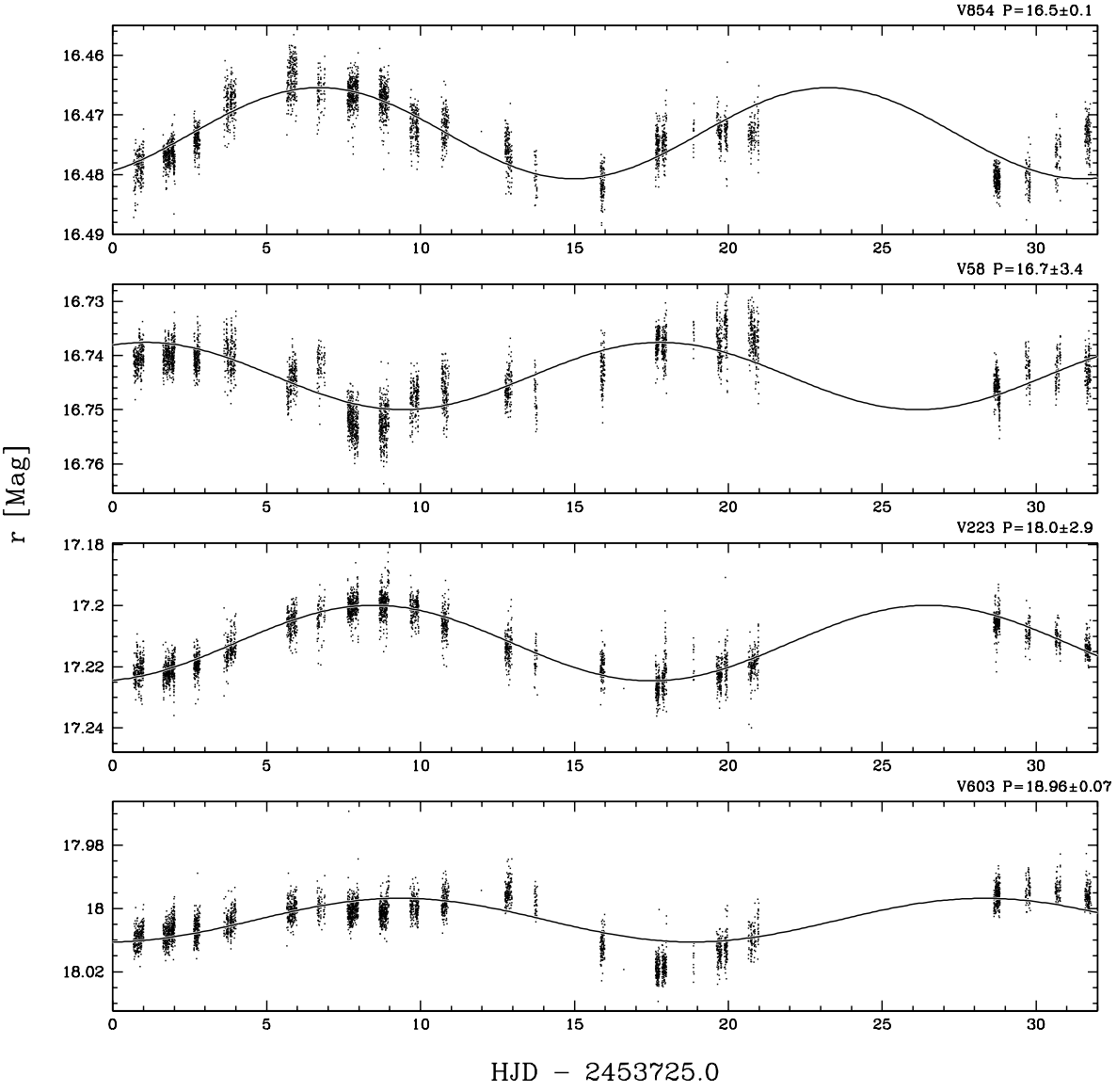

Fig. 6.— Light curves of four variable stars that are photometrically selected candidate cluster members with long periods ($P > 15$ days and $(B-V)_0 < 1.2$). The listed periods are in days and the solid line shows the best fit sinusoid to each light curve. V223 has an RV that is consistent with cluster membership; we do not have RV information for the other three stars. We exclude one long period star that is in the clean sample shown in figure 2 but has an RV that is inconsistent with it being a member of the cluster.

3.3.1. Period Uncertainties

Uncertainties in the period can be divided into two classes: errors due to aliasing or choosing the wrong harmonic of the true period and random errors. Aliasing generally yields a discrete set of peaks in the periodogram of a light curve resulting in an uncertainty in choosing the peak that corresponds to the physical period of the star. Random errors correspond to the uncertainty in the centroid of each periodogram peak, these errors are typically assumed to be Gaussian. There are at least four factors which contribute to random uncertainties in the stellar rotation period inferred from starspots. These factors include:

1. Noise in the photometry.
2. Inadequacies in the model used to determine the period (e.g. the light curve is periodic but not sinusoidal).
3. Spot evolution.
4. Differential rotation.

In Paper II we conducted bootstrap simulations of the period detection for each star. This effectively determines the contribution of photometric noise to the period uncertainty. We redo these bootstrap simulations here for the multi-harmonic AoV period determinations.

To assess the uncertainty due to inadequacies in the model and due to spot evolution we conduct Monte Carlo simulations. We simulate light curves for 1000 spotted stars using the spot model due to Dorren (1987). For each simulation we place three spots with random angular sizes between 0.05 and 0.5 radians, random latitudes and random longitudes on the surface of a star, assign the star a random rotation period between 0.2 and 20 days, and allow the spots to vary sinusoidally in angular size. The amplitude, phase and period of the variation are chosen randomly for each spot. We limit the period for spot size variation to lie between 5 and 20 times the rotation period. We generate light curves for each simulated star using the same time sampling as our observations. We then measure the period of each simulated light curve using the multi-harmonic AoV algorithm, rejecting light curves for which $N = 1, 2$ and 3 do not return the same period within 10%. Figure 7 shows an example of a simulated light curve and the detected period as a function of the injected period for all simulations. We find the RMS difference between the injected and recovered periods is $\sim 5\%$. We also find that the $N = 2$ period has the lowest RMS deviation from the injected rotation period. Note that this estimate for the error is conservative since most of the stars that we observed do not show as much spot evolution as our models do.

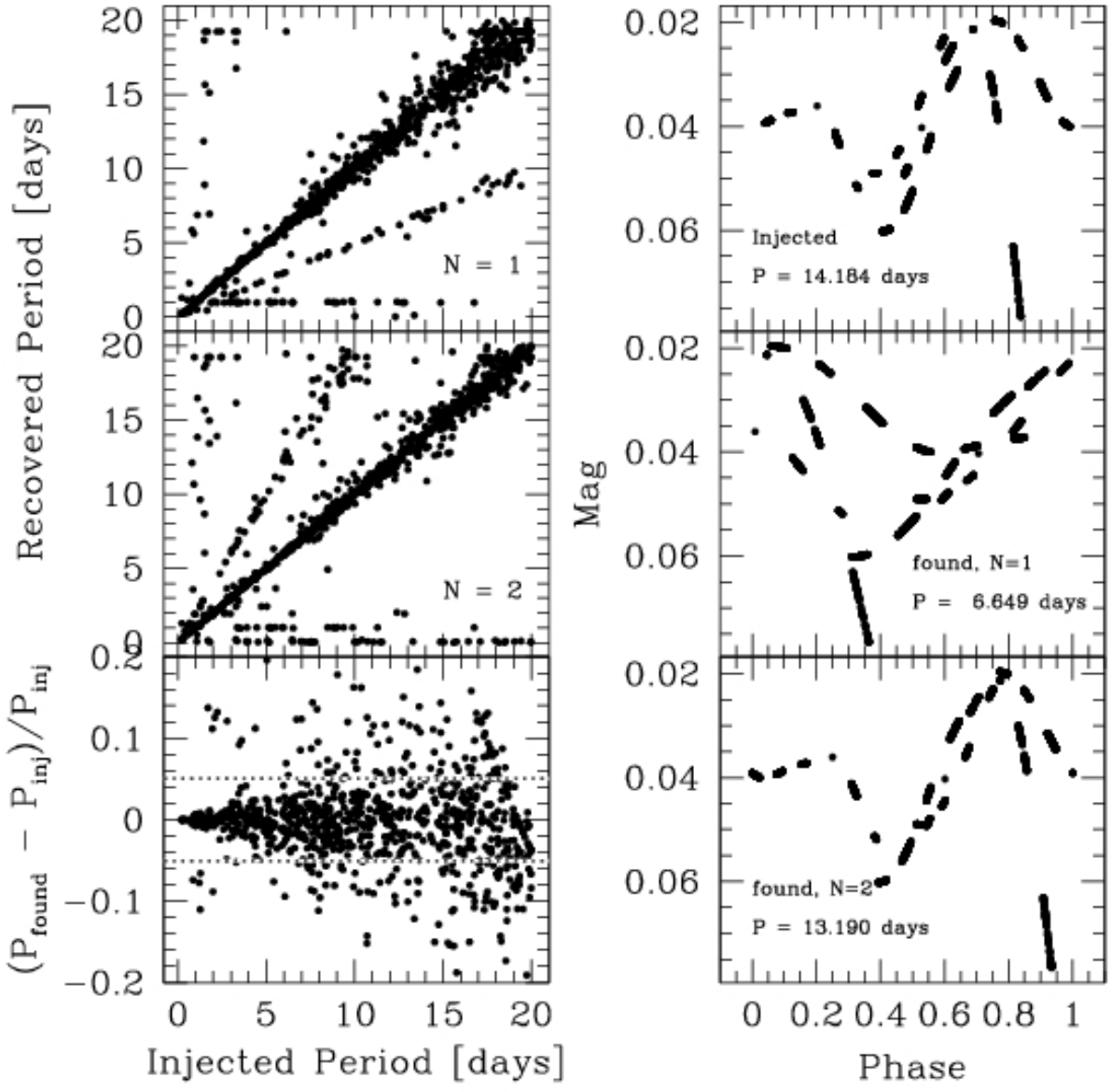

Fig. 7.— Left: Injected versus recovered period for simulated spot evolution light curves. The periods are recovered using the multi-harmonic AoV algorithm with $N = 1$, 2 and 3. We plot the results for $N = 1$ and $N = 2$ only. The bottom left panel shows the fractional difference between the recovered and injected periods for $N = 2$. The dotted line shows the RMS. Right: A simulated light curve of a star exhibiting spot evolution is phased at the injected rotation period (top) as well as at the recovered periods for $N = 1$ and $N = 2$.

The rotation periods measured for an ensemble of stars with spots located at different latitudes may exhibit scatter even if all stars of a given mass have the same equatorial rotation period. The Sun exhibits differential rotation that can be modeled as

$$P_\beta = P_{EQ}/(1 - k \sin^2 \beta) \tag{2}$$

where P_β is the rotation period at latitude β and P_{EQ} is the equatorial rotation period. Observations of spots on the Sun yield $k = 0.19$ while surface radial velocity measurements give $k = 0.12$ (Kitchatinov 2005). Theoretical simulations of turbulent convection predict that k should decrease with increasing rotation rate (Brown et al. 2004), this has been confirmed by observations of starspots on κ^1 Ceti by the MOST satellite which yield $k = 0.09$ for this solar-like star rotating with $P = 8.77$ days (Walker et al. 2007). While sunspots are rarely seen with $|\beta| > 30°$, there are indications that younger stars may have spots at any latitude. For example, the aforementioned observations of κ^1 Ceti found 7 spots over the range $10° < |\beta| < 80°$. Assuming spots may be uniformly distributed over the surface of a star (i.e. uniformly distributed in $\sin \beta$), a value of $k = 0.09$ will yield an RMS spread in detected periods of $\sim 3\%$. We adopt this as an estimate for the expected contribution of differential rotation to the period uncertainty for stars in M37.

3.3.2. Color Uncertainties

There are several effects that contribute to the uncertainty in the color of a star including uncertainties in the photometric precision, photometric variability and binarity. All of these effects can cause the measured color to differ from the photosphere color of the star (or the star with the measured rotation period in the case of a multiple star system). The net uncertainty from all of these effects can be determined empirically from the spread of the main sequence on a CMD. Following the procedure described in §7, we draw a fiducial main sequence by eye through the rotational variables plotted on $B - V$, $V - I_C$, $g - r$ and $g - i$ CMDs. We then calculate for each variable the difference between its observed color and the color along the fiducial main sequence interpolated at the V magnitude of the star. The data are binned in magnitude and we calculate the RMS of the color residuals for each bin. The resulting uncertainties in $(B - V)_0$, $(V - I_C)_0$, $g - r$ and $g - i$ as a function of absolute magnitude are listed in table 4. The drop in the RMS of the color residuals at $M_V = 11$ for $(V - I_C)_0$, $g - r$ and $g - i$ is due to incompleteness in the selection of probable members at this magnitude.

3.4. Completeness

Incompleteness in the selection of variable stars can bias the observed period-color and period-amplitude distributions. To assess the completeness of our sample of rotation periods we conduct Monte Carlo simulations of the variable star selection process. We inject sinusoidal variations, and spot signals (generated using the model described in § 3.3.1) into the light curves of 1081 stars that pass the cuts used to select candidate cluster members discussed in § 3.1 but were not selected as variable stars. For each star we conduct 1000 simulations. For the sinusoid models we inject signals with random phases, periods uniformly distributed in logarithm between 0.1 and 20.0 days and semi-amplitudes uniformly distributed in logarithm between 1 mmag and 0.1 mag. We attempt to recover the injected signals using the L-S algorithm in combination with the multi-harmonic AoV algorithm. An injected signal is considered to be recovered if it does not have a period falling within one of the rejected period bins discussed in Paper II, has a formal L-S false alarm probability logarithm that is less than -150 and if the N=1, 2 and 3 periods returned by AoV agree with one another to within 10%. To make the problem computationally feasible we use a lower period resolution in the L-S algorithm than what we used to select the variables in Paper II (we sample at 0.1 times the Nyquist frequency rather than 0.005 times the Nyquist frequency).

In figure 8 we show the recovery fraction as a function of period and of amplitude for the sinusoid injections and the spot model injections while figure 9 shows the recovery fraction as a function of magnitude. When we don't apply the multi-harmonic AoV selection, the recovery fraction is more or less insensitive to period between 0.1 and 20 days for semi-amplitudes larger than 0.01 mag. The recovery fraction for stars brighter than $r \sim 20$ is close to 100% for the sine-curve model and is between $80 - 100\%$ for the spot model. The recovery fraction drops at a few periods ($\sim$ 1 day and $2 - 4$ days) due to the period rejection that we perform in selecting the variables. For the sinusoid models applying the multi-harmonic AoV selection reduces the recovery fraction dramatically to $10 - 20\%$. This is due to the degeneracy between harmonic number and period (i.e. doubling the period and setting the amplitude of the first harmonic to one and all other harmonics to zero yields the same signal as using the correct period and setting the amplitude of the fundamental to one and all harmonics to zero). Because we limit the period search to 20 days, periods longer than 10 days cannot be recovered at twice the period or three times the period, and periods longer than 7 days cannot be recovered at three times the period. As a result the recovery fraction for long periods using the multi-harmonic AoV selection is close to the recovery fraction when the AoV selection is not used. For more realistic spot models the degeneracy between choosing the fundamental mode with the true period or either of the harmonics with a longer period is broken, so applying the multi-harmonic AoV selection does not have as

significant an effect on the recovery fraction. In this case the recovery fraction is reduced by $\sim 20\%$ independent of period. Based on the results for the spot model signals we conclude that the rotation period-color diagram may be biased toward brighter stars, but at fixed magnitude, it is not strongly biased in period due to incompleteness.

3.5. Field Contamination

In addition to incompleteness, the presence of field stars may also bias the observed period-color and period-amplitude distributions. Based on spectroscopic observations of several of the candidate rotational variables that we discuss in § 5 we estimate that $\sim 20\%$, or ~ 115 of the stars in our catalog (~ 74 after applying the multi-harmonic AoV selection) are field stars. While the field star variables located away from the cluster main sequence on a CMD do not show an obvious correlation between color and rotation period (figure 10), we cannot infer that the same is true for the field stars near the cluster main sequence since these stars generally have different masses and radii. To disentangle the period-color distribution of field stars from cluster members would require either a complete spectroscopic survey of all the rotational variables, or a time series study of a field off the cluster. Note that the estimated contamination fraction is small enough that the conclusions of the paper should not be strongly affected by the contamination.

Out of a total sample of ~ 1450 cluster members with $14.5 < r < 22.3$ that we have observed, we estimate that ~ 460 are detected as variables, and ~ 220 have semi-amplitudes greater than 0.01 mag. Note that we used a stricter χ^2-based membership selection for choosing candidate variable cluster members than what was used to estimate the total number of surveyed cluster members in Paper I. The number of cluster members that could have potentially been selected as variable cluster members is thus likely to be slightly smaller than the estimate of ~ 1450. Based on the completeness estimates for spot-model injected light curves without multi-harmonic AoV selection, we estimate that we have detected $\sim 70\%$ of the large-amplitude cluster member variables in this sample, so we estimate that $\sim 20\%$ of cluster members are variable with semi-amplitudes greater than 0.01 mag.

3.6. Comparison with the RACE-OC Project

Messina et al. (2008) have recently presented rotation periods for a number of stars in M37 as part of the RACE-OC project. We find that 91 of the 106 candidate cluster member stars listed in table 2 of Messina et al. (2008) that are not classified as δ-Scuti, RR Lyr or

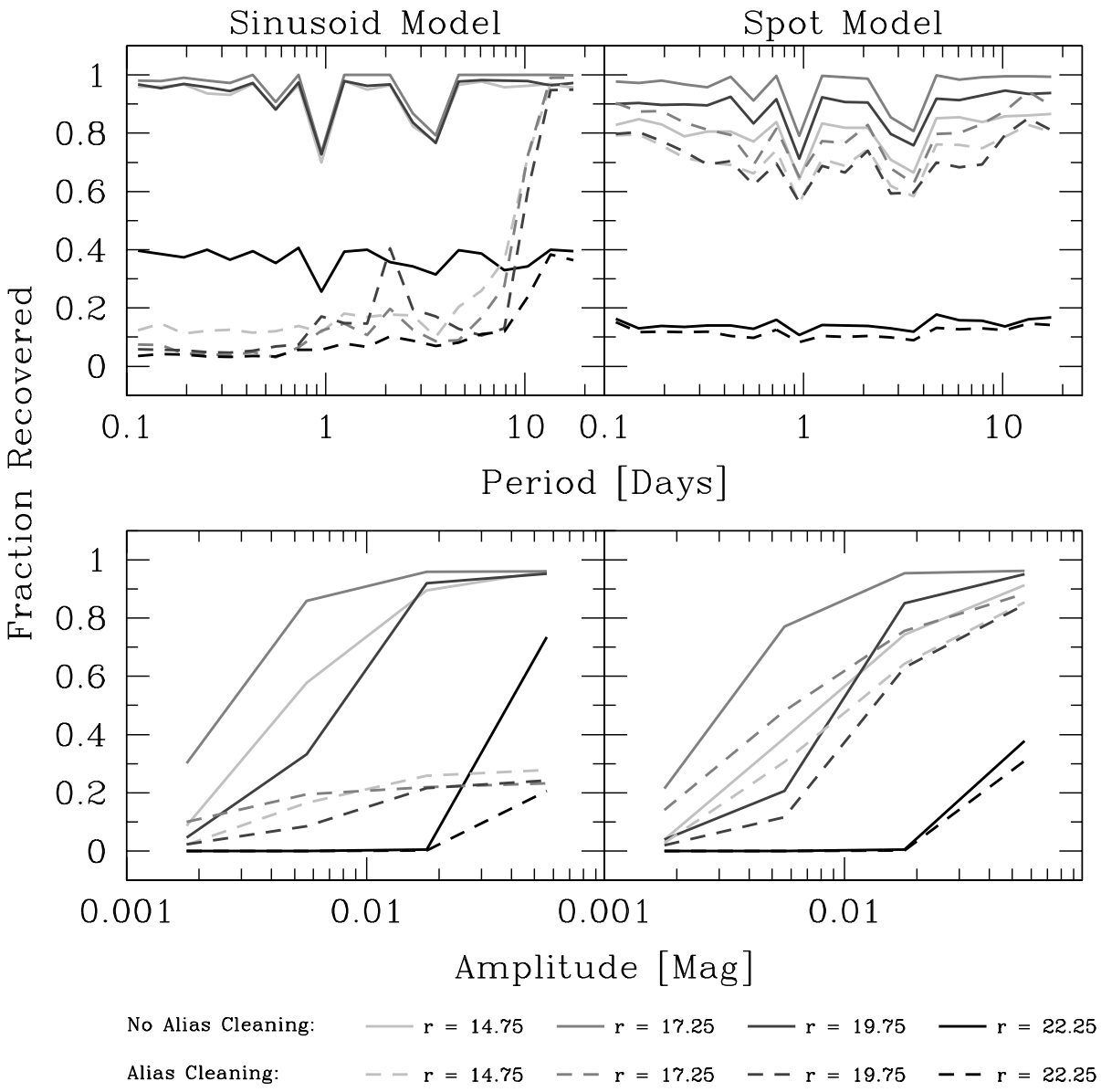

Fig. 8.— The recovery fraction for injected sinusoid (left) and spot (right) models as a function of period (top) and amplitude (bottom). We show the results for several magnitudes with and without applying the multi-harmonic AoV selection. For the top plot we include all simulations with semi-amplitudes greater than 0.01 mag.

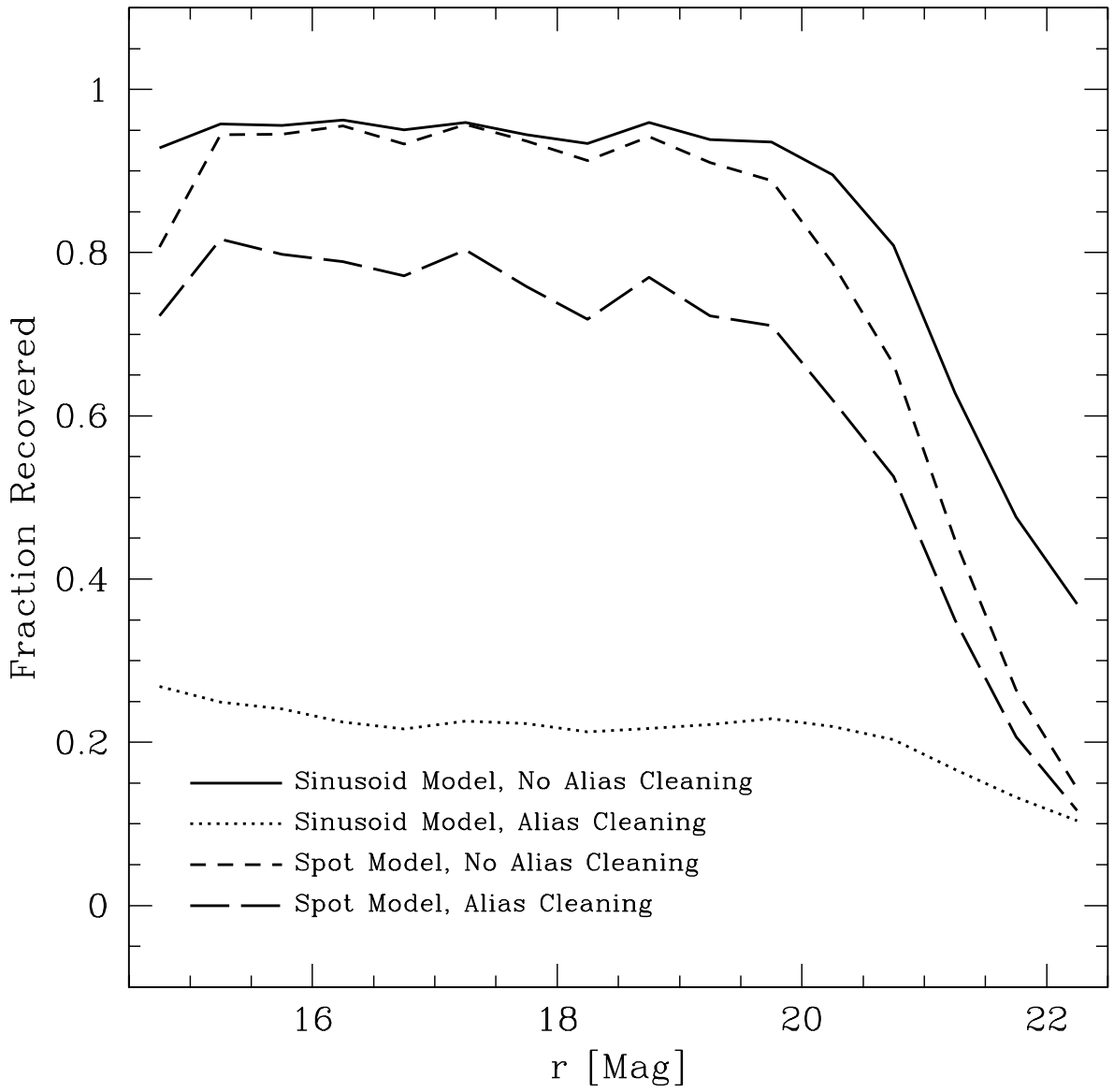

Fig. 9.— The recovery fraction as a function of magnitude for simulations that have periods uniformly distributed in logarithm between 0.1 and 20 days, and semi-amplitudes uniformly distributed in logarithm between 0.01 and 0.1 mag.

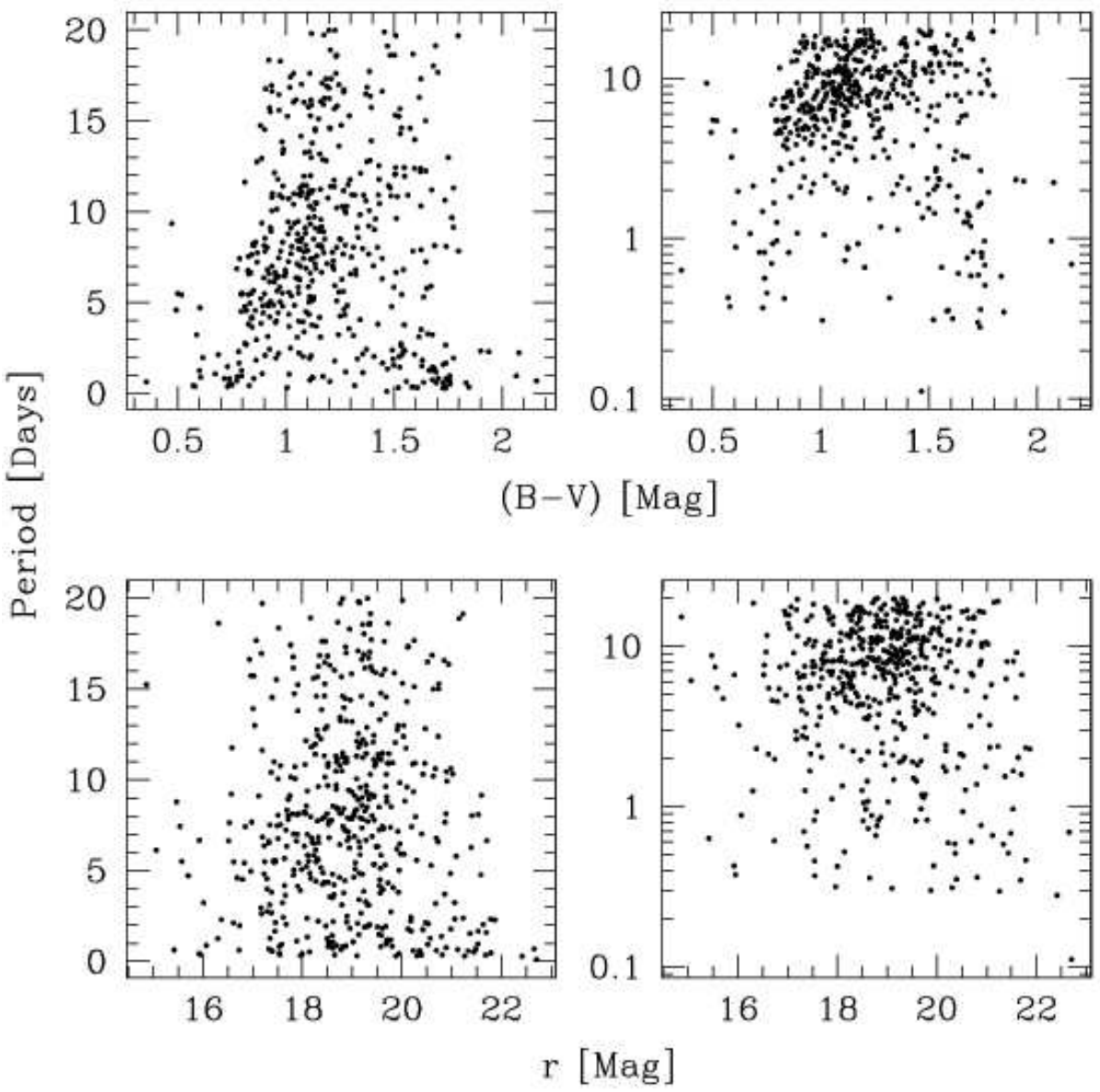

Fig. 10.— r-magnitude and $(B-V)$ vs. Period for variable field stars located away from the cluster main sequence on a CMD. We exclude eclipsing binaries and pulsating variables from this plot. The period is shown on a linear scale on the left-hand-side and on a logarithmic scale on the right-hand-side. Note that no correction for redenning has been applied to the colors.

eclipsing binaries match to stars in our point source catalog. To do the matching we allow for a second-order polynomial transformation from the Messina et al. (2008) coordinates to our coordinates, and match stars within a radius of 5″. For sources that match to multiple stars in our catalog we choose the match with the smallest magnitude difference. Thirteen of the 15 unmatched sources lie on a Megacam chip gap, while stars 2835 and 3021 do not lie within 5″ of any stars in our point source catalog. We have independently detected periodic variability for 58 of the 91 matched stars. We classify 38 of these stars as potential cluster members, 21 are not classified as potential cluster members, while 2 stars do not have BV photometry from Kalirai et al. (2001) and are excluded from the catalog of rotating candidate cluster members presented in this paper. Note that the membership classification by Messina et al. (2008) is based on photometry through two filters while our classification utilizes five filters. Of the 32 stars that we do not classify as variables, 19 are saturated in more than two-thirds of our time-series observations, 11 have a light curve RMS that is higher than the median RMS as a function of magnitude, while two have an RMS that is lower than the median RMS as a function of magnitude.

In figure 11 we compare our periods to those measured by Messina et al. (2008) for the 22 matching stars which are included in our clean sample, we also compare the resulting period-magnitude diagrams. Note that the Messina et al. (2008) periods are generally shorter than the periods that we measure. The period measurements disagree by more than 20% for the following 8 stars: V424 (M3208), V589 (M3245), V827 (M2257), V888 (M2395), V961 (M3866), V1008 (M2549), V1025 (M2895), V1135 (M4134), where the identification listed in parentheses for each star is taken from Messina et al. (2008). In each case we find that our light curve does not phase at the period reported by Messina et al. (2008), while inspection of the Scargle-periodograms displayed in figures 17-26 of Messina et al. (2008) reveals additional peaks near the periods that we have measured. Note that our light curves contain an order of magnitude more observations obtained on more than twice as many nights as the light curves used by Messina et al. (2008), as a result the periods presented here are less susceptable to aliasing.

4. The Period-Color Sequence in M37

The relation between period and color for the clean sample of M37 stars seen in figure 2 is similar to that seen for stars in the Hyades (Radick et al. 1987). As we will discuss in §8, this sequence provides a powerful test for theories of stellar angular momentum evolution. In this section we provide an analytic fit to the period-color relation, and also evaluate the spread in rotation periods about this fit as a function of mass.

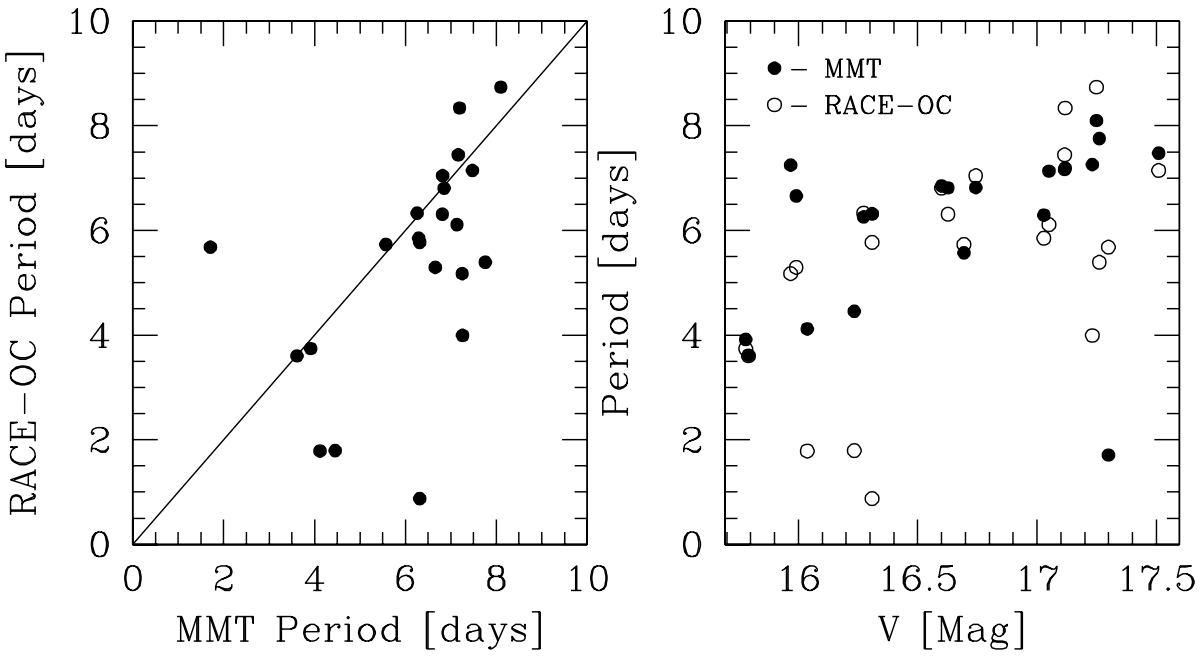

Fig. 11.— (Left) Comparison between the periods presented in this paper (MMT Period) and the Lomb-Scargle periods measured by the RACE-OC project for the 22 matching stars included in our clean sample. Note that our periods are generally longer than the periods measured by the RACE-OC project. (Right) We show the period-magnitude relation for the matching stars using the MMT periods (filled circles) and the RACE-OC periods (open circles).

The selection of stars in the $(B-V)_0$-period sequence is shown in figure 12. We take the period uncertainty for each star to be the quadrature sum of the bootstrap error for the star, 0.05% to account for errors in the model, and 0.03% to account for differential rotation. The color error for each star is interpolated from table 4. We fit two models of the form:

$$P = a_{lin}(B-V)_0 + b_{lin} \tag{3}$$

and

$$P = \frac{a_{bpl}}{\left(\frac{(B-V)_0}{0.5}\right)^{b_{bpl}} + \left(\frac{(B-V)_0}{0.5}\right)^{-1}} \tag{4}$$

by minimizing the total χ^2_{tot}

$$\chi^2_{tot} = \sum_i \left(\left(\frac{x_i - x_{i,0}}{\sigma_{x,i}} \right)^2 + \left(\frac{y(x_i) - y_{i,0}}{\sigma_{y,i}} \right)^2 \right) \tag{5}$$

where $x_{i,0}$ is the observed $(B-V)_0$ value of star i, x_i is the predicted $(B-V)_0$ value for star i and is treated as a free parameter, $\sigma_{x,i}$ is the uncertainty in $(B-V)_0$ for star i, and the y values correspond to periods with $y(x_i)$ being given by equation 3 or 4 for the free a and b parameters.

We use the downhill simplex algorithm (Nelder and Mead 1965; Press et al. 1992) to fit each relation solving for the a and b parameters as well as the x_i values for each star. Note that this is equivalent to minimizing the orthogonal χ^2 distance between each point and the model. The resulting parameters with uncertainties are listed in table 5. We list the 1σ uncertainties from 1000 bootstrap simulations (i.e. simulating data sets by resampling with replacement from the original data set), and from 1000 Monte Carlo simulations (i.e. simulating data sets by adjusting each observed x and y value by random variables drawn from normal distributions with standard deviations σ_x and σ_y). We find that χ^2 per degree of freedom for the linear and broken power-law relations are given respectively by $\chi^2_{dof,lin} = 3.23$ and $\chi^2_{dof,bpl} = 2.48$, where there are 242 degrees of freedom. We note, therefore, that we do detect a significant spread in rotation period about the main period-color sequence beyond what is due to observational uncertainties in the period and color (at the 16σ level for the broken power-law). This can be seen both from the deviation of χ^2_{dof} from 1 and from the fact that the parameter errors from the bootstrap simulations are consistently larger than the parameter errors from the Monte Carlo simulations. In table 6 we list the residual RMS and χ^2 per degree of freedom in $(B-V)_0$ bins for both the linear and broken power-law relations. Note that the spread in period is significant at greater than the 3σ level for all color bins with $(B-V)_0 < 1.5$.

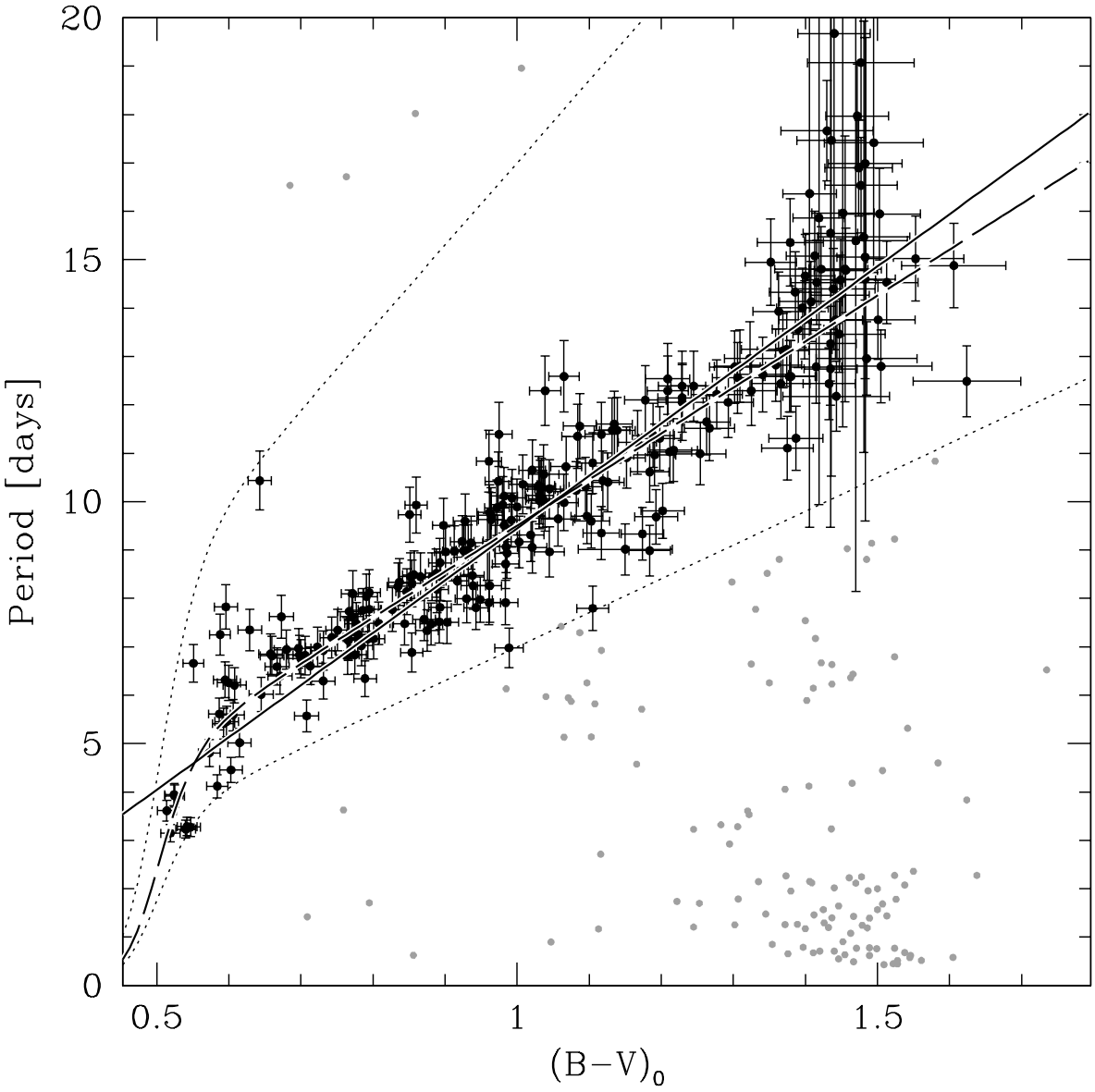

Fig. 12.— The selection of stars on the main period-color sequence in M37. Dark points are used to plot stars in the sequence, while light points plot stars not on the sequence. The dotted lines show the boundaries for this selection. The solid and dashed lines show a linear and broken power-law fit to the sequence respectively (equations 3 and 4).

5. Comparison With Spectroscopy

Of the 127 stars for which we obtained spectra with Hectochelle, 41 match to candidate rotational variables. Of these, 33 have an average radial velocity that is within 3σ of the cluster systemic radial velocity (see Paper I).

In figure 13 we show the stars with spectroscopy on the $(B-V)_0$-period relation. Using the measured $v \sin i$ and rotation periods, together with the stellar radii inferred from the best fit YREC isochrone, we can estimate the inclination angle of the rotation axis via:

$$\sin i = \frac{P v \sin i}{2\pi R}. \tag{6}$$

In figure 13 we plot the sine of the angle as a function of $(B-V)_0$ for the 33 stars with RV consistent with being cluster members.

For all but three stars in the clean sample the measured values of P and $v \sin i$ appear to be consistent with the inferred radii since we find values that are consistent with $\sin i < 1$. The errors on this determination are dominated by the errors on $v \sin i$.

6. Amplitude Distribution

Because photometric observations of spotted stars are only sensitive to changes in the flux integrated over the visible hemisphere of the star, much of the information on the actual surface brightness distribution is lost. Due to well known degeneracies between the latitude, area, and temperature of a spot, it is not generally possible to obtain a unique fit to a single-filter light curve using a simple single spot model (e.g. Dorren 1987). When multiple spots are present their individual signals merge into a rather featureless spot-wave. Nonetheless, by studying an ensemble of stars it may be possible to gain insight on the activity-rotation relation from our data. Moreover, from an observational point of view, knowing the distribution of amplitudes is useful for planning purposes since the amplitude and period will determine if the rotation period of a star can be measured.

We calculate the amplitudes for the clean sample of 372 stars using equation 1 with $N = 2$. We take the amplitude (A_r) to be the peak-to-peak amplitude of the Fourier series.

As seen in figure 14 the amplitude appears to be anti-correlated with the period and positively correlated with the $(B-V)_0$ color. There is a fairly steep selection effect, however, between the amplitude and $(B-V)_0$ which is caused by the drop in photometric precision for fainter stars. Due to the non-trivial relation between period and color, the selection in the period-amplitude plane is complicated.

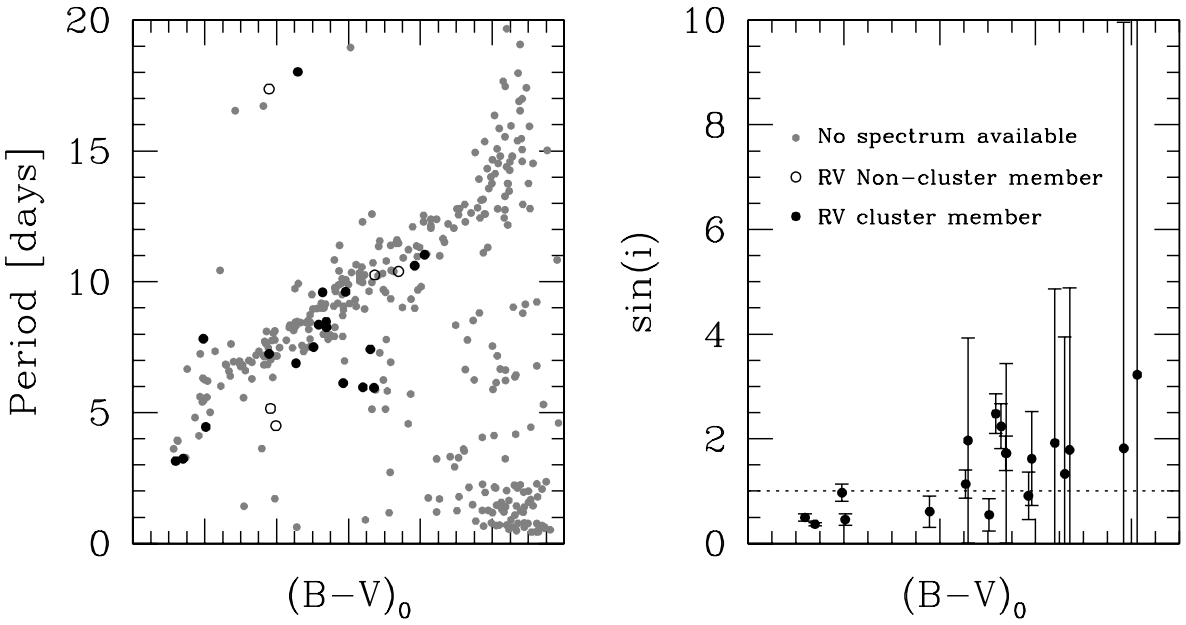

Fig. 13.— (Left) Rotation period versus $(B-V)_0$ for stars in the clean sample with and without spectroscopy. (Right) $\sin i$ determined via equation 6 versus $(B-V)_0$ for 19 rotational variables in the clean sample with Hectochelle spectra that have an average radial velocity consistent with being members of the cluster. The errors are dominated by uncertainties in $v \sin i$, which are estimated from the scatter in $v \sin i$ measured on four different nights. The dotted line shows $\sin i = 1$, points below this line have consistent $v \sin i$, period and radius values.

To evaluate whether or not the observed correlations are due to selection effects we determine for each light curve the minimum amplitude that the signal could have had and still have been detected. To do this, we find α such that

$$LS(r(t) - (1-\alpha)\tilde{r}(t), P) = -150 \tag{7}$$

where $LS(x, P)$ is the logarithm of the Lomb-Scargle (L-S) formal false alarm probability for light curve x with period P (see Press et al. 1992), $\tilde{r}(t)$ is the model signal in eq. 1, $r(t)$ is the observed light curve, and -150 is the selection threshold used to select variables in Paper II. For the purposes of this investigation we do not include stars that were not selected with L-S; we also reject stars for which no positive α can be found that satisfies eq. 7 as these are light curves for which the simple model in eq. 1 does not adequately describe the periodic signal. We then take the minimum observable amplitude to be:

$$A_{min} = \alpha A_r \tag{8}$$

Note that we have ignored the by-eye selection that light curves are passed through following the selection on L-S. We also caution that stars with light curves that are not well modeled by the simple Fourier series will have minimum observable amplitudes that are underestimated. The minimum observable amplitudes for each point are also shown in figure 14.

To evaluate the significance of the apparent correlation in the presence of the selection we use Kendell's τ (non-parametric correlation statistic) modified for the case of data suffering a one-sided truncation (Tsai 1990; Efron and Petrosian 1992, 1999). Letting the data set be represented by the set of points $\{(x_i, y_i, y_{min,i})\}$, where $y_{min,i}$ is the minimum value of y_i that could have been measured for observation i, define the set of comparable pairs

$$\mathcal{C} = \{(i,j) \,|\, y_i \geq y_{min,j} \text{ and } y_j \geq y_{min,i}\}. \tag{9}$$

Define the risk-set numbers by

$$N_j = \#\{i \,|\, y_{min,i} \leq y_j \text{ and } y_i \geq y_j\}. \tag{10}$$

The normalized correlation statistic is then

$$\hat{T} = \left(\sum_{(i,j)\in\mathcal{C}} \text{sign}((x_i - x_j)(y_i - y_j)) \right) / \sigma \tag{11}$$

with the variance of the numerator given by

$$\sigma^2 \approx 4 \sum_i \frac{N_i^2 - 1}{12}. \tag{12}$$

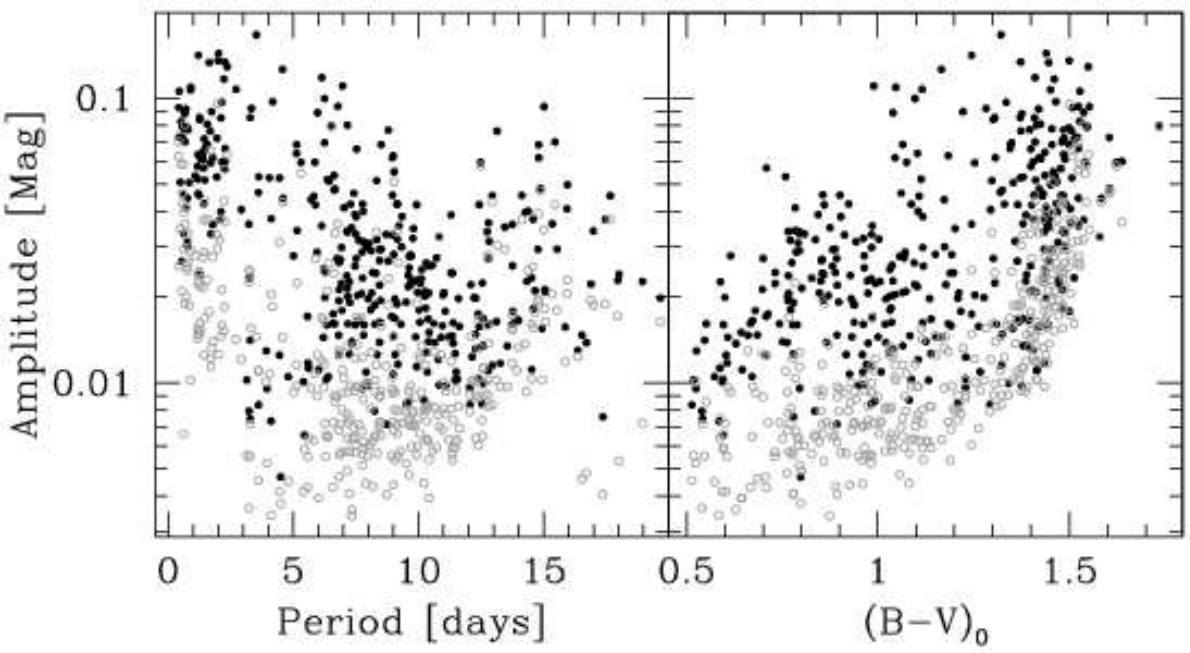

Fig. 14.— The amplitude of the rotational variables is plotted against period and $(B-V)_0$. The light colored open circles show the minimum amplitude that each star could have had and still have been detected.

The statistic is normalized such that a value of $\hat{T} = 1$ corresponds to a 1σ rejection of the null hypothesis of non-correlation.

Applying eq 11 to the (P, A_r) and $((B-V)_0, A_r)$ data we find $\hat{T} = -11091$ and $\hat{T} = 3900$ respectively. We conclude, therefore, that there is a significant anti-correlation between rotation period and amplitude and a positive correlation between $(B-V)_0$ and amplitude for the lower main sequence stars in this cluster.

As shown by Noyes et al. (1984), there is a tight correlation between stellar activity, measured via the ratio of emission in the cores of the Ca II H and K lines to the total luminosity of the star, and the Rossby number (R_O, the ratio of the rotation period to the characteristic time scale of convection). Messina et al. (2001) find that the light curve amplitude also appears to be anti-correlated with R_O.

To compute R_O for each star we use the empirical expression for the convective time-scale from Noyes et al. (1984)

$$\log \tau_c = \begin{cases} 1.362 - 0.166x + 0.025x^2 - 5.323x^3, & x > 0 \\ 1.362 - 0.14x, & x < 0 \end{cases} \tag{13}$$

where τ_c is the convective time-scale in days and $x = 1.0-(B-V)_0$. We plot the amplitude of the variables against R_O in figure 15, showing stars with $(B-V)_0 < 1.36$ and $(B-V)_0 > 1.36$ separately. For comparison we also show the candidate field rotators from Paper II.

The anti-correlation between R_O and A_r appears to be steeper for stars with $(B-V)_0 < 1.36$ than for stars with $(B-V)_0 > 1.36$. We note that the empirical constraints on the convective time-scale are less stringent for redder stars, so the values of R_O are more susceptible to systematic errors for $(B-V)_0 > 1.36$. Focusing on cluster members with $(B-V)_0 < 1.36$, the relation between R_O and A_r appears to flatten out, or saturate, for stars with $R_O < 0.3$. There appears to be a dearth of low-amplitude stars with $R_O < 0.2$, note that stars with peak-to-peak amplitudes $A_r > 0.02$ mag should have been detectable. There is also a hint that the relation between R_O and A_r is flat for $R_O > 0.6$. Note that as seen in figure 16 many of the stars with $R_O > 0.6$ fall above the main period-color sequence. As we discuss below, it is possible that the periods measured for these stars are not the rotation periods but rather the spot-evolution timescales.

Applying eq 11 to the (R_O, A_r) data we find $\hat{T} = -16462$ for all stars in the clean data set, $\hat{T} = -10520$ for 233 stars with $(B-V)_0 < 1.36$ and $\hat{T} = -1150$ for 129 stars with $(B-V)_0 > 1.36$. For comparison, the $((B-V)_0, A_r)$ data has $\hat{T} = 3846$ for $(B-V)_0 < 1.36$ and $\hat{T} = -540$ for $(B-V)_0 > 1.36$, while the (P, A_r) data has $\hat{T} = -5430$ for $(B-V)_0 < 1.36$ and $\hat{T} = -1145$ for $(B-V)_0 > 1.36$. For $(B-V)_0 < 1.36$ the correlation for (R_O, A_r) is more significant than for $((B-V)_0, A_r)$ or (P, A_r).

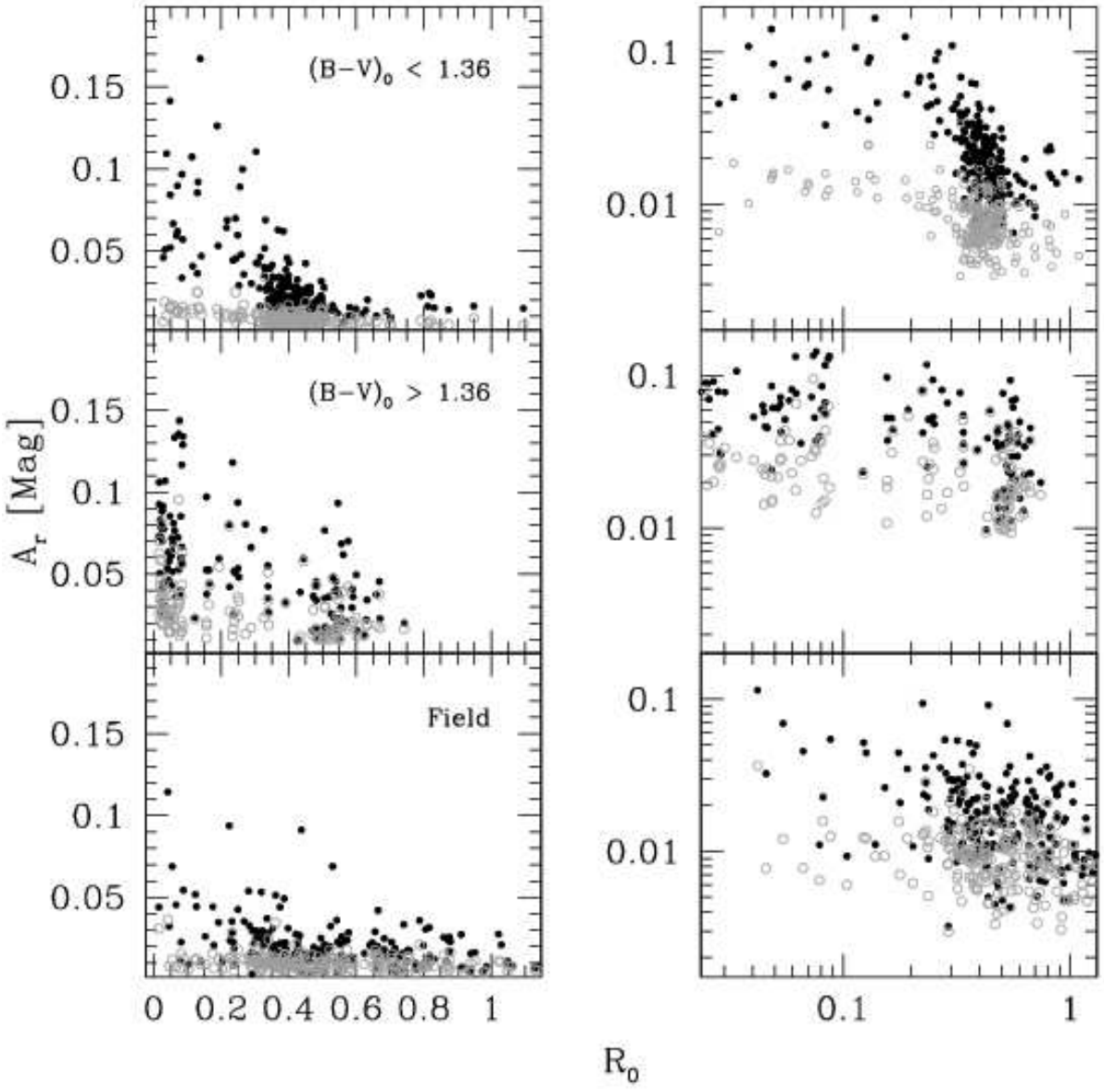

Fig. 15.— The r-band peak-to-peak amplitude A_r is plotted against the Rossby number R_O. The top two rows show the sample of clean cluster members that have $(B-V)_0 < 1.36$ and $(B-V)_0 > 1.36$. The bottom row shows the relation for field variables presented in Paper II, note that these stars all have $(B-V)_0 < 1.36$. The left column is on a linear scale, the right column is on a logarithmic scale. The solid points show the measured amplitudes, the open circles show the minimum detectable amplitude for each star. Notice that for cluster members with $(B-V)_0 < 1.36$, R_O and A_r are strongly anti-correlated above $R_O > 0.3$ while the relation flattens below $R_O < 0.3$. Stars with $R_O < 0.3$ appear to have a minimum amplitude of $A_r \sim 0.03$ mag. Cluster members with $(B-V)_0 > 1.36$ show a relatively flat relation even above $R_O > 0.3$. The field stars also show a relatively flat relation.

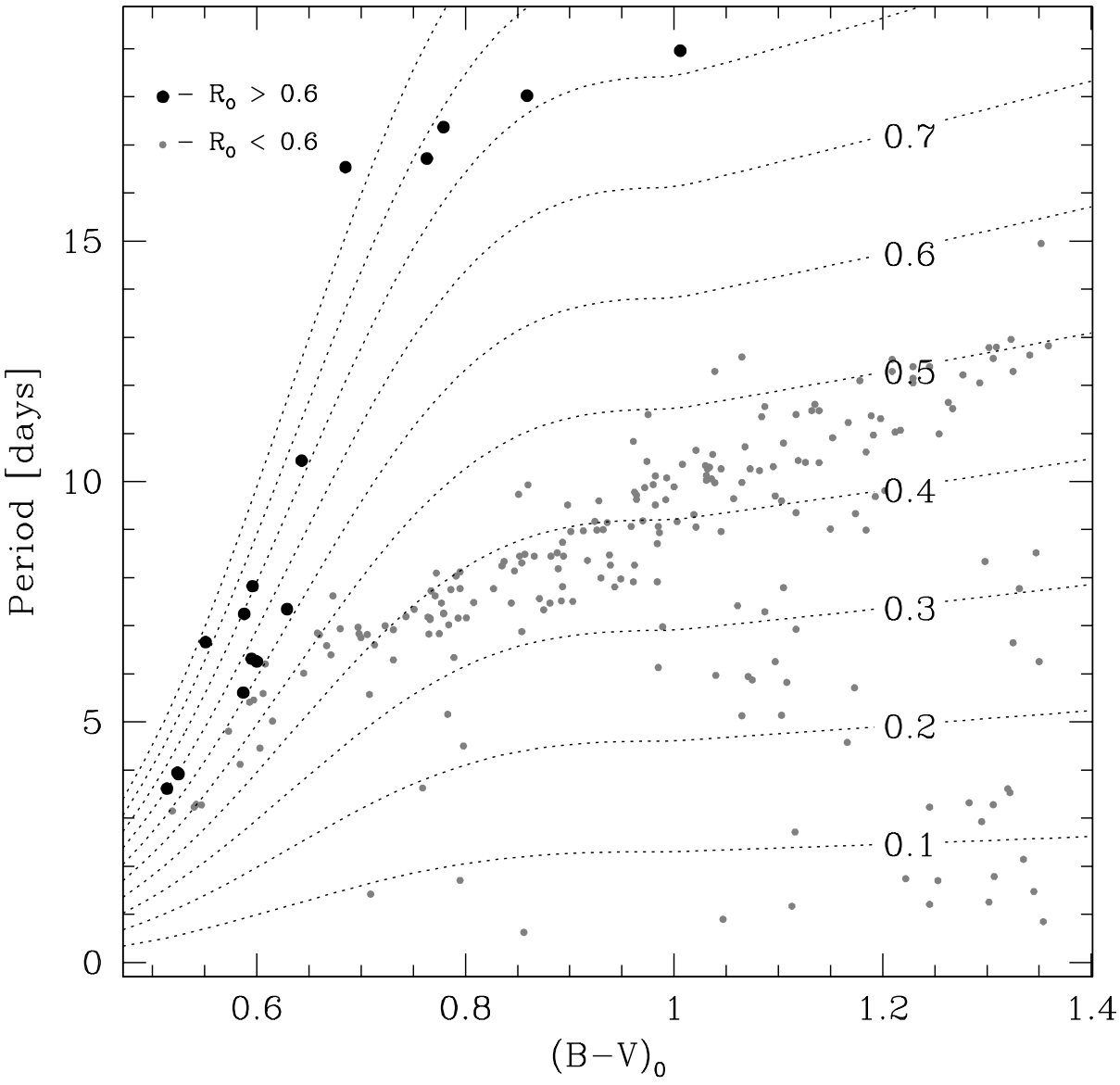

Fig. 16.— Comparison of stars with $R_O < 0.6$ and $R_O > 0.6$ on the $(B-V)_0$-P plot. Only stars in the clean sample with $(B-V)_0 < 1.36$ are shown. The dotted lines are lines of constant R_O.

For $(B-V)_0$, $R_O < 0.6$ the selection on A_r does not appear to bias the (R_O, A_r) distribution. We find that the (R_O, A_r) data for cluster members with $(B-V)_0 < 1.36$ and $R_0 < 0.6$ can be fit with the function:

$$A_r = \frac{0.078 \pm 0.008}{1 + \left(\frac{R_O}{0.31 \pm 0.02}\right)^{3.5 \pm 0.5}} \tag{14}$$

where the errors listed are the 1σ errors from 1000 bootstrap simulations. Figure 17 shows this relation. We also show the approximate location of the Sun on this diagram, assuming a typical large sunspot with an area that is 500 millionths that of the solar disk, a temperature ratio to the photosphere of 0.7, the bolometric corrections for the r-band from Girardi et al. (2004) and $(B-V)_\odot = 0.656$ (Gray 1992) to convert the bolometric amplitude to an r-band amplitude, and the solar equatorial rotation period of 24.79 days (Howard, Gilman and Gilman 1984). The error bar shows the approximate range of values for the Sun, where the upper limit is for the largest sunspot group observed to date (the giant sunspot group of April, 1947 had an area of ~ 6000 millionths that of the solar disk and was large enough to be seen without optical aid, see Taylor 1989).

As noted above, there appears to be a minimum amplitude of ~ 0.03 mag for stars with $(B-V)_0 < 1.36$, $R_O < 0.2$. The fact that there are stars with $R_O > 0.3$ that have amplitudes down to the minimum detectable limits below 0.01 mag shows that this is not likely a result of underestimating the minimum detectable amplitude and is likely to be a real effect. This indicates that these rapidly rotating stars may have a distribution of spot-sizes that is peaked, or that they have several spots. To illustrate this we have conducted Monte Carlo simulations of spotted star light curves for four different models of the spot-size and spot-number distributions. For the spot-size distribution we either fixed the spot area to 1% that of the stellar surface area or we allowed the spot-sizes to be uniformly distributed in logarithm between 10^{-5} times the stellar surface area and 10% of the stellar surface area. We calculated models with two spots per star or with ten spots per star. For each model we simulate 1000 light curves using the latest version of the Wilson-Devinney program (Wilson & Devinney 1971; van Hamme & Wilson 2003). The simulations are conducted assuming a spot to photosphere temperature ratio of 0.7, random orientations for the rotation axis, and that the spots are distributed randomly over the surface of the star. Figure 18 shows the distribution of A_r for the model simulations together with the observed A_r distribution for stars with $(B-V)_0 < 1.36$, $R_O < 0.3$. While fitting a model to the observed distribution is beyond the scope of this paper, we note that the models with a fixed spot-size or ten spots per star have peaked A_r distributions whereas the model with a broad spot-size distribution and only two spots per star results in a broad A_r distribution that is inconsistent with our observations. This suggests that the logarithmic distribution of spot filling-factors (i.e. the fraction of the stellar surface that is covered by spots) is peaked.

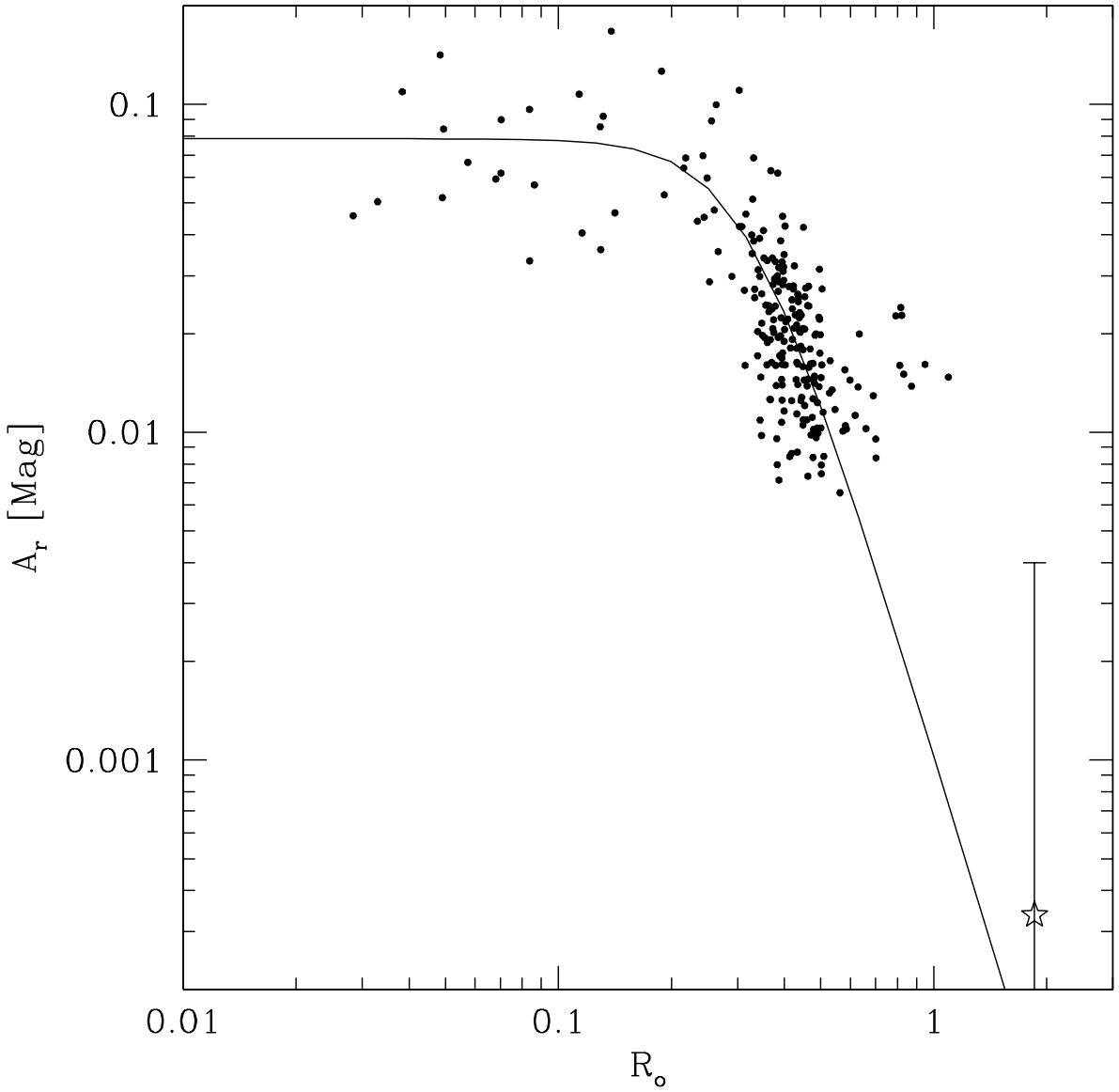

Fig. 17.— The r-band peak-to-peak amplitude A_r is plotted against the Rossby number R_O for the sample of clean stars that were selected by L-S and have $(B-V)_0 < 1.36$. The solid line shows equation 14 which is a fit to the data with $R_O < 0.6$. The star shows the approximate location of the Sun for a typical large sunspot, while the errorbar indicates the approximate upper limit on the amplitude.

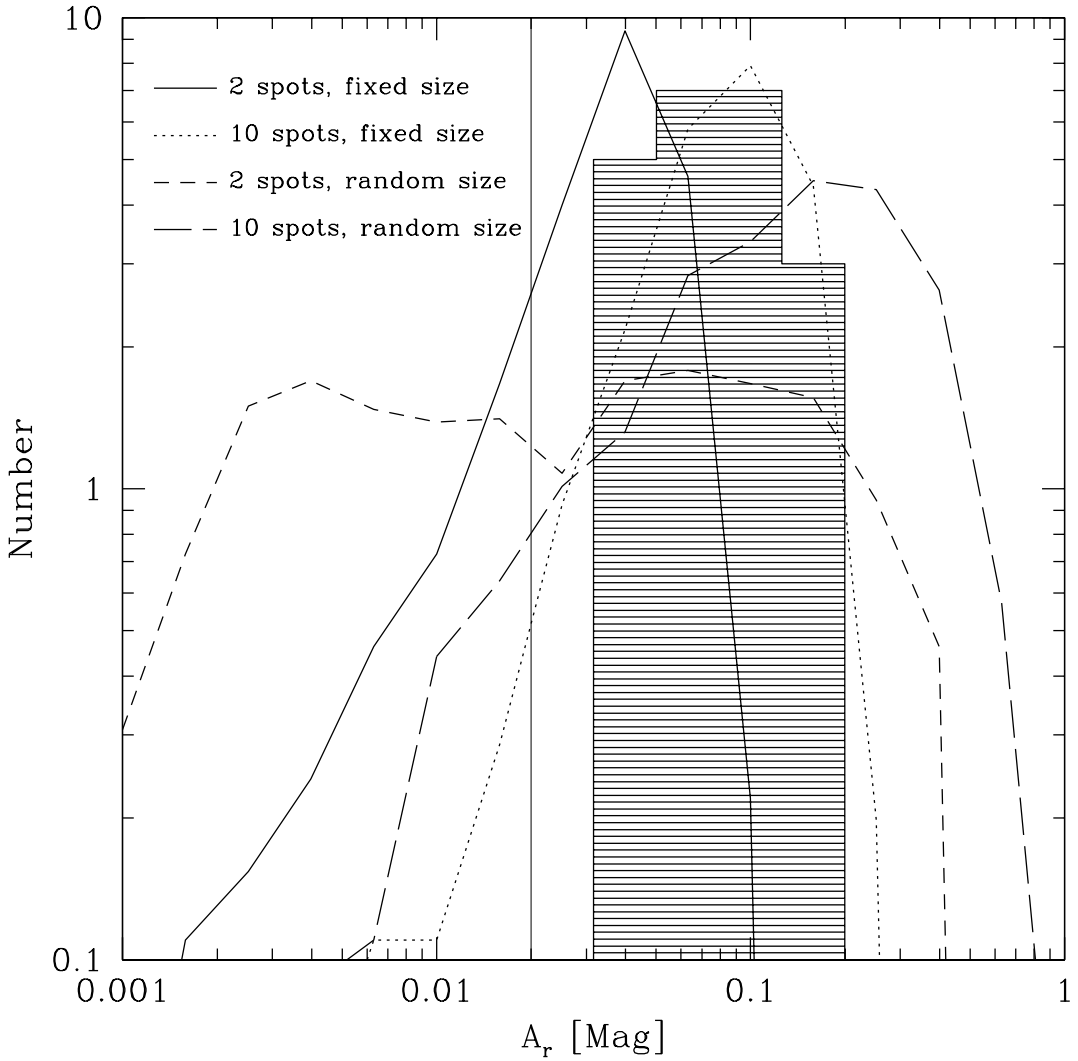

Fig. 18.— The distribution of peak-to-peak r-band amplitude measurements (A_r) for stars with $(B-V)_0 < 1.36$, $R_O < 0.2$ (shaded histogram) compared with model simulations. The models have been normalized to have the same total number of stars as the observed distribution. The simulations assume either a fixed spot size that is 1% of the stellar surface area or allow the spot-sizes to be uniformly distributed in logarithm between 10^{-5} times the stellar surface area and 10% of the stellar surface area. The simulations also assume either two spots per star or ten spots per star. The vertical line indicates the minimum detectable amplitude for stars in the cluster. Note that the lack of observed stars with $0.02 < A_r < 0.03$ indicates that the observed distribution is peaked at $A_r > 0.03$ mag. Models with a fixed spot-size result in a peaked A_r distribution whereas models that allow a broad spot-size distribution result in a broad A_r distribution that is inconsistent with the observations. Increasing the number of spots per star can tighten up the A_r distribution when the spot-size distribution is broad.

7. The Blue K Dwarf Phenomenon in M37

It is well known that the K dwarfs in the Pleiades fall blueward of a main sequence isochrone when plotted on a $B-V$ CMD (see Stauffer et al. 2003, hereafter S03). S03 have argued that this is due to differences in the spectral energy distribution of the Pleiades stars and the field dwarfs which are used to define the main sequence. They argue that this difference is due to more significant cool spots and plage areas on the photospheres of the young, rapidly rotating, heavily spotted Pleiades stars than are present on the older, slowly rotating, less heavily spotted field dwarfs. The plage areas result in excess flux in the B and V bands, while spots cause excess flux in the near infrared. As evidence for this explanation they show that the discrepancy at fixed color between the magnitude of the Pleiades stars and the main sequence isochrone correlates with $v \sin i$. An et al. (2007, hereafter A07) have also shown that the K dwarfs in the young cluster NGC 2516 are too blue in $B-V$ and that the discrepancy correlates with $v \sin i$.

Using our rotation periods we can look for this phenomenon in M37. We first define two groups of stars: those which lie on the main color-rotation period band (with the selection performed as in §4), and rapid rotators with $P < 2$ days. In figure 19 we show the locations of these two groups of stars on $B-V$ and $V-I_C$ CMDs and in figure 20 we show them on $g-r$ and $g-i$ CMDs. The results appear to be similar to that found by S03 and A07. In the $B-V$ and $g-r$ CMDs the rapid rotators appear to be bluer than the slower rotators at a fixed magnitude along the lower main sequence. While in the $V-I_C$ and $g-i$ CMDs the rapid rotators are slightly redder at fixed magnitude than the slower rotators.

To illustrate these effects quantitatively we bin the data by magnitude and plot in figures 21-24 the rotation period of the variables against the color difference $c_{obs} - c_{fid}$ where c_{fid} is the color interpolated within a fiducial main sequence, at the V magnitude of the star; the fiducial sequence is drawn by eye. We use a fiducial sequence rather than a theoretical sequence because the discrepancy between the observed and theoretical sequences varies with magnitude, and correlations between period and magnitude could lead to spurious correlations between period and color difference. For each bin we calculate the Spearman rank-order correlation coefficient (r_s) as well as the two-sided significance level of its deviation from zero, we ignore uncertainties in the photometry in calculating this statistic.

As seen in figure 21, there is a significant correlation (greater than 98% significance) between period and $(B-V)_{obs}-(B-V)_{fid}$ at fixed V for stars with $6.5 < M_V < 9.5$. Fitting a linear relation of the form $(B-V)_{obs}-(B-V)_{fid} = mP+b$ gives a slope of $m \sim 0.005$ for the bin with the most significant correlation detection. When using $(V-I_C)_0$ we find anti-correlations with greater than 80% significance between period and $(V-I_C)_{obs}-(V-I_C)_{fid}$ for stars with $8.5 < M_V < 10.5$ (figure 22). In $g-r$, the stars with $6.5 < M_V < 9.5$ or

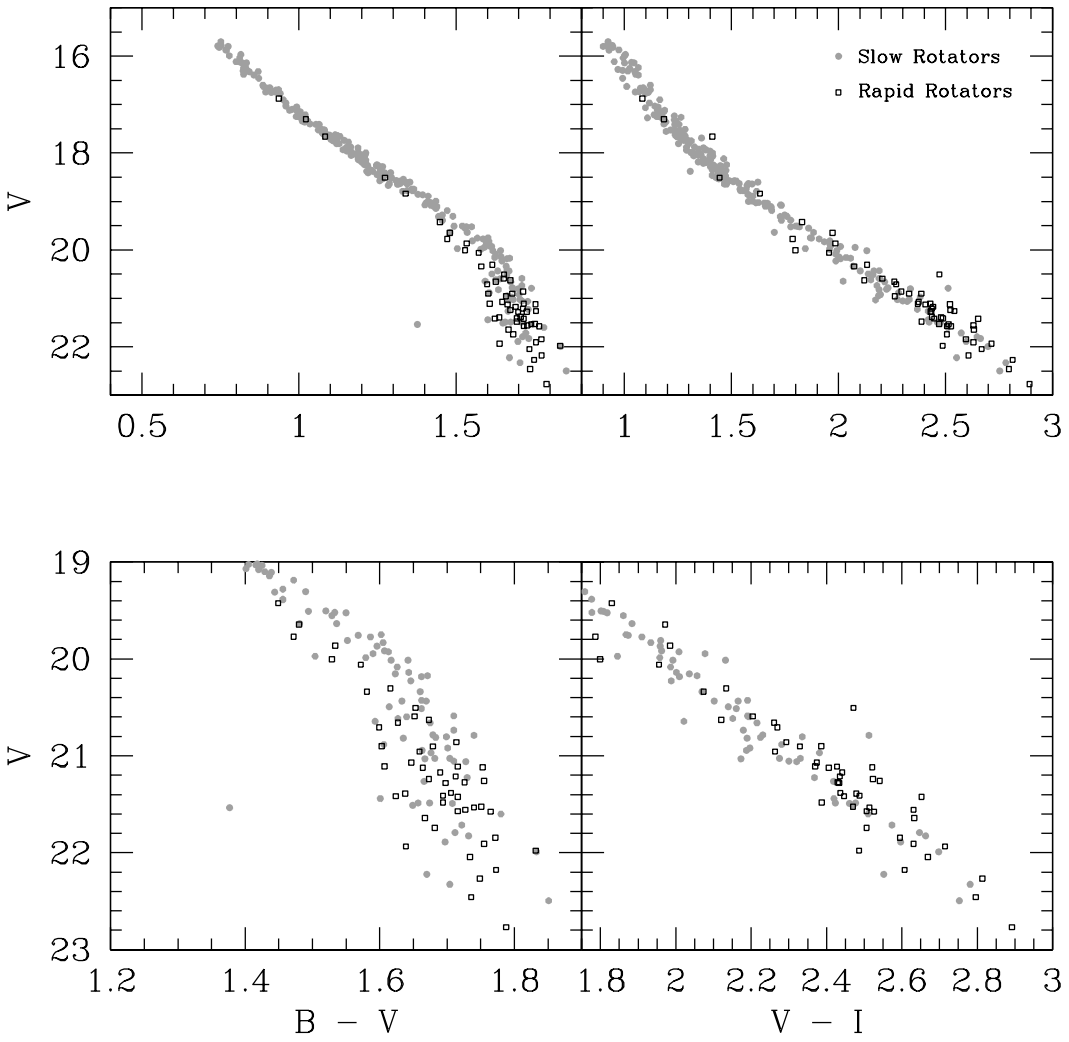

Fig. 19.— Stars located on the main color-rotation period band (filled, light points) and rapidly rotating stars with $P < 2$ days are plotted on $B-V$ and $V-I_C$ CMDs. The bottom panels show a close up on the lower main sequence. Along the lower main sequence the rapidly rotating stars appear to be slightly bluer in $(B-V)$ at given V and slightly redder in $(V-I_C)$ at given V than the slower rotators.

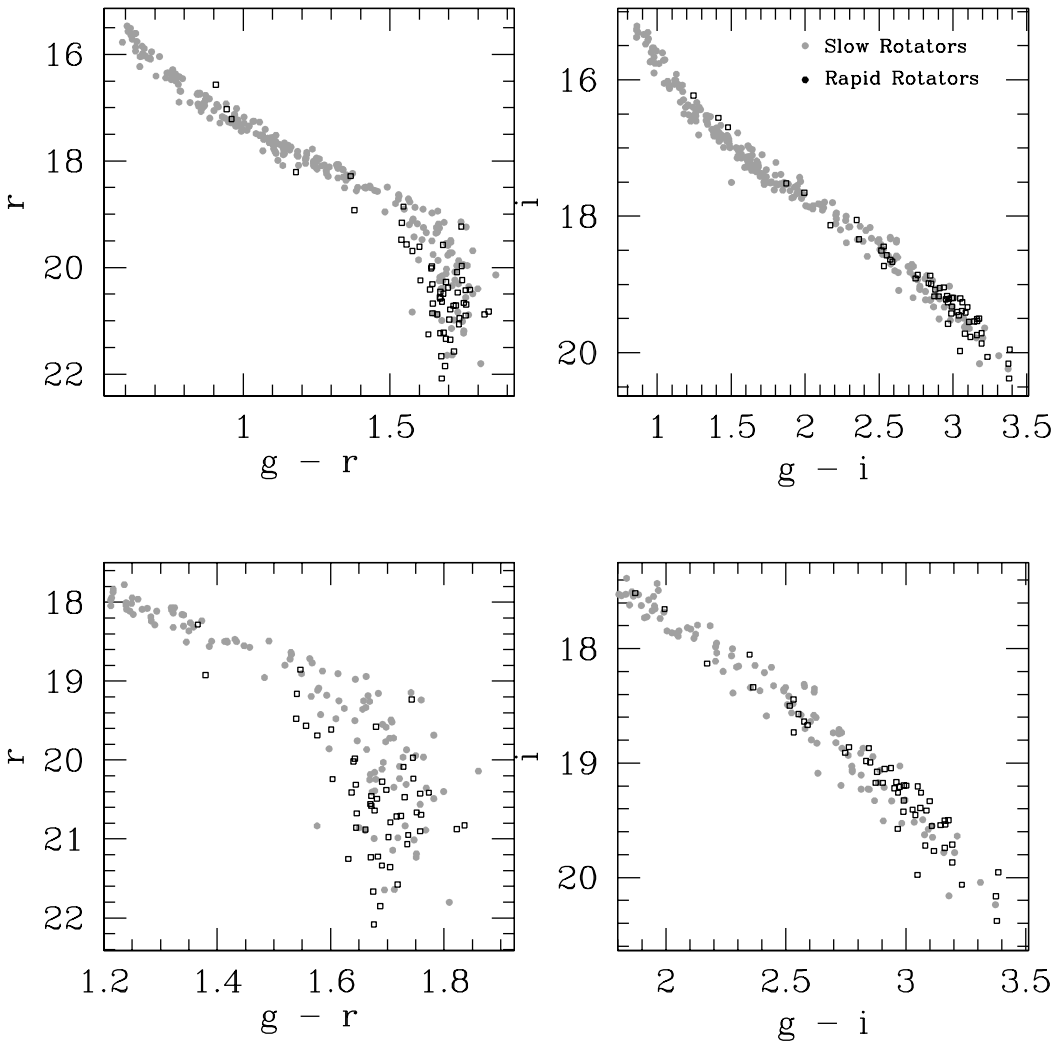

Fig. 20.— Same as figure 19 here we show $g-r$ and $g-i$ CMDs.

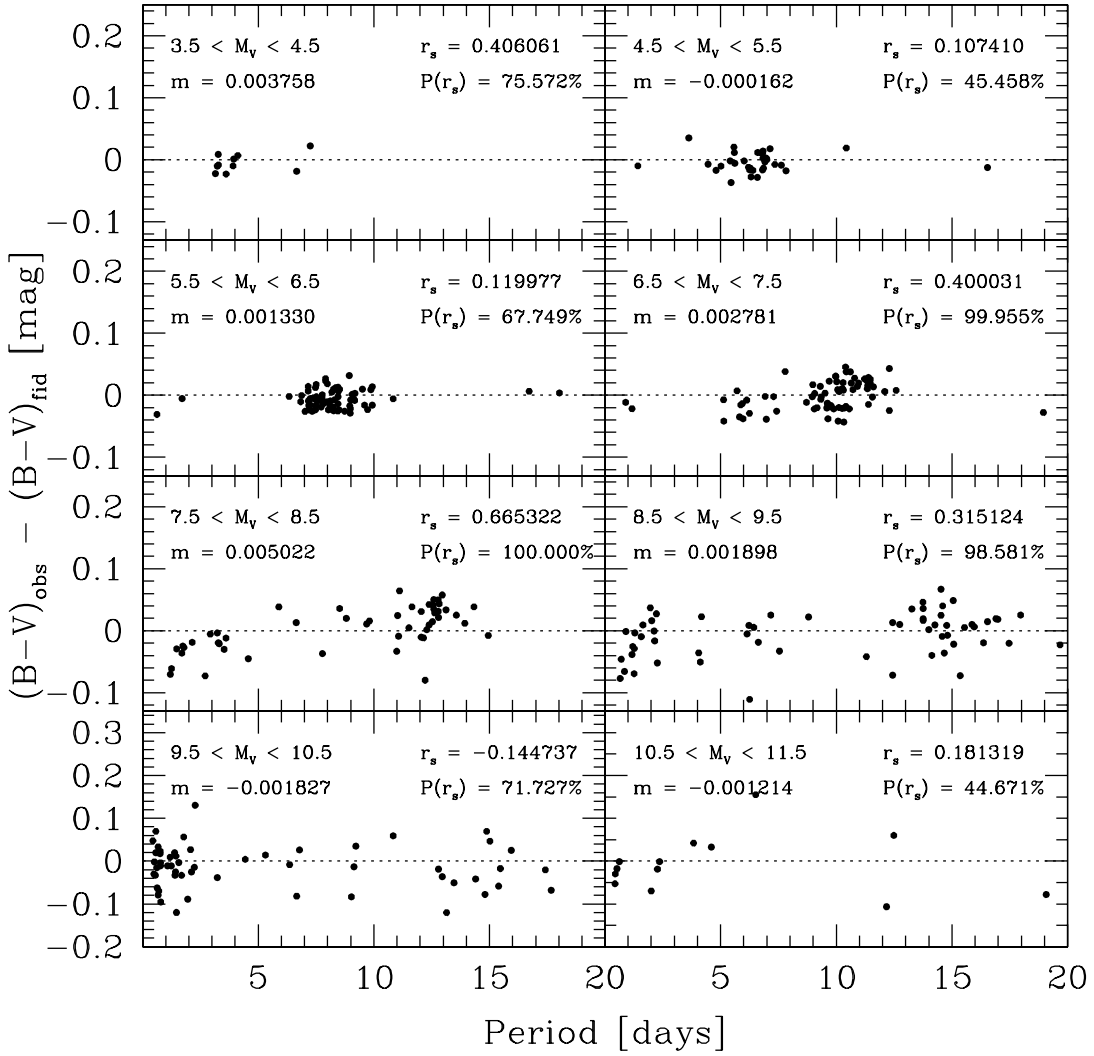

Fig. 21.— Period versus $(B-V)_{obs} - (B-V)_{fid}$, where $(B-V)_{fid}$ is the color on the fiducial main sequence at the V magnitude of each star. This is plotted for stars in different M_V bins (assuming a distance modulus of $(m-M)_V = 11.572$ from Paper I). In each bin we calculate the Spearman rank-order correlation coefficient (r_s) as well as the two-sided significance level of its deviation from zero ($P(r_s)$); we also fit a linear relation of the form $(B-V)_{obs} - (B-V)_{fid} = mP + b$ listing the slope in each bin. Stars in the magnitude bins ($6.5 < M_V < 9.5$) show a significant correlation between P and $(B-V)_{obs} - (B-V)_{fid}$.

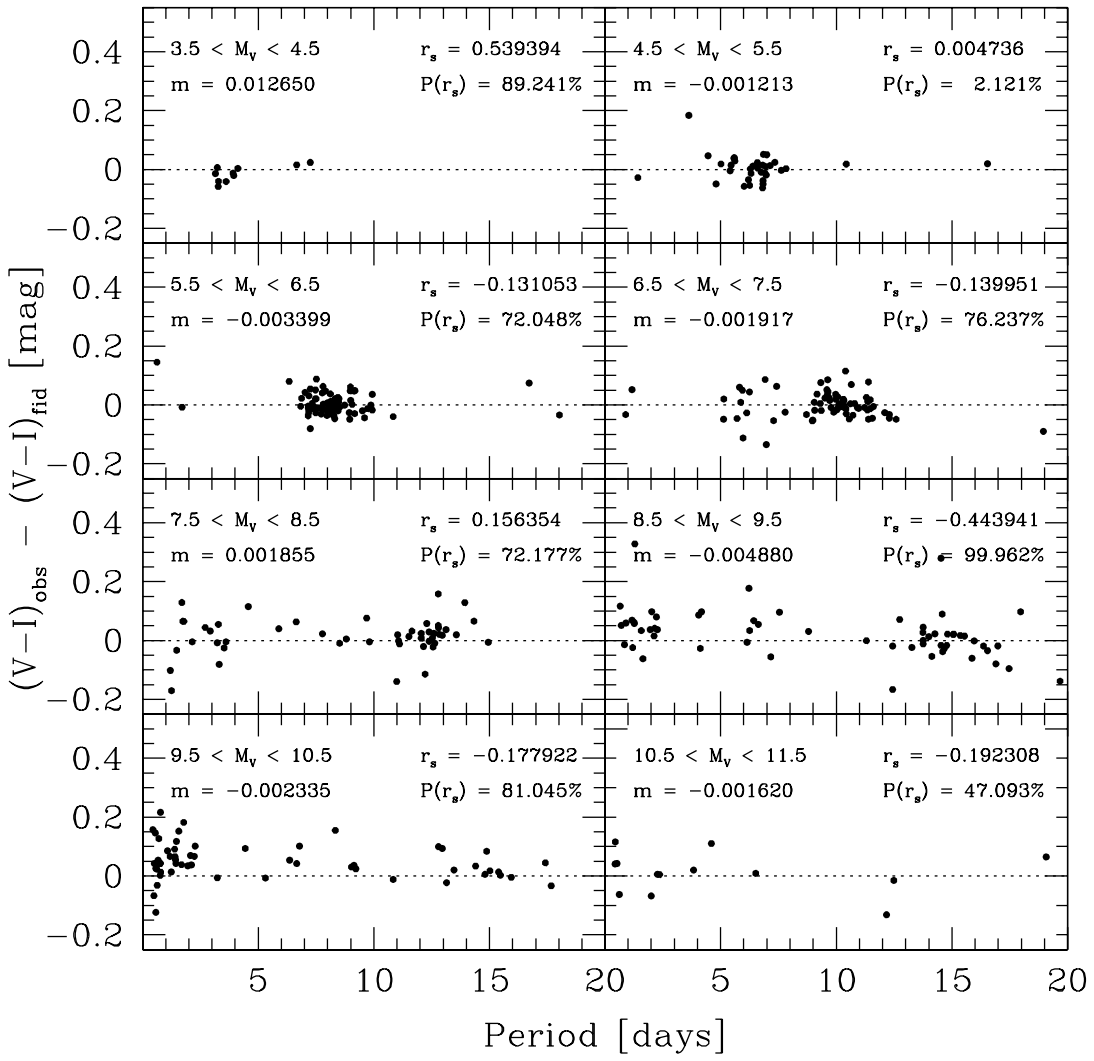

Fig. 22.— Same as figure 21, here $(V - I_C)_{fid}$ is calculated at the V magnitude of the stars. In this case stars with $8.5 < M_V < 10.5$ show an anti-correlation between P and $(V - I_C)_{obs} - (V - I_C)_{fid}$.

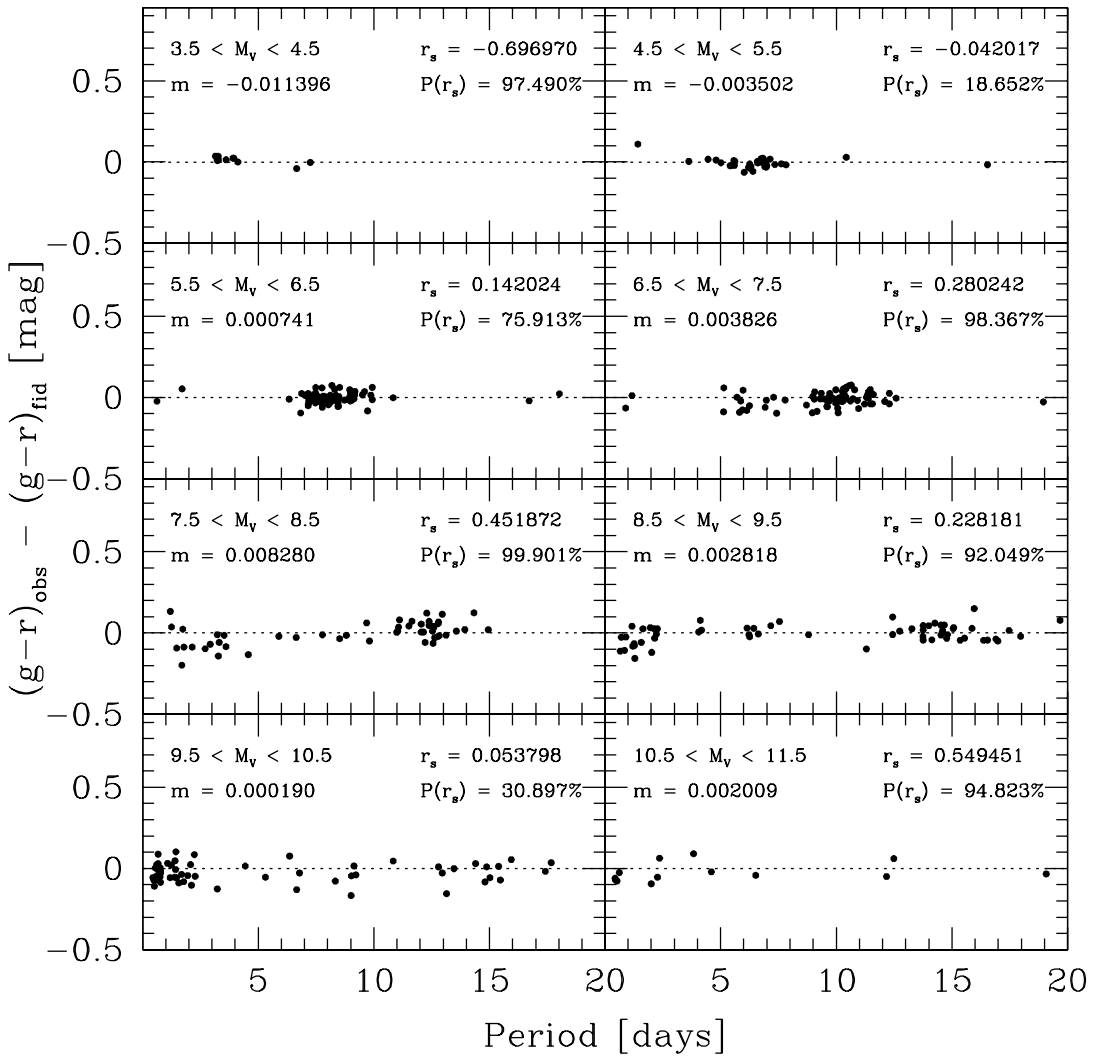

Fig. 23.— Same as figure 21, this time using $g - r$. The stars with $6.5 < M_V < 9.5$ or $10.5 < M_V < 11.5$ show a significant correlation between P and $(g - r)_{obs} - (g - r)_{fid}$.

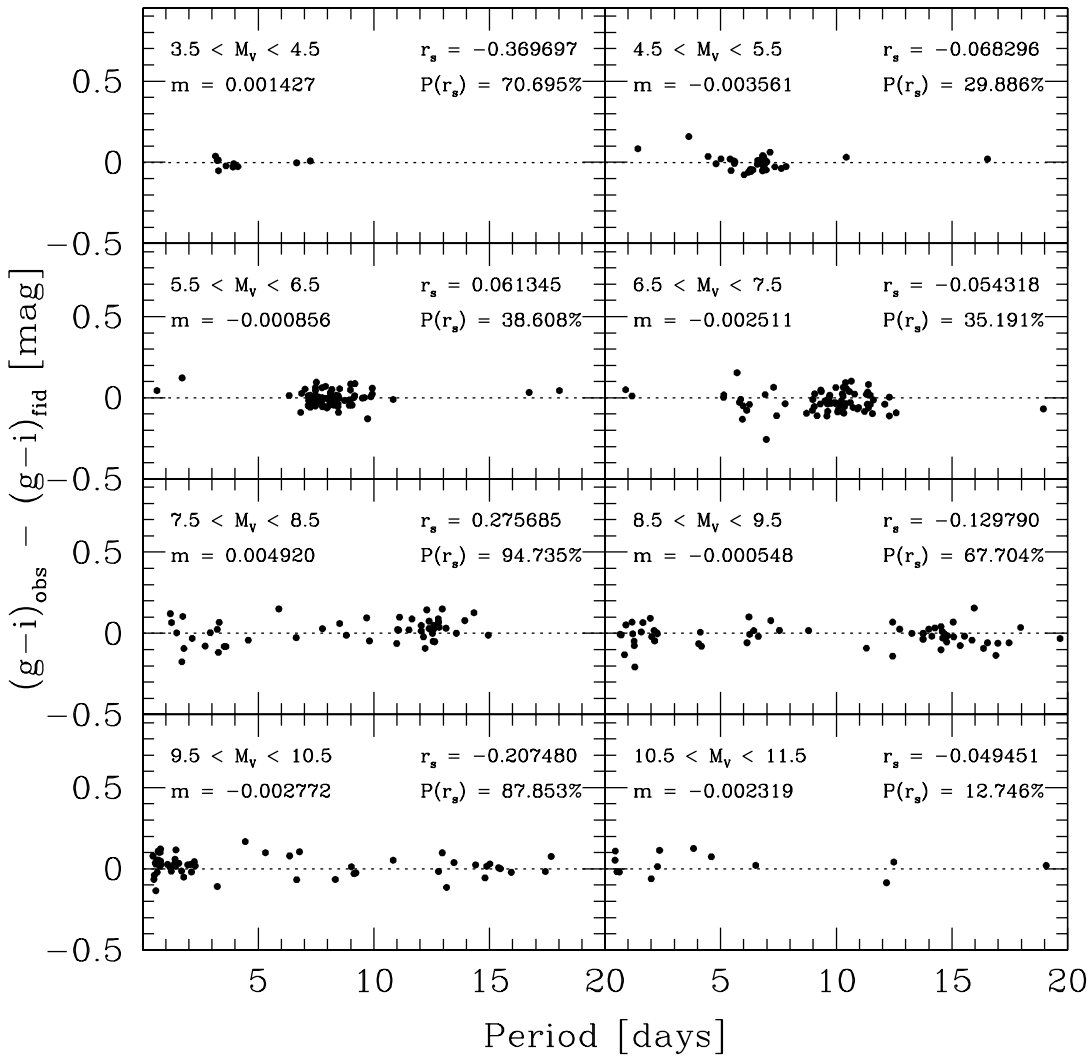

Fig. 24.— Same as figure 21, this time using $g - i$. Stars with $7.5 < M_V < 8.5$ show a positive correlation between P and $(g - i)_{obs} - (g - i)_{fid}$ while stars with $9.5 < M_V < 10.5$ show an anti-correlation.

$10.5 < M_V < 11.5$ show a positive correlation between period and $(g-r)_{obs} - (g-r)_{fid}$ (figure 23). Finally in $g-i$, stars with $7.5 < M_V < 8.5$ have a positive correlation between period and $(g-i)_{obs} - (g-i)_{fid}$ (figure 24) while stars with $9.5 < M_V < 10.5$ show a negative correlation.

The positive correlations seen in $B-V$ and $g-r$, together with the anti-correlations in $V-I_C$ and $g-i$ for the red stars is consistent with the blue K dwarf phenomenon in the Pleiades described by S03. This effect has been seen in the Pleiades and in NGC 2516 amongst stars with $0.8 < (B-V)_0 < 1.2$ ($6 \lesssim M_V \lesssim 7.5$; see A07). We find that this phenomenon extends into the M dwarf regime where $(B-V)_0$ saturates at ~ 1.5 mag ($M_V \gtrsim 9.5$).

These observations bear on a well-known problem in the theory of low-mass stars. In recent years studies of M-dwarf eclipsing binaries have revealed that these stars have radii that are $\sim 10\%$ larger than predicted by theory (Torres and Ribas 2002; Ribas 2003; López-Morales & Ribas 2005; Ribas 2006; Torres 2007). Note that the Torres (2007) finding is for an M-dwarf orbited by a short-period transiting Neptune-mass planet. The observed luminosities of these stars are in good agreement with theoretical predictions, but their effective temperatures are lower than predicted. The observed low-mass eclipsing binary systems generally have short periods, and it has been suggested that the discrepancy between theory and observations may be due to enhanced magnetic activity on these rapidly rotating stars (Ribas 2006; Torres et al. 2006; López-Morales 2007). There is also evidence that the discrepancy may be correlated with metallicity (López-Morales 2007). Recently Morales, Ribas and Jordi (2007) have shown that for fixed luminosity, active stars tend to have lower temperatures than inactive stars. This result was based on a sample of isolated field stars.

Our observations show that, at fixed luminosity, rapidly rotating late-K and early-M dwarfs tend to be bluer in $(B-V)$ but redder in $(V-I_C)$ than slowly rotating dwarfs. Since the bulk of the flux from these stars is emitted in the near infrared, it is reasonable to suppose that the correlation between $(V-I_C)$ and period more closely represents the correlation between effective temperature and period for these stars than the correlation between $(B-V)$ and the period does. For stars with $8.5 < M_V < 9.5$ we find that the slope between $(V-I_C)$ and the period is ~ -0.005 mag/day. Using the best fit YREC isochrone for M37 (see Paper I), a difference in $(V-I_C)$ of 0.1 mag (corresponding to a difference in period of 20 days, which is comparable to the difference between an old field star and a tidally synchronized binary) would result in a $\sim 3\%$ difference in effective temperature at fixed luminosity, or a $\sim 6\%$ difference in radius. This is comparable to, but still slightly less than, the radius discrepancy from eclipsing binaries. Since the flux through the V filter may

be slightly enhanced for rapidly rotating stars, it is likely that colors using only near-infrared filters will be more strongly anti-correlated with period than $(V - I_C)$ is. Deep near-infrared observations of this cluster would confirm or refute this hypothesis. Note that because our present sample of stars are all members of the same cluster, we can rule out age effects as the source of the color discrepancy. This is a conclusion which is not possible to make using samples of field stars.

8. Angular Momentum Evolution

By comparing the distribution of stellar rotation periods between star clusters of different ages we can study the evolution of stellar angular momentum. Both changes in the moment of inertia of a star and changes in its angular momentum contribute to changes in the rotation period. After ~ 100 Myr stars have settled onto the main sequence and their moment of inertia changes very little until they evolve onto the sub-giant branch. During this time period the rotation evolution is thought to be dominated by angular momentum loss via a magnetized wind. In this section we compare our observations of M37 with observations of other open clusters to test a simple model of stellar angular momentum evolution.

8.1. Data for Other Clusters

Besides M37, there are four clusters older than ~ 100 Myr that have significant, publicly available, samples of rotation periods; these are the Pleiades (100 Myr; Meynet, Mermilliod and Maeder 1993), NGC 2516 (140 Myr; Meynet, Mermilliod and Maeder 1993), M34 (200 Myr; Jones & Prosser 1996) and the Hyades (625 Myr; Perryman et al. 1998).

8.1.1. Pleiades

We used the WEBDA database[3] to obtain the rotation periods for 50 Pleiads; the periods are compiled from a number of sources (Stauffer et al. 1987; Prosser et al. 1993a,b, 1995; Marilli, Catalano, and Frasca 1997; Krishnamurthi et al. 1998; Terndrup et al. 1999; Messina 2001; Clarke, MacDonald and Owens 2004; Scholz & Eislöffel 2004). For stars with multiple periods listed we took the average value. We do not include 11 low-mass stars with periods for which optical photometry is unavailable.

[3]http://www.univie.ac.at/webda/webda.html

We also used WEBDA to obtain the photometry for this cluster. We took the mean photoelectric BV measurements (Johnson and Morgan 1953; Johnson and Mitchell 1958; Iriarte 1967, 1974; Mendoza 1967; Jones 1973; Robinson and Kraft 1974; Landolt 1979; Stauffer 1980, 1982b, 1984; Stauffer and Hartmann 1987; Prosser, Stauffer and Kraft 1991; Andruk et al. 1995; Messina 2001), Kron VI_K measurements (Stauffer 1982b, 1984; Prosser, Stauffer and K 1991; Stauffer and Hartmann 1987), Johnson VI_J measurements (Mendoza 1967; Iriarte 1969; Landolt 1979) and Johnson-Cousins VI_C measurements (Stauffer et al. 1998). Following A07 we converted VI_K to VI_C using the transformation from Bessell & Weis (1987) and VI_J to VI_C using the transformation given in A07.

To obtain $(B-V)_0$, $(V-I_C)_0$ and M_V for each star we take $E(B-V) = 0.02$, and $(m-M)_0 = 5.63$ (A07). We also assume $R_V = 3.1$ and $E(V-I_C)/E(B-V) = 1.37$ (see A07).

8.1.2. NGC 2516

The rotation periods for 362 stars in NGC 2516 come from Irwin et al. (2007, hereafter I07). These authors also provide VI_C photometry for all of their rotators. We find, however, that when adopting $E(B-V) = 0.125$, $(m-M)_0 = 8.03$ for this cluster (A07), the $(V-I_C)_0$ vs. M_V lower main sequence falls ~ 0.1 mag to the red of the sequence for M37, despite the cluster having a metallicity of $[Fe/H] = -0.07 \pm 0.06$ (A07) or 0.01 ± 0.07 (Terndrup et al. 2002) compared with $[Fe/H] = 0.045 \pm 0.044$ for M37 (Paper I). When taking the VI_C photometry for NGC 2516 from Jeffries, Thurston and Hambly (2001, hereafter J01) or Sung et al. (2002) the sequence is in good agreement with the M37 sequence. We therefore transform the photometry from I07 to match the J01 photometry via:

$$V_{J01} = 1.014V_{I07} - 0.172(V-I_C)_{I07} + 0.043 \quad (15)$$

$$I_{C,J01} = 0.972I_{C,I07} + 0.040(V-I_C)_{I07} + 0.314. \quad (16)$$

Finally there is BV photometry from J01 for 73 of the I07 rotators.

8.1.3. M34

The rotation periods for 105 stars in M34 were taken from Irwin et al. (2006, hereafter I06). We adopt the VI_C photometry from this paper as well. The lower main sequence in this case appears to be quite comparable to that for M37 when taking $E(B-V) = 0.07$ (Canterna, Crawford and Perry 1979) and $(m-M)_0 = 8.38$ (Jones & Prosser 1996). Note

that this cluster appears to be slightly more metal rich than M37, with $[Fe/H] = +0.07 \pm 0.04$ (Schuler et al. 2003). There is BV photometry from Jones & Prosser (1996) for 25 of the I06 rotators.

8.1.4. Hyades

As for the Pleiades we obtained the rotation periods for 25 Hyads from WEBDA; the periods are compiled from three sources (Radick et al. 1987, 1995; Prosser et al. 1995) and we take the average value for stars with multiple measurements. We also take the average photoelectric BV photometry (Johnson and Knuckles 1955; Argue 1966; Eggen 1968, 1974; Mendoza 1968; van Altena 1969; Sturch 1972; Robinson and Kraft 1974; Upgren and Weis 1977; Upgren, Weis and Hanson 1985; Stauffer 1982a; Herbig, Vrba, and Rydgren 1986; Weis & Upgren 1982; Weis & Hanson 1988; Andruk et al. 1995), Kron VI_K photometry (Upgren and Weis 1977; Upgren, Weis and Hanson 1985; Weis & Upgren 1982; Weis & Hanson 1988; Stauffer 1982a), Johnson VI_J photometry (Mendoza 1967; Johnson, MacArthur, and Mitchell 1968; Mendoza 1968; Sturch 1972; Carney & Aaronson 1979), and Johnson-Cousins VI_C photometry (Reid 1993). We transform the VI_K and VI_J photometry to the VI_C system using the same relations that we used for the Pleiades. Finally, we adopt $E(B-V) = 0.003 \pm 0.002$ (Crawford 1975; Taylor 1980) and an average distance modulus of $(m-M)_0 = 3.33 \pm 0.01$ (Perryman et al. 1998).

8.2. Comparison of Period-Age Data with Models

In figure 25 we compare the $(B-V)_0$ vs. Period relation for M37 to each of the four clusters discussed above. In figure 26 we show the $(V-I_C)_0$ vs. Period relation.

The convergence of stellar rotation periods into a sequence for $(B-V)_0 < 1.3$ is clearly seen in M37 and the Hyades. A sequence may also be present in the Pleiades and M34 (this is more clearly seen in the less complete BV data for M34). The data for NGC 2516 is incomplete for stars hotter than $(B-V)_0 \sim 1.3$ as the I07 survey was focused on very low mass stars.

The formation of such a sequence can be explained by an angular momentum loss law that is a steep function of the angular frequency. Typically modelers adopt a modified Kawaler (1988) $N = 1.5$ wind law (Chaboyer, Demarque and Pinsonneault 1995), where N is a parameter used in modeling the geometry of the coronal magnetic field of the star and can vary between 0 and 2, with $N = 3/7$ for a dipolar field and $N = 2$ for a purely radial

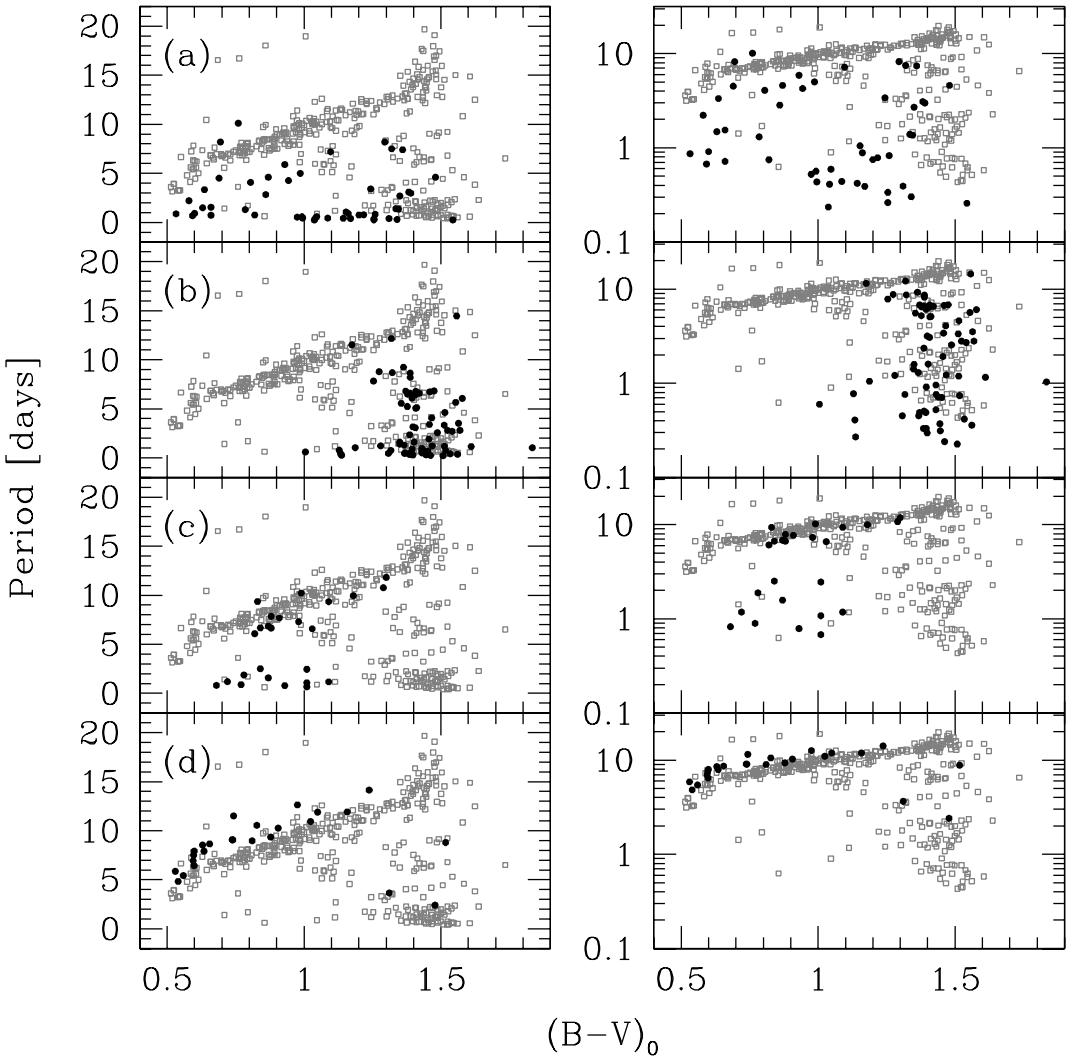

Fig. 25.— Comparison of the $(B-V)_0$-period relation between M37 (light open points) and (a) the Pleiades, (b) NGC 2516, (c) M34, and (d) the Hyades. Dark filled points are used for the other clusters. On the left the periods are plotted on a linear scale, on the right they are plotted on a log scale. Note the general evolutionary trend toward longer periods from the youngest cluster (the Pleiades) to the oldest cluster (the Hyades). Note that we use only the clean sample of stars for M37.

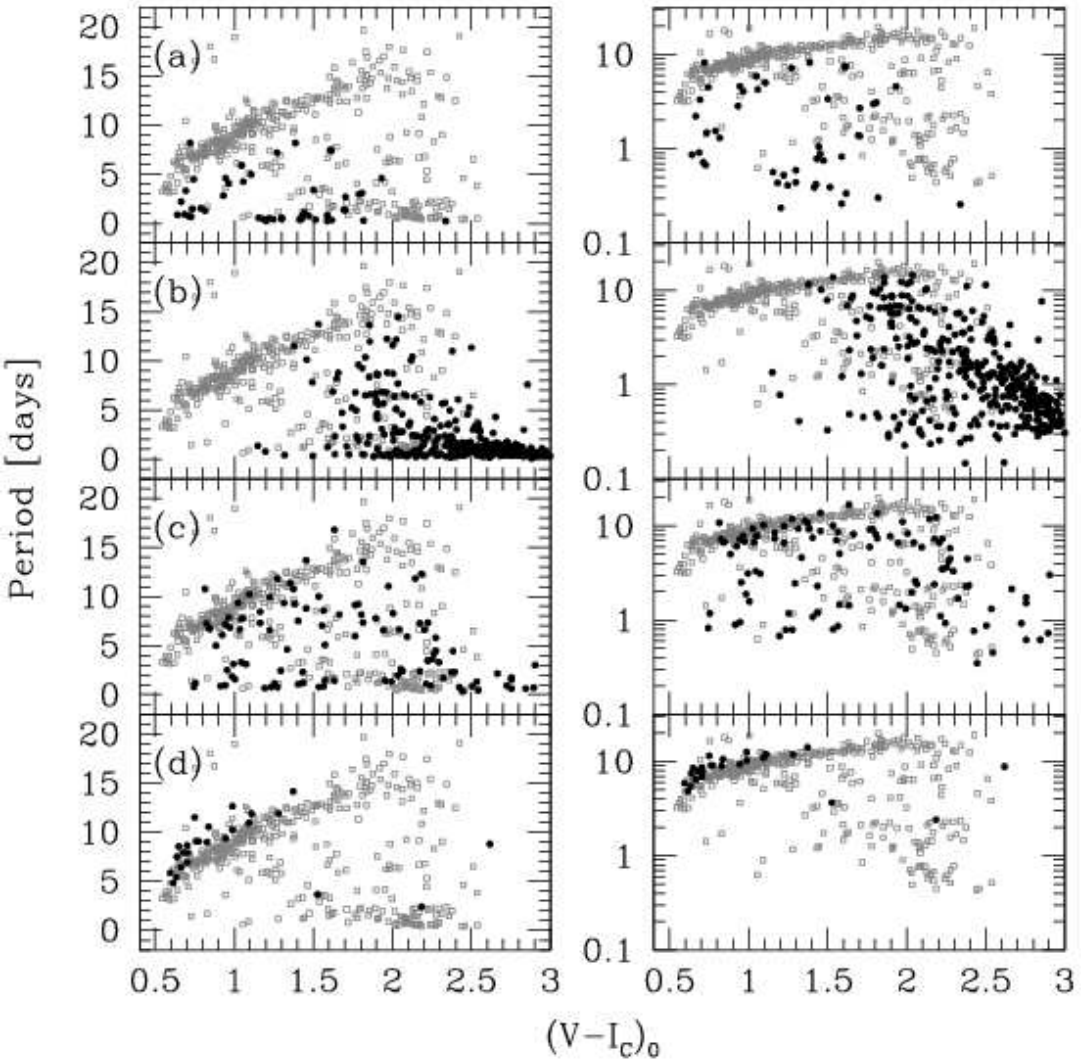

Fig. 26.— Same as figure 25, here we show the $(V - I_C)_0$-period relation.

field. The general law has the form:

$$\frac{dJ}{dt} = \begin{cases} f_k K_w \omega^{1+4N/3} \left(\frac{R}{R_\odot}\right)^{2-N} \left(\frac{M}{M_\odot}\right)^{-N/3} \left(\frac{\dot{M}}{10^{-14} M_\odot \mathrm{yr}^{-1}}\right)^{1-2N/3}, & \omega < \omega_{sat} \\ f_k K_w \omega \omega_{crit}^{4N/3} \left(\frac{R}{R_\odot}\right)^{2-N} \left(\frac{M}{M_\odot}\right)^{-N/3} \left(\frac{\dot{M}}{10^{-14} M_\odot \mathrm{yr}^{-1}}\right)^{1-2N/3}, & \omega \geq \omega_{sat} \end{cases} \tag{17}$$

Here ω_{sat} is a saturation angular frequency, which is needed to account for the presence of rapid rotators in the Pleiades. The leading constant $f_k K_w$ determines the overall angular momentum loss rate. Kawaler (1988) gives $f_k K_w = 2.035 \times 10^{33} (24.93 K_V^{-1/2})^n K_B^{4n/3}$, where K_V is the ratio of the wind speed to the escape velocity at a radius of r_A, the radius out to which the stellar wind co-rotates with the star, and K_B is a constant of proportionality between the surface magnetic field strength and the stellar rotation rate. Chaboyer, Demarque and Pinsonneault (1995) let $K_w = 2.036 \times 10^{33} (1.452 \times 10^9)^N$ in cgs units, for $K_V = 1.0$ and K_B set to the value obtained from calibration to the solar global magnetic field strength, and introduce f_k as a dimensionless parameter to account for our ignorance of K_V and K_B. For $N = 1.5$ this reduces to

$$\frac{dJ}{dt} = \begin{cases} -K\omega^3 \left(\frac{R}{R_\odot}\right)^{0.5} \left(\frac{M}{M_\odot}\right)^{-0.5}, & \omega < \omega_{sat} \\ -K\omega\omega_{sat}^2 \left(\frac{R}{R_\odot}\right)^{0.5} \left(\frac{M}{M_\odot}\right)^{-0.5}, & \omega \geq \omega_{sat} \end{cases} \tag{18}$$

where $f_k K_w$ is combined into a single calibration constant K. Bouvier (1997) determined a value of $K = 2.7 \times 10^{47}$ g cm^2 s by requiring that the law reproduce the rotation frequency of the Sun at 4.5 Gyr assuming $\omega_{sat} = 14\omega_\odot$ for a $1 M_\odot$ star.

For rigid body rotation, the angular frequency obeys the differential equation:

$$\frac{d\omega}{dt} = \frac{1}{I}\frac{dJ}{dt} - \frac{\omega}{I}\frac{dI}{dt} \tag{19}$$

where I is the moment of inertia of the star. Helioseismology suggests that the rigid body rotation approximation is reasonable for the Sun (Gough 1990), though it is uncertain whether this approximation is valid for younger stars. Previous investigations have found that the rigid body approximation reproduces the observed angular velocity distribution of stars older than the Pleiades, while models incorporating internal differential rotation are needed to reproduce the observations of younger clusters (e.g. Sills, Pinsonneault, & Terndrup 2000). In simple models where the core and envelope of the star are assumed to rotate as distinct rigid bodies, I and ω in equation 19 are replaced with I_{conv} and ω_{conv} because the magnetic wind is tied to the convective envelope. Additional terms are then required to allow for coupling between the core and the envelope (see I07).

In figures 27 and 28 we plot the rotation period as a function of age for stars in the clusters presented in figures 25 and 26. Following I07, we show the 10th, and 90th percentile

rotation periods for each cluster within color bins. We conduct 1000 bootstrap simulations for each cluster to estimate the $1-\sigma$ uncertainties on these percentiles. For clusters with less than 10 points in a bin, we take the minimum and maximum observed periods in the bin as estimates of the 10th and 90th percentiles. We do not show clusters with less than 4 points in a bin. We include the Sun in the bluest color bins. Note that while the period of the Sun ($P_\odot = 24.79$ days) is very well determined, we do expect stars at the age of the Sun to exhibit a range in rotation periods. Based on the models described above, we estimate this range to be ~ 1.0 day at 4.5 Gyr. We therefore adopt this as the uncertainty on the rotation period of a Sun-like star.

For each color bin we fit a model given eq. 19 to the 10th and 90th percentile periods letting $\omega_{0,10}$, $\omega_{0,90}$, K, and ω_{sat} be the free parameters. Here $\omega_{0,10}$ and $\omega_{0,90}$ are the ω_0 values at $t_0 = 100$ Myr for the 10th and 90th percentiles respectively. Note that in solving eq. 19 we use evolutionary tracks computed with the YREC isochrones (Terndrup et al. 2008, in preparation) to determine I and R as functions of M and t. As seen in figure 27, the model can reproduce the observed spin-down and convergence of rotation periods for stars with $0.5 < (B-V)_0 < 0.7$ or $1.1 < (B-V)_0 < 1.5$, however we find that for $0.7 < (B-V)_0 < 1.1$ ($0.76M_\odot < M < 0.99M_\odot$) the model fails to fit the Pleiades, M34, M37 and the Hyades simultaneously with greater than 95% confidence. In this color-range, the models predict a greater degree of convergence in the rotation periods at the age of M37 than is observed. The models also under-predict the periods of the slowest rotators in M34. When using $(V-I_C)_0$, the models for stars with $1.0 < (V-I_C)_0 < 2.5$ ($0.56M_\odot < M < 0.82M_\odot$) fit the M37 observations, but fail to fit the younger clusters. The difference between the $(V-I_C)_0$ and $(B-V)_0$ data is that the $(V-I_C)_0$ data is more complete for M34 and NGC 2516 than the $(B-V)_0$ data, but is less complete for the Hyades.

Table 7 gives the parameters for the models displayed in figures 27 and 28. To simplify the comparison with the data presented in this paper we list periods rather than angular frequencies so that P_{sat} corresponds to ω_{sat}, etc. A few points bear mentioning. The first is that the saturation period appears to increase with decreasing stellar mass, as found by other authors (e.g. I07). The second is that while there is no clear trend between K and stellar mass, we find that to reproduce M37, the Hyades and the Sun K must be a factor of ~ 1.2 larger than what was found by Bouvier (1997).

Throughout this subsection we have implicitely assumed that the samples of stars with rotation period measurements are unbiased in period. Given the relation between period and amplitude (figure 14), however, it is likely that the samples are biased towards short-period rotators (though as we saw in § 3.4 any bias in period is relatively minor for the M37 data). Since we cannot tell how this bias may differ from sample to sample, it is unclear what

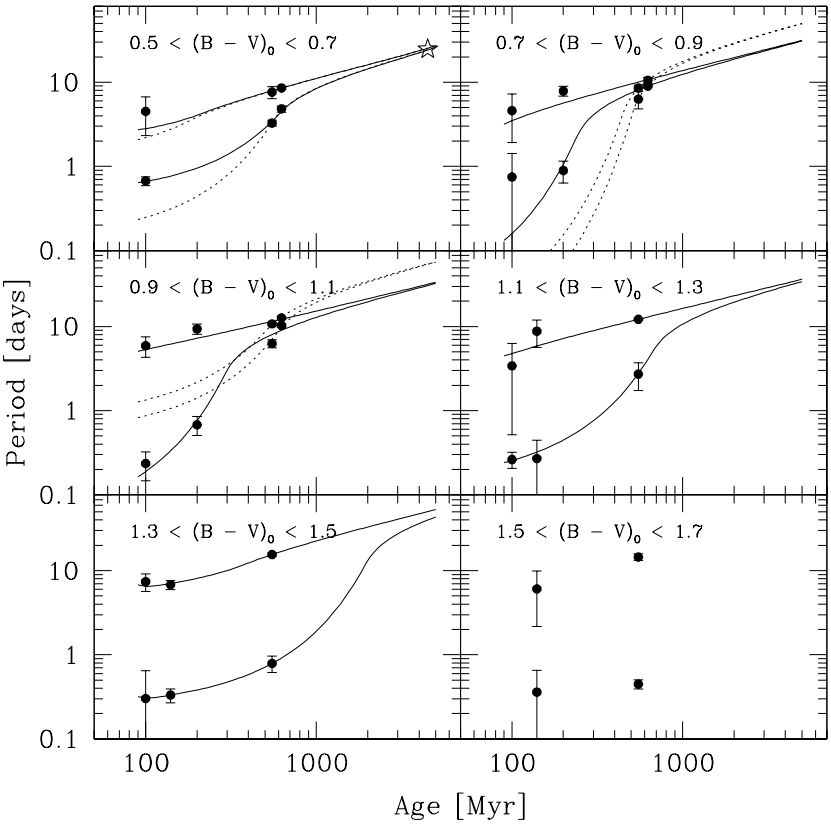

Fig. 27.— The rotation period is plotted as a function of age for stars in the clusters presented in figure 25. The period-age relation is shown for different $(B-V)_0$ color bins. We include the Sun, plotted as an open star, in the $0.5 < (B-V)_0 < 0.7$ bin, and assume that this is equal to the 10th and 90th percentile of 4.5 Gyr solar-mass stars with an uncertainty of ~ 1.0 days. The solid points show the 10th and 90th percentile rotation periods for stars in each cluster and color bin. We only show clusters that have at least four points in a given bin. The $1-\sigma$ error bars are estimated by conducting 1000 bootstrap simulations for each cluster. The solid lines show a model fit (equation 19) to the 10th and 90th percentile periods in each color bin for the Sun and the clusters that have at least 4 points. The dotted lines show a fit that is restricted to M37, the Hyades and the Sun (for the bluest color bin) only. While the model can reproduce the observed spin-down and convergence of rotation periods for stars with $0.5 < (B-V)_0 < 0.7$ or $1.1 < (B-V)_0 < 1.5$, there are noticeable discrepancies for stars with $0.7 < (B-V)_0 < 1.1$. We do not attempt to fit the model to color bins with fewer than 3 clusters.

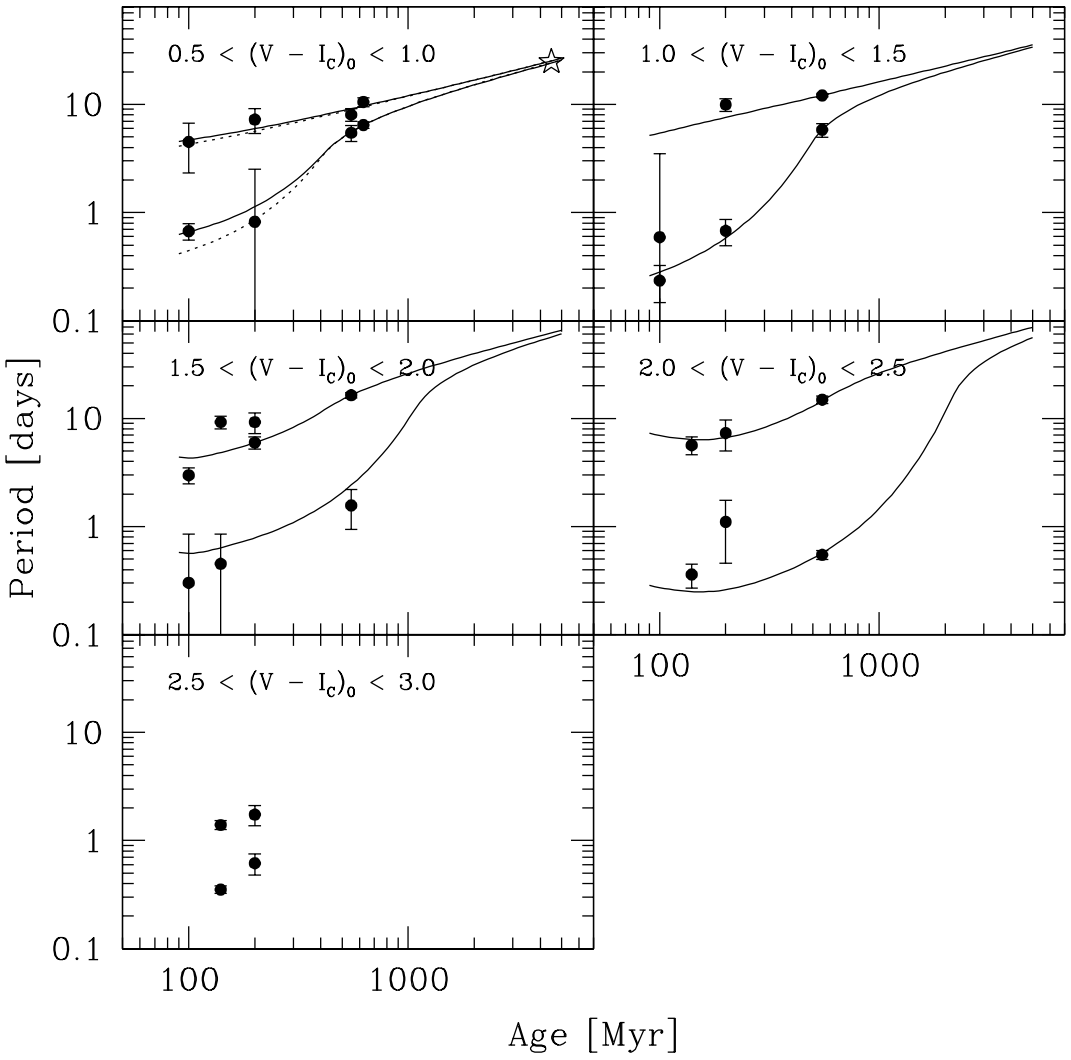

Fig. 28.— Same as figure 27, this time for $(V - I_C)_0$. In this case the model provides a good fit to the stars with $0.5 < (V - I_C)_0 < 1.0$ and a reasonable fit to the stars with $2.0 < (V - I_C)_0 < 2.5$, but fails to fit the stars with $1.0 < (V - I_C)_0 < 2.0$ with greater than 95% confidence. Note that for $1.5 < (V - I_C)_0 < 2.5$ the fastest rotators in M34 have periods that are signficantly longer than the fastest rotators in M37. This is particularly apparent in the $1.5 < (V - I_C)_0 < 2.0$ bin. The models cannot reproduce the lack of rapid rotators in M34 in these color bins. The models also under-predict the rotation periods of the slowest rotators in M34 with $1.0 < (V - I_C)_0 < 2.0$ and the slowest rotators in NGC 2516 with $1.5 < (V - I_C)_0 < 2.0$ and over-predict the rotation periods of the slowest rotators in the Pleiades with $1.0 < (V - I_C)_0 < 2.0$. We do not attempt to fit the model to color bins with fewer than 3 clusters.

affect this has on the above conclusions. Given the fairly sharp upper limit on the period as a function of mass for M37 and the Hyades, we do not expect the estimates of the 90th percentile period measurements for M37 and the Hyades to be substantially different from the actual values for $(B-V)_0 < 1.1$. We also note that we have not included uncertainties in the fundamental cluster parameters in this analysis. Including these uncertainties will reduce the signficance of the discrepancy between the models and the observed period distributions.

9. Discussion

We have measured rotation periods for 575 candidate members of the open cluster M37. This is the largest sample of rotation periods for a cluster older than 100 Myr and only the second cluster older than 500 Myr with a large sample of rotation periods (the other cluster being the Hyades with 25 stars that have measured periods). As mentioned in the introduction, this is the second set of rotation periods published for this cluster. Messina et al. (2008) have recently published periods for 122 cluster members. Using this data we have investigated the Rossby number-amplitude and period-color distributions.

We find that for stars with $(B-V)_0 < 1.36$ the amplitude and Rossby number are anti-correlated, and are related via equation 14. Extrapolating this relation to higher Rossby number values, we expect A_r to drop below 1 mmag at $R_O \sim 1.1$. For a Skumanich spin-down, we expect stars to reach this Rossby number at ~ 2 Gyr. We note that stellar activity will be a non-negligible effect to consider when conducting surveys for transiting planets with amplitudes of ~ 1 mmag (e.g. Neptune-sized planets orbiting sun-sized stars) that orbit stars younger than ~ 2 Gyr. However, since the rotation and transit time-scales typically differ by ~ 2 orders of magnitude, it should be possible to find these planets nonetheless. We also find that for stars with $R_O < 0.2$, $(B-V)_0 < 1.36$, the logarithmic distribution of A_r appears to be peaked above 0.03 mag which suggests that the distribution of spot filling-factors is peaked for these rapidly rotating stars.

We have also investigated the effect of rotation on the shape of the main sequence on CMDs. We find that at fixed V magnitude rapid rotators tend to lie blueward of slow rotators on a $B-V$ CMD and redward of slow rotators on a $V-I_C$ CMD. This effect, seen previously for early K-dwarfs in the Pleiades and NGC 2516, extends down to early M-dwarf stars ($M_V < 10.5$). We note that the relation between $V-I_C$ and rotation period is consistent with observations by Morales, Ribas and Jordi (2007) who found that at fixed luminosity more active M-dwarfs tend to have lower effective temperatures. Our observations quantitatively and qualitatively support the hypothesis that the well-known discrepancy between the observed and predicted radii and effective temperatures of M-dwarfs is due to

stellar activity/rotation and is not an age effect.

We have also investigated the rotation period-color distribution for this cluster. We find that, like the Hyades, the rotation periods of stars in M37 with $0.4 < (B-V)_0 < 1.0$ follow a tight sequence. At the blue end of this color range stars have rotation periods of ~ 3 days while at the red end stars have rotation period of ~ 10 days. Redward of $(B-V)_0 \sim 1.0$ the maximum rotation period as a function of color continues to follow this sequence, however there is also a broad tail of stars with shorter rotation periods.

We have identified a group of 4 stars with $(B-V)_0 < 1.2$ and $P > 15$ days that fall well above the main period-color sequence. The fact that at least one of these stars, V223, is a likely cluster member warrants discussion. If the measured period corresponds to the rotation period, this star would pose a significant challenge to the theory of stellar angular momentum evolution. While the periods of some of the stars may be shorter than the measured values, the light curve of V223 appears to be well-modeled by a sinusoid with a period of 18.0 ± 2.9 days (fig. 6), the star also has a spectroscopic temperature consistent with its photometric colors assuming that it is a cluster member and $v \sin i = 4.6 \pm 4.6$ km/s that is consistent with a rotation period of 18.0 days. Note that the r-band amplitude of the star, 0.024 mag, is an order of magnitude higher than the characteristic amplitude extrapolated to a Rossby number of 0.82.

Standard rotation evolution models predict a strong convergence of stellar surface rotation rates for a wide range of initial rotation rates (e.g. Sills, Pinsonneault, & Terndrup 2000). There is no plausible initial rotation rate that would yield a period of 18 days for V223, which is more than twice as long as the periods of similar stars on the main period-color sequence, at ~ 500 Myr. To explain such a long rotation period the surface of the star would have to spin-down very rapidly relative to the other stars in the cluster. This may indicate that the internal angular momentum transport varies from star to star as predicted by some theoretical models involving magnetic angular momentum transport (e.g. Charbonneau & MacGregor 1993). Alternatively the slow rotation of these stars might be explained by a threshold effect. For example, stars rotating faster than some threshold may have sufficient mixing to erase gravitational settling, while slower rotators cannot prevent a μ gradient from being established, and as a result experience core-envelope decoupling. The latter explanation would predict a bimodal distribution of rotation periods, while the former class of models might produce a continuous spectrum.

It is also possible that the variation is due to the evolution of permanently visible spots (e.g. on the pole of an inclined star), rather than the rotational modulation of spots. In that case the measured period corresponds to a spot evolution time-scale rather than to the rotation period.

Finally, we have combined our observations of M37 with previous observations of the Pleiades, NGC 2516, M34, the Hyades, and the Sun to perform a test of a simple theory of stellar angular momentum evolution which assumes rigid body rotation and an $N = 1.5$ wind-model including saturation for short periods. We find that the model provides a good fit to the data for stars with $0.5 < (B-V)_0 < 0.7$ ($0.99M_\odot < M < 1.21M_\odot$) or $1.1 < (B-V)_0 < 1.5$ ($0.53M_\odot < M < 0.76M_\odot$), but for stars with $0.7 < (B-V)_0 < 1.1$ ($0.76M_\odot < M < 0.99M_\odot$) the model fails to fit the Pleiades, M34, M37 and the Hyades simultaneously at the $2-4\sigma$ level. In this color-range, the best-fit models predict a greater degree of convergence in the rotation periods at the age of M37 than is observed. The models also under-predict the periods of the slowest rotators in M34. When using $(V-I_C)_0$, the models for stars with $1.0 < (V-I_C)_0 < 2.0$ ($0.56M_\odot < M < 0.82M_\odot$) fit the M37 observations, but fail to fit the younger clusters. Taking the parameters from the best fit models at face value, we find that the saturation period increases with decreasing stellar mass, which is consistent with the results from previous studies (see I07).

Comparing our results to the survey of M37 by Messina et al. (2008), we note that both groups have found that there does not appear to be significant spin-down between M34 and M37 for stars with $(B-V)_0 \lesssim 1.0$, while there is significant spin-down between M37 and the Hyades. While the rotation periods and photometry are independent for each group, both groups adopt the same fundamental parameters for the clusters. The results from the two surveys are thus not independent against errors in these parameters. Our survey goes more than 2 magnitudes deeper than Messina et al. (2008) (the faintest star with a measured period in the Messina et al. (2008) survey has $V \sim 20$, while the faintest star in our survey has $V \sim 22.8$), as a result we are able to study the rotation evolution for late K and early M dwarfs as well as late F, G and early K dwarfs (note the Messina et al. (2008) survey has measured periods for early F stars that are saturated in our survey). We find that for later spectral-type stars there is a noticeable spin-down between the slowest rotators in M34 and M37.

The survey presented in this paper compliments previous surveys of younger clusters. The recent results from the Monitor project, in particular, have provided a wealth of data for testing the rotation evolution of low-mass stars at ages between 5 and 200 Myr (Irwin et al. 2006, 2007, 2008a,b). Studying stellar evolution at these young ages yields insight into processes such as disk regularization, which may be important for stellar and planetary formation theory, and internal differential rotation. Other processes, such as non-saturated angular momentum wind-loss are more significant for the older cluster studied in this paper.

The discrepancies between this simple theory of stellar angular momentum evolution and the observed rotation periods of subsolar mass stars in clusters older than ~ 100 Myr

may suggest that one or more of the assumptions in the theory is wrong. In particular, it may be necessary to relax the assumption that these stars rotate as rigid bodies, or to revise the assumed wind model. A detailed test of more complicated models is beyond the scope of this paper. Additional observations of the rotation periods of stars in clusters with ages $\gtrsim 100$ Myr and a thorough treatment of all sources of observational errors are needed to map the period-age evolution in detail and understand the physical mechanisms behind angular momentum evolution.

We are grateful to C. Alcock for providing partial support for this project through his NSF grant (AST-0501681). Funding for M. Holman came from NASA Origins grant NNG06GH69G. We would like to thank G. Fürész and A. Szentgyorgyi for help in preparing the Hectochelle observations, S. Barnes, S. Saar, N. Brickhouse and S. Baliunas for helpful discussions, and the staff of the MMT, without whom this work would not have been possible. We are grateful to the anonymous referee for providing a thoughtful critique which improved the quality of this paper. We would also like to thank the MMT TAC for awarding us a significant amount of telescope time for this project. This research has made use of the WEBDA database, operated at the Institute for Astronomy of the University of Vienna; it has also made use of the SIMBAD database, operated at CDS, Strasbourg, France.

REFERENCES

Alard, C. & Lupton, R. H. 1998, ApJ, 503, 325

Alard, C. 2000, A&AS, 144, 363

Allain, S., Fernandez, M., Martín, E. L, & Bouvier, J. 1996, A&A, 314, 173

An, D., Terndrup, D. M., Pinsonneault, M. H., Paulson, D. B., Hanson, R. B., & Stauffer, J. R. 2007, ApJ, 655, 233 (A07)

Andruk, V., Kharchenko, N., Schilbach, E., & Scholz, R.-D. 1995, AN, 316, 225

Argue, A. N. 1966, MNRAS, 133, 475

Barnes, J. R., Collier Cameron, A., Unruh, Y. C., Donati, J. F., & Hussain, G. A. J. 1998, MNRAS, 299, 904

Barnes, S. A. 1998, Ph.D. thesis, Yale University

Barnes, S. A., Sofia, S., Prosser, C. F., Stauffer, J. R. 1999, ApJ, 516, 263

Barnes, S. A. 2003, ApJ, 586, 464

Barnes, S. A. 2007, ApJ, in press, arXiv:0704.3068v2 [astro-ph]

Bessell, M. S., & Weis, E. W. 1987, PASP, 99, 642

Bouvier, J. 1997, MmSAI, 68, 881

Bouvier, J., Forestini, M., & Allain, S. 1997, A&A, 326, 1023

Brown, B. P., Browning, M. K., Brun, A. S., & Toomre, J. 2004, in Proceedings of the SOHO 14 / GONG 2004 Workshop (ESA SP-559). "Helio- and Asteroseismology: Towards a Golden Future". Editor: D. Danesy., p. 341

Canterna, R., Crawford, D. L., & Perry, C. L. 1979, PASP, 91, 263

Carney, B. W., & Aaronson, M. 1979, AJ, 84, 867

Chaboyer, B., Demarque, P., & Pinsonneault, M. H. 1995, ApJ, 441, 865

Charbonneau, P., & MacGregor, K. B. 1993, ApJ, 417, 762

Cieza, L., & Baliber, N. 2006, ApJ, 649, 862

Clarke, D., MacDonald, E. C., & Owens, S. 2004, A&A, 415, 677

Crawford, D. L. 1975, AJ, 80, 955

Devor, J. 2005, ApJ, 628, 411

Dorren, J. D. 1987, ApJ, 320, 756

Efron, B., & Petrosian, V. 1992, ApJ, 399, 345

Efron, B., & Petrosian, V. 1999, JSTOR, 94, 447, p. 824-834

Eggen, O. J. 1968, ApJS, 16, 49

Eggen, O. J. 1974, PASP, 86, 697

Girardi, L., Grebel, E. K., Odenkirchen, M., & Chiosi, C. 2004, A&A, 422, 205

Gough, D. O. 1990, in: Angular Momentum Evolution of Young Stars, eds. S. Catalano, J. R. Stauffer, 271

Gray, D. F. 1992, PASP, 104, 1035

Hartman, J. D., et al. 2008a, ApJ, 675, 1233.

Hartman, J. D., et al. 2008b, ApJ, 675, 1254.

Herbig, G. H., Vrba, F. J., & Rydgren, A. E. 1986, AJ, 91, 575

Herbst, W., Bailer-Jones, C. A. L., Mundt, R., Meisenheimer, K., & Wackermann, R. 2002, A&A, 396, 513

Howard, R., Gilman, P. A., & Gilman, P. I. 1984, ApJ, 283, 373

Iriarte, B. 1967, BOTT, 4, 79

Irairte, B. 1969, BOTT, 5, 89

Iriarte, B. 1974, BITon, 1, 73

Irwin, J., Aigrain, S., Hodgkin, S., Irwin, M., Bouvier, J., Clarke, C., Hebb, L., & Moraux, E. 2006, MNRAS, 370, 954

Irwin, J., Hodgkin, S., Aigrain, S., Hebb, L., Bouvier, J., Clarke, C., Moraux, E., & Bramich, D. M. 2007, MNRAS, 377, 741 (I07)

Irwin, J., Hodgkin, S., Aigrain, S., Bouvier, J., Hebb, L., & Moraux, E. 2008a, MNRAS, 383, 1588

Irwin, J., Hodgkin, S., Aigrain, S., Bouvier, J., Hebb, L., Irwin, M., & Moraux, E. 2008b, MNRAS, 384, 675

Jeffries, R. D., Thurston, M. R., & Hambly, N. C. 2001, A&A, 375, 863 (J01)

Johnson, H. L., & Morgan, W. W. 1953, ApJ, 117, 313

Johnson, H. L., & Knuckles, C. F. 1955, ApJ, 122, 209

Johnson, H. L., & Mitchell, R. I. 1958, ApJ, 128, 31

Johnson, H. L., MacArthur, J. W., & Mitchell, R. I. 1968, ApJ, 152, 465

Jones, B. F. 1973, A&AS, 9, 313

Jones, B. F., & Prosser, C. F. 1996, AJ, 111, 1193

Kalirai, J. S., Ventura, P., Richer, H. B., Fahlman, G. G., Durrell, P. R., D'Antona, F., & Marconi, G. 2001, AJ, 122, 3239

Kawaler, S. D. 1988, ApJ, 333, 236

Kiss, L. L., Szabó, Gy. M., Sziládi, K., Furész, G., Sárneczky, K., & Csák, B. 2001, A&A, 376, 561

Kitchatinov, L. L. 2005, Physics - Uspekhi 48 (5), 449

Königl, A. 1991, ApJ, 370, L39

Kovács, G., Zucker, S., & Mazeh, T. 2002, A&A, 391, 369

Kovács, G., Bakos, G., & Noyes, R. W. 2005, MNRAS, 356, 557

Krishnamurthi, A., et al. 1997, ApJ, 480, 303

Krishnamurthi, A., et al. 1998, ApJ, 493, 914

Kurtz, M. J., & Mink, D. J. 1998, PASP, 110, 934

Kurucz, R. L. 1993, ASPC, 44, 87

Lamm, M. H., Mundt, R., Bailer-Jones, C. A. L., & Herbst, W. 2005, A&A, 430, 1005

Landolt, A. U. 1979, ApJ, 231, 468

Lomb, N. R. 1976, Ap&SS, 39, 447

López-Morales, M., & Ribas, I. 2005, ApJ, 631, 1120L

López-Morales, M. 2007, ApJ, 660, 732L

Magnitskii, A. K. 1987, Soviet Astron. Lett., 13, 451

Marilli, E., Catalano, S., & Frasca, A. 1997, MmSAI, 68, 895

Martín, E. L., & Zapatero Osorio, M. R. 1997, MNRAS, 286, L17

McLeod, B. A., Conroy, M., Gauron, T. M., Geary, J. C., & Ordway, M. P. 2000, in Proc. International Conference on Scientific Optical Imaging, Further Developments in Scientific Optical Imaging, ed. M. Bonner Denton (Cambridge: Royal Soc. Chemistry), 11

Mendoza, E. E. 1967, BOTT, 4, 149

Mendoza, E. E. 1968, PDAUC, 1, 106

Mermilliod, J.-C., Huestamendia, G., del Rio, G., & Mayor, M. 1996, A&A, 307, 80

Messina, S., Rodonò, M., & Guinan, E. F. 2001, A&A, 366, 215

Messina, S. 2001, A&A, 371, 1024

Messina, S., Distefano, E., Parihar, P., Kang, Y. B., Kim, S.-L., Rey, S.-C., & Lee, C.-U. 2008, A&A, in press (arXiv:0803.1134)

Meynet, G., Mermilliod, J.-C., & Maeder, A. 1993, A&AS, 98, 477

Morales, J. C., Ribas, I., & Jordi, C. 2007, A&A, in press (arXiv:0711.3523v1)

Nelder, J. A., & Mead, R. 1965, Computer Journal, 7, 308

Nilakshi, & Sagar, R. 2002, A&A, 381, 65

Noyes, R. W., Hartmann, L., Baliunas, S. L., Duncan, D. K., & Vaughn, A. H. 1984, ApJ, 279, 763

O'Dell, M. A., & Collier Cameron, A. 1993, MNRAS, 262, 521

O'Dell, M. A., Hendry, M. A., & Collier Cameron, A. 1994, MNRAS, 268, 181

O'Dell, M. A., Hilditch, R. W., Collier Cameron, A., & Bell, S. A. 1997, MNRAS, 284, 874

Patten, B. M., & Simon, T. 1996, ApJS, 106, 489

Perryman, M. A. C., et al. 1998, A&A, 331, 81

Pinsonneault, M. H. 1997, ARA&A, 35, 557

Pinsonneault, M. H., Terndrup, D. M., Hanson, R. B., & Stauffer, J. R. 2004, ApJ, 600, 946

Press, W. H., & Rybicki, G. G. 1989, ApJ, 338, 277

Press, W. H., Teukolsky, S. A., Vetterling, W. T., & Flannery, B. P. 1992, Numerical Recipes in C, second edition (Cambridge University Press, New York, NY) 575

Prosser, C. F. 1991, PhD Thesis, University of California, Santa Cruz

Prosser, C. F., Stauffer, J. R., & Kraft, R. P. 1991, AJ, 101, 1361

Prosser, C. F., Schild, R. E., Stauffer, J. R., & Jones, B. F. 1993a, PASP, 105, 269

Prosser, C. F., et al. 1993, PASP, 105, 1407

Prosser, C. F., et al. 1995, PASP, 107, 211

Prosser, C. F., & Randich, S. 1998, AN, 319, 201

Prosser, C. F., Randich, S., & Simon, T. 1998, AN, 319, 215

Radick, R. R., Thompson, D. T., Lockwood, G. W., Duncan, D. K., & Baggett, W. E. 1987, ApJ, 321, 459

Radick, R. R., Skiff, B. A., & Lockwood, G. W. 1990, ApJ, 353, 524

Radick, R. R., Lockwood, G. W., Skiff, B. A., & Thompson, D. T. 1995, ApJ, 452, 332

Reid, N. 1993, MNRAS, 265, 785

Ribas, I. 2003, A&A, 398, 239

Ribas, I. 2006, Ap&SS, 304, 89

Robinson, E. L., & Kraft, R. P. 1974, AJ, 79, 698

Scargle, J. D. 1982, ApJ, 263, 835

Scholz, A., & Eislöffel, J. 2004, A&A, 421, 259

Scholz, A., & Eislöffel, J. 2007, MNRAS, in publication (arXiv:0708.2274)

Schuler, S. C., King, J. R., Fischer, D. A., Soderblom, D. R., & Jones, B. F. 2003, AJ, 125, 2085

Schwarzenberg-Czerny, A. 1989, MNRAS, 241, 153

Schwarzenberg-Czerny, A. 1996, ApJ, 460, 107L

Shu, F., Najita, J., Ostriker, E., Wilkin, F., Ruden, S., & Lizano, S. 1994, ApJ, 429, 781

Shu, F. H., Najita, J. R., Shang, H., & Li, Z.-Y. 2000, in Protostars and Planets IV, ed. V. Mannings et al. (Tucson: Univ. of Arizona), 789

Sills, A., Pinsonneault, M. H., & Terndrup, D. M. 2000, ApJ, 534, 335

Skrutskie, M. F., et al. 2006, AJ, 131, 1163

Skumanich, A. 1972, ApJ, 171, 565

Soderblom, D. R., Stauffer, J. R., MacGregor, K. B., & Jones, B. F. 1993, ApJ, 409, 624

Stassun, K. G., & Terndrup, D. 2003, PASP, 115, 505

Stauffer, J. R. 1980, AJ, 85, 1341

Stauffer, J. R. 1982(a), AJ, 87, 899

Stauffer, J. R. 1982(b), AJ, 87, 1507

Stauffer, J. R. 1984, ApJ, 280, 189

Stauffer, J. R., Hartmann, L. W., Burnham, J. N., & Jones, B. F. 1985, ApJ, 289, 247

Stauffer, J. R., Schild, R. A., Baliunas, S. L., & Africano, J. L. 1987, PASP, 99, 471

Stauffer, J. R., & Hartmann, L. W. 1987, ApJ, 318, 337

Stauffer, J. R., Hartmann, L. W., & Jones, B. F. 1989, ApJ, 346, 160

Stauffer, J. R., Schild, R., Barrado y Navascues, D., Backman, D. E., Angelova, A. M., Kirkpatrik, J. D., Hambly, N., & Vanzi, L. 1998, ApJ, 504, 805

Stauffer, J. R., Jones, B. F., Backman, D., Hartmann, L. W., Barrado y Navascués, D., Pinsonneault, M. H., Terndrup, D. M., & Muench, A. A. 2003, AJ, 126, 833 (S03)

Sturch, C. 1972, PASP, 84, 666

Sung, H., Bessell, M. S., Lee, B.-W., & Lee, S.-G. 2002, AJ, 123, 290

Szentgyorgyi, A. H., Cheimets, P., Eng, R., Fabricant, D. G., Geary, J. C., Hartmann, L., Pieri, M. R., & Roll, J. B. 1998, in Proc. SPIE 3355, Optical Astronomical Instrumentation, ed. S. D'Odorico, 242-252

Taylor, B. J. 1980, AJ, 85, 242

Taylor, P. O. 1989, JAVSO, 18, 65

Terndrup, D. M., Krishnamurthi, A., Pinsonneault, M. H., & Stauffer, J. R., 1999, AJ, 118, 1814

Terndrup, D. M., Pinsonneault, M. H., Jeffries, R. D., Ford, A., Stauffer, J. R., & Sills, A. 2002, ApJ, 576, 950

Torres, G., & Ribas, I. 2002, ApJ, 567, 1140

Torres, G., Lacy, C., H., Marschall, L. A., Sheets, H. A., & Mader, J. A. 2006, ApJ, 640, 1018

Torres, G. 2007, ApJ, 671L, 65

Tsai, W. 1990, Biometrika, 77, 169

Upgren, A. R., & Weis, E. W. 1977, AJ, 82, 978

Upgren, A. R, Weis, E. W., & Hanson, R. B. 1985, AJ, 90, 2039

van Altena, W. F. 1969, AJ, 74, 2

van Hamme, W., & Wilson, R. E. 2003, ASPC, 298, 323

Van Leeuwen, F., & Alphenaar, P. 1982, ESO Messenger, 28, 15

Van Leeuwen, F., Alphenaar, P., & Meys, J. J. M. 1987, A&AS, 67, 483

Walker, G. A. H., et al. 2007, ApJ, 659, 1611

Webber, E. D., & Davis, L. 1967, ApJ, 148, 217

Weis, E. W., & Upgren, A. R. 1982, PASP, 94, 475

Weis, E. W., & Hanson, R. B. 1988, AJ, 96, 148

Wilson, R. E., & Devinney, E. J. 1971, ApJ, 166, 605

This preprint was prepared with the AAS LaTeX macros v5.2.

Table 1. Candidate Cluster Members with Measured Rotation Periods: Coordinates and Periods

ID	RA (J2000)	DEC (J2000)	Chip	Period[a] (days)	σ_P (days)	$P_{N=1}$[b] (days)	$\sigma_{P_{N=1}}$ (days)	$P_{N=2}$[b] (days)	$\sigma_{P_{N=2}}$ (days)	$P_{N=3}$[b] (days)	$\sigma_{P_{N=3}}$ (days)	Clean[c]
25	05:51:17.45	+32:40:08.7	29	7.96596671	0.02481300	7.93346085	0.01864600	15.94418247	0.04626800	15.78239472	1.78339100	0
26	05:51:18.34	+32:40:31.9	29	8.21743495	0.01027100	8.38240366	0.01186800	8.35987638	0.02384200	8.35987638	0.02914300	1
43	05:51:20.55	+32:32:01.6	32	6.32258130	0.01705700	6.38618354	0.01925000	12.74358869	0.04080600	12.90215678	0.02950900	0
47	05:51:21.37	+32:35:39.1	31	1.69921452	0.00069700	1.70573845	0.00064600	1.70107340	0.00045400	1.70107340	0.00045400	1
57	05:51:22.06	+32:31:02.6	33	7.62148720	0.03865000	7.73616016	0.02092800	7.77483129	0.02163400	7.75544752	0.01871000	1
58	05:51:22.14	+32:29:42.4	33	15.58862440	0.25834300	17.36856505	1.97524300	16.71526061	3.35777700	16.19318063	2.72763000	1
61	05:51:22.34	+32:37:54.3	30	8.45071991	0.01507800	4.17488928	0.00342200	8.34977855	0.00851300	12.47444192	0.02091000	0
71	05:51:24.23	+32:38:01.3	30	8.73549565	0.02335200	8.66251740	0.02124000	8.47374013	0.01470200	8.71103332	0.04233500	1
73	05:51:24.55	+32:28:31.7	34	8.45038568	0.09496900	8.13125735	0.02317700	16.15149769	0.05990400	16.15149769	0.05770400	0
78	05:51:24.82	+32:29:37.3	33	1.25855603	0.00075200	1.25883615	0.00031000	1.25985582	0.00034000	1.25985582	0.00039700	1
81	05:51:25.06	+32:39:28.8	30	11.60712687	0.03841500	11.64623736	0.04880800	11.22594731	0.07203800	11.18558073	0.03799100	1
84	05:51:25.28	+32:39:31.9	30	8.41870095	0.01294100	8.56708896	0.01238000	8.56708896	0.01596700	17.18149682	0.10037800	0
86	05:51:25.42	+32:37:59.9	30	9.08103926	0.04919900	8.96199942	0.01478500	8.96199942	0.01407500	8.96199942	0.01453300	1
91	05:51:25.72	+32:31:06.3	33	0.71158870	0.00048600	0.71067830	0.00028000	1.42229893	0.00045300	1.42229893	0.00047600	0
94	05:51:25.86	+32:23:49.6	35	3.25558346	0.00669400	3.25014105	0.00753300	3.23661430	0.00609200	3.21653397	0.01078100	1
98	05:51:26.09	+32:34:06.9	32	3.52788205	0.00155800	3.53048462	0.00121900	3.53048462	0.00195300	3.52648226	0.00101500	1
99	05:51:26.14	+32:44:22.2	28	6.05726804	0.01754600	5.96950681	0.00731700	5.94668323	0.00763800	5.95807317	0.00779300	1
103	05:51:26.34	+32:25:04.1	35	7.22580720	0.00653700	7.35218624	0.01453900	7.24938243	0.01132000	7.21575041	0.00874000	1
104	05:51:26.79	+32:40:24.7	29	10.03454839	0.02957100	9.80987070	0.03066200	19.80082750	0.08107000	19.92767457	0.18444700	0
105	05:51:26.83	+32:37:41.1	30	7.44901820	0.01415900	3.67218746	0.00467700	7.45794773	0.00801900	7.45794773	0.00914900	0
106	05:51:26.91	+32:35:33.9	31	9.90195829	0.01885900	9.90353453	0.01656900	9.87210482	0.01608600	9.80984008	0.01578800	1
115	05:51:28.20	+32:24:26.0	35	11.76071834	0.05457200	11.60279746	0.06066000	11.55968042	0.06551700	11.47440059	0.24772400	1
122	05:51:28.63	+32:31:53.6	32	9.97022436	0.02819600	10.16239791	0.04186300	2.11742563	0.00112000	2.11598531	0.00135900	0
123	05:51:28.76	+32:27:35.0	34	7.39896076	0.01717600	7.22491002	0.02547200	14.49593719	0.05393800	7.32699762	0.02047300	0
124	05:51:28.82	+32:24:07.0	35	0.85131637	0.00027800	0.84989754	0.00018600	0.85106016	0.00018600	0.85106016	0.00018300	1
127	05:51:28.92	+32:37:47.5	30	6.88972315	0.00993000	6.89583241	0.01267700	13.81923590	0.02822200	13.69753413	2.68678300	0
133	05:51:29.32	+32:25:35.8	35	12.12752437	0.05572300	11.91386442	0.07324000	12.29043856	0.05691900	12.33919080	0.81425900	1
139	05:51:30.08	+32:33:11.8	32	9.52306750	0.02707900	9.62770040	0.02997800	9.56847124	0.04163100	19.80082750	0.06876500	0
140	05:51:30.09	+32:25:21.4	35	3.58997115	0.00322600	3.57101366	0.00315300	3.61248403	0.00282900	3.61248403	0.00357400	1
142	05:51:30.13	+32:32:02.6	32	0.62538148	0.00005800	0.62550723	0.00007000	0.62525577	0.00005400	0.62538148	0.00005800	1
143	05:51:30.20	+32:24:57.4	35	12.22282908	0.35579400	11.22594731	0.03606000	11.30756089	0.03949200	11.18558073	0.04745100	1
144	05:51:30.26	+32:44:23.3	28	2.26233455	0.00257200	2.25397435	0.00211800	2.27374461	0.00329700	2.26217002	0.00581700	1
145	05:51:30.35	+32:40:34.6	29	9.25806548	0.05784100	9.22785524	0.04161400	9.22785524	0.03982400	9.22785524	0.04814600	1
151	05:51:30.75	+32:40:08.3	29	7.55760447	0.00621400	7.56679640	0.04801500	15.24110730	0.10383800	7.62242098	0.02833200	0

Table 1—Continued

ID	RA (J2000)	DEC (J2000)	Chip	Period[a] (days)	σ_P (days)	$P_{N=1}$[b] (days)	$\sigma_{P_{N=1}}$ (days)	$P_{N=2}$[b] (days)	$\sigma_{P_{N=2}}$ (days)	$P_{N=3}$[b] (days)	$\sigma_{P_{N=3}}$ (days)	Clean[c]
153	05:51:30.82	+32:40:20.8	29	12.38833134	0.15882700	12.38833134	0.03830800	12.43786485	0.04950800	12.29043856	0.04384300	1
157	05:51:31.24	+32:30:59.5	33	9.08103926	0.36258200	8.68670762	0.02189400	17.08242724	0.03896500	17.56470920	1.93205600	0
160	05:51:31.66	+32:21:54.3	36	6.56135434	0.02968400	6.58287244	0.01372300	13.26029493	0.02826900	19.89044240	3.31998500	0
161	05:51:31.81	+32:27:09.8	34	7.06302611	0.03030600	6.93503109	0.03663600	6.81353174	0.02628300	7.27559573	0.05093700	1
163	05:51:31.87	+32:42:33.8	29	8.47604905	0.01643000	8.42782444	0.01770400	16.53753323	1.45872300	16.62592197	0.17353200	0
164	05:51:31.91	+32:37:57.3	30	7.11670098	0.01530300	7.11670098	0.10039200	7.16588344	0.01073500	7.11670098	0.00997400	1
165	05:51:31.95	+32:33:30.3	32	1.39275129	0.00039000	1.39113188	0.00050100	1.39237724	0.00044400	1.39175428	0.00044000	1
169	05:51:32.18	+32:20:35.8	36	12.95388042	0.05647200	13.14821874	0.05287100	13.14821874	0.04456900	13.14821874	0.04256000	1
171	05:51:32.23	+32:32:24.7	32	7.81585427	0.02037000	7.83356837	0.04065300	16.02632664	0.06285400	16.27791732	0.10407500	0
174	05:51:32.61	+32:35:08.4	31	10.56085398	0.31818300	10.75994237	0.28105000	10.26294898	0.02647000	10.40019960	0.02584800	0
182	05:51:33.29	+32:38:09.4	30	11.25030741	0.02575800	11.30756089	0.03730400	11.34881430	0.04035100	11.14550340	0.02563500	1
183	05:51:33.32	+32:36:28.0	31	12.59396802	0.07667400	12.58882036	0.09986400	12.95583983	0.06345600	12.95583983	0.06447600	1
187	05:51:33.68	+32:37:53.0	30	16.45007932	0.35694500	0.97879551	0.00029800	17.36856505	4.71821000	17.27212660	0.19604500	0
192	05:51:34.12	+32:38:26.4	30	7.38885986	0.01383800	7.36960436	0.01574700	14.80585435	0.03742700	14.73571767	0.03364400	0
194	05:51:34.27	+32:43:34.2	28	12.46527750	0.38295400	12.19408075	0.07317000	12.29043856	0.09058100	12.29043856	0.08360800	1
198	05:51:34.48	+32:31:55.9	32	10.67138937	0.03896500	10.47024571	0.03117700	10.33115244	0.03336300	10.33115244	0.02943800	1
208	05:51:35.46	+32:36:19.9	31	12.27104576	0.05402400	12.29039040	0.06087200	12.53807965	0.07022000	12.58882036	0.07621500	1
209	05:51:35.46	+32:30:00.2	33	13.73381898	0.14852400	13.75811588	0.12092800	14.00589824	2.26891600	19.19006786	1.83856900	0
211	05:51:35.59	+32:32:10.3	32	6.38749487	0.01011200	6.37309977	0.01068700	12.69159527	0.03152300	12.69159527	0.65241900	0
214	05:51:35.85	+32:33:38.3	32	9.73618153	0.06612100	9.59799445	0.01844100	9.59799445	0.02041400	9.59799445	0.01950600	1
216	05:51:36.06	+32:38:53.7	30	1.38253778	0.00169100	1.37941111	0.00277500	1.37575074	0.00159200	4.13603244	0.00623700	0
218	05:51:36.57	+32:35:59.3	31	7.79331656	0.12709000	7.64112616	0.01655600	7.79429292	0.01276000	15.02025630	0.04773200	0
220	05:51:36.68	+32:20:55.1	36	0.65662980	0.00012300	0.65643584	0.00010000	0.65657437	0.00007400	0.65643584	0.00009800	1
223	05:51:36.99	+32:22:04.6	36	18.25537171	0.24547100	18.02272490	0.05907300	18.02272490	2.91424600	18.02272490	3.49727000	1
229	05:51:37.89	+32:20:42.1	36	6.31728528	0.01921900	6.31561821	0.11318900	12.51362667	0.03722400	12.61510360	0.02832600	0
232	05:51:38.07	+32:40:26.2	29	1.78632709	0.00038300	1.79695569	0.00116800	1.78663489	0.00031400	1.78560932	0.00036100	1
233	05:51:38.22	+32:38:51.2	30	12.69159527	0.28711800	13.69753413	0.06639900	12.74358869	0.07315700	12.58887090	0.06316800	1
234	05:51:38.30	+32:32:05.2	32	6.39405961	0.02943200	6.25771475	0.04547100	12.74358869	0.03947800	18.39568303	0.08038300	0
237	05:51:38.41	+32:33:40.5	32	14.88377990	0.13006000	14.00589824	0.08778400	14.94814993	0.19412700	15.02032834	1.22340400	1
240	05:51:38.72	+32:23:40.5	35	16.24391645	0.22923800	15.16679668	0.25085200	16.36354550	6.82287900	16.45007932	6.13551000	1
241	05:51:38.84	+32:30:30.2	33	6.03318464	0.01915100	6.00407257	0.00779900	12.03136724	0.02236100	17.86737507	0.04626400	0
248	05:51:39.35	+32:36:38.4	31	8.76256366	0.04844600	9.17340291	0.06080100	9.50993760	0.03466600	9.48095282	0.01821800	1
249	05:51:39.41	+32:40:18.5	29	4.57457353	0.00890400	4.57390090	0.01038600	4.54715685	0.01018300	13.88090138	0.04732700	0
251	05:51:39.76	+32:27:35.4	34	7.96738284	0.01992400	8.19551405	0.03691400	7.72735017	0.02343300	8.00572009	0.03872800	1

Table 1—Continued

ID	RA (J2000)	DEC (J2000)	Chip	Period[a] (days)	σ_P (days)	$P_{N=1}$[b] (days)	$\sigma_{P_{N=1}}$ (days)	$P_{N=2}$[b] (days)	$\sigma_{P_{N=2}}$ (days)	$P_{N=3}$[b] (days)	$\sigma_{P_{N=3}}$ (days)	Clean[c]
253	05:51:39.97	+32:24:08.3	35	9.53766672	0.16117400	9.11964233	0.04977100	9.50996637	0.01563600	9.50996637	0.01536800	1
257	05:51:40.37	+32:35:20.0	31	5.65583655	0.00714800	5.64453721	0.00798900	5.67543227	0.00965900	16.98903938	0.05079700	0
258	05:51:40.64	+32:40:23.3	29	4.52466909	0.00834500	4.52072373	0.01158500	4.50109970	0.00873100	4.43689916	0.02674900	0
261	05:51:40.87	+32:30:19.0	33	8.28307815	0.03827400	8.33746985	0.01126000	8.40505269	0.01085600	16.53753323	4.07381100	0
262	05:51:40.95	+32:40:19.7	29	7.46869148	0.01674300	7.44011002	0.00697000	7.40468936	0.00994100	14.94814993	0.02082000	0
269	05:51:41.51	+32:30:43.4	33	7.27566366	0.00781400	7.33485027	0.00591100	7.33485027	0.00841300	7.28332943	0.00768300	1
286	05:51:43.45	+32:21:59.7	36	0.51694990	0.00011500	0.51711058	0.00015300	0.51650965	0.00009800	0.51650965	0.00015500	1
287	05:51:43.68	+32:30:58.2	33	11.45116878	0.17991700	11.55968042	0.03914500	11.47440059	0.07647700	11.43223080	0.05118900	1
288	05:51:43.76	+32:43:39.1	28	2.71416979	0.00102200	2.70708380	0.00108800	2.71180368	0.00155000	2.71180368	0.00136900	1
290	05:51:44.46	+32:30:14.0	33	6.83672527	0.01571900	6.86539395	0.50090700	12.74358869	0.04850400	12.69159527	1.33522800	0
292	05:51:44.62	+32:33:49.7	32	6.18431412	0.00712800	3.08877966	0.00228800	3.14817326	0.00453900	3.14817326	0.00246400	1
294	05:51:44.67	+32:20:38.2	36	13.12049509	0.09591800	12.98361224	0.03913200	12.82307629	0.04574700	12.82307629	0.04700600	1
295	05:51:44.93	+32:39:37.2	30	9.97022436	0.04219400	10.12930641	0.05999800	10.64946936	0.04744500	10.75997925	0.05609800	1
298	05:51:45.27	+32:34:04.5	32	8.51083447	0.02622000	8.45071991	0.03053000	16.90143983	0.08754600	17.17675317	0.11577600	0
299	05:51:45.30	+32:43:51.8	28	10.87660839	0.04410400	10.83493556	0.05850900	11.86840900	0.04757000	18.39568303	1.58935600	0
300	05:51:45.37	+32:30:14.0	33	6.49307724	0.01064800	5.13367226	0.00954400	6.47138373	0.01191100	13.07679112	0.33795200	0
303	05:51:45.87	+32:21:48.2	36	9.53848489	0.02160300	9.58402797	0.01299400	19.10919141	0.05330100	19.13092910	0.05767900	0
305	05:51:45.96	+32:30:38.1	33	16.28368586	0.06601500	16.04510937	0.08419700	15.96275919	4.32109000	15.96275919	7.24161100	1
307	05:51:49.41	+32:35:58.3	22	6.28539962	0.02354800	6.26703607	0.00862600	6.25443394	0.00961300	6.17987284	0.01021800	1
311	05:51:49.77	+32:37:42.4	21	6.27232829	0.00496000	6.25216124	0.00643400	6.25216124	0.00603300	6.25216124	0.00381700	1
314	05:51:50.07	+32:35:11.5	22	3.90744975	0.00728600	3.91581267	0.00616700	3.91581267	0.00498100	3.91581267	0.02995100	1
315	05:51:50.22	+32:27:28.4	25	17.67448920	0.10977400	18.18054892	0.14755800	16.89675830	0.12600700	17.17665888	4.58114500	1
318	05:51:50.45	+32:35:03.0	22	13.82368889	0.06861000	13.92892969	0.06812900	13.92892969	0.05267500	13.92892969	0.04499700	1
319	05:51:50.47	+32:23:43.4	26	5.94782027	0.01126200	5.93533677	0.01381500	5.71716596	0.00936300	12.05234405	0.03035800	0
320	05:51:50.52	+32:28:31.1	25	6.26527714	0.04403400	6.07440739	0.02552900	6.20775073	0.02227900	6.19538718	0.02092000	1
321	05:51:50.54	+32:25:12.9	26	2.11901226	0.00732200	2.11454694	0.00590900	2.11311052	0.00214200	2.11311052	0.00251300	1
322	05:51:50.56	+32:27:32.1	25	10.63490632	0.06855700	10.16236504	0.07126800	10.91090561	0.03467700	10.91090561	1.18596500	1
324	05:51:50.74	+32:39:13.0	21	10.12846865	0.11687200	10.04832542	0.04678500	19.86377450	0.11283200	10.17983509	0.05650500	0
326	05:51:50.92	+32:39:43.2	21	1.57040905	0.00085800	1.56767911	0.00059700	1.56846942	0.00053500	1.56846942	0.00057300	1
327	05:51:50.95	+32:23:55.9	26	6.16409393	0.02585600	6.08630405	0.01351000	6.01568362	0.01464900	6.08630405	0.01056300	1
328	05:51:51.13	+32:38:22.6	21	8.18753421	0.40840600	6.87374456	0.01725400	6.99742033	0.00996400	7.15841750	0.00961500	1
332	05:51:51.47	+32:29:09.8	24	1.19146907	0.00029900	1.19019248	0.00028300	1.19201702	0.00029200	1.19156036	0.00026800	1
334	05:51:51.59	+32:26:38.9	25	8.69639755	0.02700100	8.68668365	0.02033500	8.71100921	0.01148500	8.71100921	0.00994000	1
335	05:51:51.62	+32:43:38.3	19	9.67561431	0.01746200	9.74838609	0.02536600	9.59799445	0.01641300	9.65759081	0.01760400	1

Table 1—Continued

ID	RA (J2000)	DEC (J2000)	Chip	Period[a] (days)	σ_P (days)	$P_{N=1}$[b] (days)	$\sigma_{P_{N=1}}$ (days)	$P_{N=2}$[b] (days)	$\sigma_{P_{N=2}}$ (days)	$P_{N=3}$[b] (days)	$\sigma_{P_{N=3}}$ (days)	Clean[c]
340	05:51:52.03	+32:35:47.5	22	1.24662525	0.00045000	1.24597604	0.00054700	1.24497859	0.00055200	1.24497859	0.00055700	1
345	05:51:52.45	+32:27:29.0	25	12.31964396	0.05267400	12.43781552	0.05657400	12.58882036	0.04838800	12.58882036	0.04927100	1
348	05:51:52.74	+32:33:12.2	23	10.25492860	0.34731100	10.82603298	0.04337600	10.25492860	0.02341900	10.39198031	0.05019000	1
350	05:51:52.80	+32:44:35.0	19	11.49985213	0.04765500	11.69000376	0.04545000	11.39036983	0.03358800	11.26660630	0.04045300	1
357	05:51:53.43	+32:35:27.5	22	14.88196172	0.65828700	14.58195030	0.27847200	15.07673291	0.29006700	15.29921299	0.07030300	1
359	05:51:53.54	+32:25:18.8	26	7.33658019	0.14107200	7.23252732	0.02096100	14.66624234	0.05245400	14.80585435	0.05525800	0
361	05:51:53.62	+32:43:36.2	19	0.88636843	0.00026800	7.85334511	0.02250500	15.94418247	0.05548100	15.78239472	0.10984200	0
362	05:51:53.65	+32:27:00.6	25	8.79598842	0.18556500	8.93622857	0.02379300	17.36846863	0.04481100	17.46598896	0.03597600	0
363	05:51:53.73	+32:35:23.5	22	5.62650145	0.04398900	5.61127548	0.00671800	11.22255097	0.01862300	11.21648035	0.01833600	0
364	05:51:53.79	+32:25:23.3	26	7.11670098	0.01894100	7.45794773	0.02204400	14.84471487	0.04282500	7.16588344	0.09387300	0
366	05:51:53.84	+32:29:54.1	24	12.39175299	0.07868500	12.52650020	0.11042600	12.62821762	0.22856900	12.42640831	0.49118500	1
368	05:51:53.90	+32:32:10.0	23	0.73048436	0.00018400	0.73041575	0.00014500	0.73041575	0.00014100	2.19073278	0.00060400	0
369	05:51:53.93	+32:26:15.2	25	5.07871037	0.01149300	5.08202094	0.01705000	10.26294898	0.03516700	10.19567324	0.03472200	0
370	05:51:54.06	+32:34:55.1	22	1.07922623	0.00056800	1.07986321	0.00038800	1.08023825	0.00058300	1.07986321	0.00053300	1
373	05:51:54.52	+32:34:51.6	22	5.96419942	0.07474600	6.13114528	0.16533600	6.29239328	0.01190800	11.59273202	0.08124900	0
374	05:51:54.53	+32:43:42.1	19	9.73465811	0.03144100	9.74838609	0.01699700	9.77903175	0.01440900	9.74838609	0.01868800	1
377	05:51:54.74	+32:35:41.1	22	9.05481805	0.03415300	9.06009321	0.03248000	9.13996474	0.05797100	9.06009321	0.05900500	1
378	05:51:54.77	+32:27:53.5	25	9.60837096	0.01572800	4.82953776	0.01060000	9.65756114	0.02292800	9.65756114	0.02141300	0
380	05:51:54.89	+32:43:33.7	19	4.64979073	0.00439900	4.65605448	0.00499500	9.31071535	0.01411500	9.25531092	0.01313600	0
381	05:51:54.92	+32:22:31.2	27	7.86029059	0.20081500	8.66251740	0.02571700	7.99462863	0.17537100	8.01522803	0.05244300	1
387	05:51:55.16	+32:31:06.6	24	8.49816940	0.01614100	8.51445387	0.02197400	8.44509910	0.02034500	8.30972482	0.02852500	1
388	05:51:55.26	+32:32:02.0	23	0.77933603	0.00027700	0.78064637	0.00027000	0.77888697	0.00032900	0.77986343	0.00041700	1
389	05:51:55.36	+32:33:06.8	23	7.46149128	0.01049800	7.45344512	0.00956600	7.41789335	0.00835200	7.41789335	0.00772300	1
394	05:51:55.67	+32:27:02.4	25	10.38634424	0.03675000	10.43508777	0.03403800	10.40019960	0.02305700	10.29692090	0.02597700	1
396	05:51:55.85	+32:29:00.6	24	7.34001180	0.01389800	3.68391567	0.00632700	7.24511996	0.01220600	7.24511996	0.01544200	0
399	05:51:56.13	+32:25:08.3	26	5.73349922	0.01048300	5.69622780	0.00959000	11.39036983	0.02673100	11.39245559	0.56994000	0
402	05:51:56.41	+32:35:14.6	22	5.54623752	0.00608000	5.52162258	0.00500600	5.57107290	0.00507200	5.56111210	0.00558900	1
404	05:51:56.47	+32:45:18.6	19	5.89484556	0.00701300	5.94668323	0.00605500	5.96950681	0.00554700	5.96950681	0.00615800	1
406	05:51:56.52	+32:42:28.2	20	1.68191944	0.00122300	1.68410481	0.00106100	1.68410481	0.00093000	1.68410481	0.00092400	1
409	05:51:56.78	+32:37:50.3	21	8.77029740	0.01343600	4.37817570	0.00668800	8.67541198	0.01976000	8.67541198	0.01816300	0
410	05:51:56.81	+32:34:55.6	22	7.79726749	0.00883900	7.69312392	0.01123100	7.80901331	0.01120300	7.78945655	0.01432000	1
413	05:51:57.02	+32:32:08.9	23	11.26931196	0.04699300	11.13612232	0.04831100	10.39198031	0.02428200	10.35737510	0.02226800	0
414	05:51:57.06	+32:27:17.1	25	8.83097260	0.01824200	9.25528368	0.02485100	8.80968930	0.03243500	9.22782816	0.01891100	1
415	05:51:57.14	+32:37:02.2	22	8.26116866	0.01718100	8.49120939	0.02432800	8.30972482	0.02399600	8.30972482	0.03646500	1

Table 1—Continued

ID	RA (J2000)	DEC (J2000)	Chip	Period[a] (days)	σ_P (days)	$P_{N=1}$[b] (days)	$\sigma_{P_{N=1}}$ (days)	$P_{N=2}$[b] (days)	$\sigma_{P_{N=2}}$ (days)	$P_{N=3}$[b] (days)	$\sigma_{P_{N=3}}$ (days)	Clean[c]
416	05:51:57.20	+32:28:38.4	25	1.84979529	0.00050800	1.84820168	0.00053200	3.69640336	0.00211900	1.84820168	0.00058700	0
417	05:51:57.24	+32:32:53.8	23	7.43296133	0.03654700	7.65523614	0.01528200	7.47134910	0.01427600	7.47134910	0.01522000	1
418	05:51:57.24	+32:30:28.5	24	1.07326777	0.00069900	1.07130851	0.00050100	14.18299134	0.06889800	14.31352968	0.06835300	0
420	05:51:57.37	+32:32:25.3	23	3.37400524	0.00343400	3.37968784	0.00163800	3.36870652	0.00181400	9.92760987	0.01648500	0
421	05:51:57.38	+32:37:57.3	21	17.61457850	7.42720000	17.41735991	1.05939700	17.41735991	2.48436800	17.32039748	2.71430000	1
422	05:51:57.43	+32:30:45.0	24	7.23248459	0.01203300	7.16170850	0.00986900	7.16170850	0.00790200	7.26203596	0.01286500	1
424	05:51:57.71	+32:39:46.0	21	6.30448430	0.01535200	6.31561821	0.01393900	6.31561821	0.01289400	6.35431448	0.01047700	1
426	05:51:57.77	+32:40:14.5	20	4.91035517	0.00596400	4.92123082	0.00691500	9.84090478	0.01359300	9.84090478	0.01864200	0
428	05:51:57.82	+32:28:14.0	25	6.52140482	0.01274400	6.49280653	0.01301000	6.63121609	0.01268700	6.61711015	0.01350800	1
430	05:51:57.89	+32:27:30.3	25	4.84118786	0.01024800	4.79973044	0.00495500	4.80714772	0.00626600	4.81458797	0.00438800	1
432	05:51:57.99	+32:39:42.4	21	3.67544359	0.00764200	3.72771528	0.00763900	7.34429337	0.01832200	7.27559573	0.02126600	0
434	05:51:58.00	+32:26:46.4	25	8.93494518	0.01310700	9.06645594	0.01267300	8.98786799	0.01384700	8.96197389	0.01342200	1
438	05:51:58.21	+32:31:16.6	24	7.73713930	0.02338100	7.52559884	0.01808700	8.09349467	0.02772700	15.29921299	0.06164600	0
442	05:51:58.37	+32:29:54.1	24	7.96499360	0.02436200	8.05159203	0.02302300	17.74289789	0.74763600	19.04672382	0.05412000	0
448	05:51:58.64	+32:21:55.4	27	7.73808458	0.01902900	7.65996060	0.02352000	7.56679640	0.01807100	7.58524750	0.01864000	1
450	05:51:58.71	+32:33:25.0	23	7.42674946	0.07116800	7.34779767	0.01529700	7.34779767	0.00882300	7.34779767	0.00722600	1
453	05:51:58.85	+32:38:23.3	21	17.07796136	4.41638200	19.13092910	0.42773800	1.04312737	0.00105900	1.04417763	0.00127500	0
454	05:51:58.95	+32:37:23.6	21	8.75179466	0.03068400	8.79807426	0.02949100	17.61457850	0.08547900	8.97574647	0.01475900	0
463	05:51:59.38	+32:40:48.4	20	5.73402765	0.14851900	5.73825862	0.01573500	11.43223080	0.03829700	11.22594731	0.06909400	0
464	05:51:59.64	+32:33:13.0	23	6.32824028	0.01541600	6.35668045	0.01482700	12.67964705	0.02964200	12.67964705	0.02612200	0
467	05:51:59.69	+32:43:39.1	19	1.95151192	0.00240500	1.94772400	0.00319500	1.95138950	0.00127300	1.95384084	0.00138000	1
468	05:51:59.70	+32:31:24.6	24	0.44587431	0.00007100	0.44597020	0.00003500	0.44597020	0.00004000	0.44597020	0.00003900	1
469	05:51:59.74	+32:30:58.4	24	6.36059305	0.01242000	6.36971124	0.01252600	6.39590788	0.00974600	6.42232088	0.00779800	1
470	05:51:59.84	+32:35:53.4	22	3.20157488	0.00286000	3.19237401	0.00394100	6.40908716	0.01008000	3.17932127	0.00336100	0
471	05:51:59.93	+32:30:32.0	24	4.15819519	0.00523300	4.15098092	0.00437600	8.30972482	0.01176600	12.27923411	0.02655800	0
472	05:52:00.00	+32:28:03.0	25	15.36524937	0.60793300	15.39185902	0.18424400	15.39185902	7.19200000	14.94807858	0.42308800	1
476	05:52:00.58	+32:30:51.0	24	2.26205818	0.00296500	2.26321036	0.00252500	2.27313455	0.00178700	2.27147448	0.00181500	1
478	05:52:00.66	+32:38:56.0	21	8.86197733	0.05228500	8.82302413	0.03111500	9.05410762	0.05827300	9.05410762	0.03334000	1
480	05:52:00.99	+32:33:06.3	23	9.40953166	0.02534800	9.33189549	0.01861200	9.33189549	0.01696000	9.33189549	0.07954900	1
481	05:52:01.00	+32:25:20.1	26	3.27408694	0.00100600	3.29140832	0.00294700	3.28099357	0.00414300	3.27408694	0.00390800	1
482	05:52:01.02	+32:33:15.7	23	1.45751176	0.00088600	1.45730621	0.00101500	1.45730621	0.00129700	4.37191863	0.00562500	0
483	05:52:01.29	+32:32:08.8	23	2.34919192	0.00321300	2.34865797	0.00257300	4.66805558	0.00428400	4.61952396	0.00613500	0
486	05:52:01.47	+32:35:21.8	22	7.77582500	0.00823200	3.86232460	0.00461100	13.33189027	0.03469000	13.21857204	0.02198200	0
487	05:52:01.58	+32:22:47.9	27	10.36557814	0.06228900	11.18558073	0.06146600	10.26298251	0.02131500	10.26298251	0.02096900	1

Table 1—Continued

ID	RA (J2000)	DEC (J2000)	Chip	Period[a] (days)	σ_P (days)	$P_{N=1}$[b] (days)	$\sigma_{P_{N=1}}$ (days)	$P_{N=2}$[b] (days)	$\sigma_{P_{N=2}}$ (days)	$P_{N=3}$[b] (days)	$\sigma_{P_{N=3}}$ (days)	Clean[c]
489	05:52:01.82	+32:25:42.0	26	1.56948032	0.00065800	1.56781916	0.00073100	1.57019333	0.00061500	1.56940114	0.00060300	1
491	05:52:02.14	+32:23:49.5	26	9.68030129	0.10312000	10.10324844	0.02480500	9.97365316	0.01749200	9.97365316	0.01764700	1
493	05:52:02.21	+32:24:52.2	26	7.37135071	0.02077300	7.36960436	0.03096800	7.47587118	0.02039900	14.87666188	0.10330800	0
494	05:52:02.21	+32:28:57.3	24	6.52060797	0.01956300	6.55772718	0.01854800	13.05216114	0.04846600	13.05216114	0.05128900	0
495	05:52:02.21	+32:32:23.0	23	9.77696810	0.03218900	9.94898164	0.01573800	9.73108278	0.01907500	9.70073110	0.01676400	1
499	05:52:02.55	+32:34:55.5	22	10.99056537	0.07601900	11.38064398	0.11471300	10.35740926	0.04578100	10.60460280	0.04364000	1
500	05:52:02.77	+32:38:19.9	21	6.24124975	0.01138100	6.30282398	0.01326200	12.71823979	0.02897100	12.71823979	0.02682800	0
501	05:52:02.86	+32:42:41.5	20	15.65530951	0.50127900	15.09320718	0.09646800	14.80585435	2.60801900	15.39193469	4.52708200	1
502	05:52:03.02	+32:37:40.6	21	10.63207122	0.02390000	10.45345899	0.02082400	10.41845427	0.02247500	10.48869973	0.03415100	1
503	05:52:03.02	+32:35:18.5	22	4.14434377	0.00539500	4.12346546	0.00470000	4.12346546	0.00758500	4.09631239	0.00721900	1
505	05:52:03.04	+32:22:51.8	27	8.90045780	0.03354300	9.09298451	0.03036700	9.06648208	0.03369300	9.04013368	0.02738100	1
506	05:52:03.28	+32:42:34.8	20	0.43234329	0.00008000	0.43233729	0.00008000	0.43227721	0.00007900	0.43221714	0.00008900	1
517	05:52:04.05	+32:32:49.0	23	9.13459648	0.00908100	9.19397253	0.01605300	9.16687572	0.01305800	9.16687572	0.01276100	1
519	05:52:04.12	+32:35:41.2	22	6.12269685	0.02102000	6.10706853	0.02096900	6.22938113	0.01782000	6.24188240	0.03758100	1
521	05:52:04.33	+32:34:53.7	22	5.97565802	0.01772600	5.93234789	0.01711300	5.89859662	0.02120300	17.74289789	0.08662300	0
522	05:52:04.37	+32:39:17.5	21	7.26082380	0.01745000	7.24172660	0.01574600	14.36210590	1.97356800	14.23072314	0.07723200	0
524	05:52:04.55	+32:42:40.1	20	18.28753674	3.26427800	18.95618525	0.38671800	19.07240956	0.41503300	18.95618525	9.95341900	1
527	05:52:05.04	+32:23:03.1	27	4.21184563	0.00970800	4.17240972	0.01261200	8.40116681	0.02582300	12.61947420	0.04079100	0
528	05:52:05.08	+32:24:53.2	26	12.24688976	0.06813900	12.09922209	0.10945000	12.14646622	0.06886600	12.19408075	0.06478400	1
529	05:52:05.23	+32:31:24.9	24	14.68868949	0.13777500	14.37970411	0.07109500	14.58195030	0.05816900	14.58195030	0.07188500	1
531	05:52:05.33	+32:35:50.7	22	0.77690271	0.00035700	0.77694152	0.00034300	0.77752419	0.00038700	2.33105748	0.00116400	0
539	05:52:05.55	+32:32:49.0	23	5.43051012	0.08159600	5.24241506	0.01603800	5.31406934	0.01771800	5.33229002	0.01682300	1
546	05:52:05.67	+32:27:07.0	25	6.76681169	0.02366100	6.88056452	0.01291000	6.82022206	0.00882100	6.82022206	0.00962800	1
548	05:52:05.74	+32:32:08.8	23	1.78754603	0.00116600	1.78313840	0.00148600	1.78313840	0.00114100	1.78313840	0.00107200	1
550	05:52:06.04	+32:32:12.3	23	7.51467162	0.02129900	7.52558087	0.01211900	7.50741635	0.00494600	7.52558087	0.00818100	1
552	05:52:06.10	+32:38:56.8	21	8.18365774	0.01266800	7.92416015	0.02271300	7.82451777	0.02014300	7.86407249	0.01634900	1
553	05:52:06.24	+32:33:19.9	23	4.85962672	0.00609200	4.87019657	0.00604800	9.76162499	0.01455000	9.76162499	0.01374300	0
555	05:52:06.40	+32:32:43.9	23	1.16960438	0.00052000	1.17180761	0.00043900	1.17180761	0.00039800	1.17180761	0.00047200	1
556	05:52:06.45	+32:36:28.0	22	6.90144067	0.03717600	6.86784885	0.01137000	7.02323356	0.01150300	7.00737940	0.01256900	1
558	05:52:06.71	+32:39:13.6	21	7.49376897	0.02835300	7.27559573	0.01564600	7.19151007	0.01538400	7.27559573	0.01783000	1
561	05:52:06.89	+32:26:29.2	25	2.72153115	0.00238100	2.72367339	0.00222400	5.43734428	0.00499500	8.18390401	0.01043900	0
563	05:52:06.92	+32:28:18.6	25	2.73709644	0.00647800	2.72367339	0.00403400	5.42833502	0.00756300	5.40898051	0.00679000	0
564	05:52:07.04	+32:37:39.5	21	8.16604462	0.02331300	8.32712309	0.02584600	2.24862355	0.00138600	7.24172660	0.20283400	0
565	05:52:07.11	+32:41:05.6	20	7.78455956	0.10369500	7.75544752	0.01314200	7.81389098	0.01917800	7.44011002	0.18862000	1

Table 1—Continued

ID	RA (J2000)	DEC (J2000)	Chip	Period[a] (days)	σ_P (days)	$P_{N=1}$[b] (days)	$\sigma_{P_{N=1}}$ (days)	$P_{N=2}$[b] (days)	$\sigma_{P_{N=2}}$ (days)	$P_{N=3}$[b] (days)	$\sigma_{P_{N=3}}$ (days)	Clean[c]
567	05:52:07.21	+32:21:20.9	27	1.97945275	0.00335700	1.97117420	0.00281300	2.00032795	0.00845500	2.00548643	0.00829600	1
571	05:52:07.50	+32:27:59.7	25	4.99712466	0.01013000	5.04084437	0.00739100	10.06373354	0.01945700	14.80578436	0.03694600	0
572	05:52:07.52	+32:33:17.1	23	9.90550987	0.03394800	9.92760987	0.04360000	10.05599756	0.03017900	10.08861502	0.03458800	1
573	05:52:07.55	+32:45:17.9	19	8.39258060	0.03067200	8.33746985	0.01483700	8.33746985	0.01524400	8.31518311	0.01350100	1
576	05:52:07.70	+32:30:03.4	24	14.23491991	0.20670600	13.92892969	0.17726800	13.56445704	0.09416800	13.50555797	0.21202000	1
579	05:52:07.90	+32:33:23.8	23	5.89411447	0.00764900	5.83222252	0.00560300	5.82130690	0.00531300	5.72487461	0.00516300	1
580	05:52:07.97	+32:25:38.3	26	8.01729381	0.03456500	8.14108872	0.04503400	16.19318063	0.08748700	16.19318063	0.17895200	0
582	05:52:08.04	+32:30:00.7	24	9.00761656	0.09433100	9.19399941	0.02868500	8.80365129	0.02314100	9.03377868	0.02507400	1
586	05:52:08.10	+32:32:46.3	23	4.90175114	0.01225900	5.60782440	0.29021900	4.93981379	0.01875000	4.80994153	0.00695600	0
587	05:52:08.18	+32:32:16.1	23	3.66723334	0.02530900	3.64422095	0.00334900	3.62720323	0.00367500	3.62297361	0.00311200	1
589	05:52:08.35	+32:41:19.3	20	7.78455956	0.00949200	7.64114468	0.01042700	7.75544752	0.01165600	7.67886941	0.01084000	1
592	05:52:08.62	+32:37:49.2	21	8.18753421	0.01507600	8.34946998	0.02025600	17.03588129	0.04906600	16.94310842	9.21598000	0
594	05:52:08.76	+32:26:57.0	25	9.73158257	0.19262500	9.48095282	0.02654900	10.29692090	0.03467700	10.29692090	0.03399700	1
596	05:52:08.84	+32:37:03.6	22	7.27392423	0.03752100	7.16170850	0.00949000	7.16170850	0.01036200	7.24511996	0.00886400	1
598	05:52:08.88	+32:33:20.6	23	5.62523638	0.00625000	2.81406724	0.00318600	5.60564453	0.00887900	5.48688737	0.00626700	0
600	05:52:08.90	+32:26:40.4	25	7.14284753	0.00902900	7.10044054	0.00896700	7.13300382	0.01114500	7.24936577	0.01101700	1
602	05:52:09.12	+32:30:24.1	24	5.13255776	0.01234800	9.92764124	0.04264000	10.02362230	0.02137400	9.92764124	0.03554500	1
603	05:52:09.22	+32:24:11.8	26	18.97873768	6.66973400	19.80082750	0.11826400	18.95618525	0.06755500	18.72793498	0.08961600	1
604	05:52:09.30	+32:38:58.5	21	3.26470409	0.00652600	3.22534340	0.00515100	3.22869047	0.00379900	3.22869047	0.00356800	1
606	05:52:09.34	+32:44:43.7	19	7.20822616	0.01753800	7.19905115	0.01362900	14.46169224	0.02775700	14.46169224	0.02270300	0
607	05:52:09.44	+32:24:22.0	26	7.17580161	0.02005000	7.21575041	0.02340100	14.39477094	0.04988900	14.32846614	0.08768300	0
608	05:52:09.44	+32:33:25.1	23	7.26665762	0.22988800	6.95334134	0.01786800	6.96907356	0.02021500	7.03272083	0.02829400	1
611	05:52:09.74	+32:28:40.5	25	8.76256366	0.01816700	8.93622857	0.01678100	17.86727302	0.05301000	17.76523321	0.04742700	0
612	05:52:09.76	+32:35:06.6	22	10.31618574	0.04943200	10.05602974	0.03393900	19.04672382	0.08397400	19.04672382	0.06561400	0
614	05:52:09.84	+32:30:38.6	24	6.61069075	0.01717800	6.51650953	0.01345600	6.65595977	0.02271700	3.53727965	0.00298100	0
619	05:52:10.65	+32:33:47.3	23	12.69522490	0.09104000	12.73154879	0.09948900	12.78387717	0.10433000	12.78387717	0.06168300	1
620	05:52:10.66	+32:33:28.0	23	10.38507546	0.09526300	10.02359032	0.05580700	9.62053968	0.02427900	9.77166299	0.02427900	1
622	05:52:10.88	+32:29:52.0	24	4.91363349	0.01936500	8.07248897	0.26712300	9.80248976	0.02947400	9.62056913	0.02507400	0
623	05:52:10.98	+32:24:00.1	26	1.18548399	0.00095500	1.19500211	0.00261500	11.95966936	0.10107200	2.38167828	0.00137400	0
625	05:52:11.19	+32:31:25.4	24	16.67737265	0.18104900	15.29921299	0.18168700	0.24929907	0.00002400	0.33236058	0.00002400	0
626	05:52:11.20	+32:28:25.1	25	6.12344508	0.01220000	6.11020230	0.01121700	12.24202227	0.02902500	18.36303340	0.05700900	0
627	05:52:11.20	+32:44:16.6	19	16.80556456	0.52715700	15.54577711	0.09718400	15.46847340	4.36466200	15.46847340	0.10741400	1
629	05:52:11.43	+32:36:54.1	22	12.42144569	0.16581600	12.78392931	0.03993700	12.78392931	0.03406500	12.73160049	0.07258200	1
633	05:52:11.68	+32:32:36.0	23	11.45609613	0.07879800	11.81283056	0.10427700	12.18299223	0.07127200	19.04660780	0.26745000	0

Table 1—Continued

ID	RA (J2000)	DEC (J2000)	Chip	Period[a] (days)	σ_P (days)	$P_{N=1}$[b] (days)	$\sigma_{P_{N=1}}$ (days)	$P_{N=2}$[b] (days)	$\sigma_{P_{N=2}}$ (days)	$P_{N=3}$[b] (days)	$\sigma_{P_{N=3}}$ (days)	Clean[c]
634	05:52:11.73	+32:34:49.4	22	4.19181941	0.00301600	4.17886605	0.00293500	4.17886605	0.00245800	4.17886605	0.00197300	1
635	05:52:11.79	+32:30:47.7	24	7.92440764	0.00852700	7.71219936	0.00961800	7.76999750	0.01209600	7.78945655	0.01085500	1
638	05:52:11.87	+32:24:51.7	26	11.43643382	0.06559900	11.06620420	0.07743200	11.10571225	0.10890500	10.75997925	0.08980100	1
639	05:52:11.88	+32:27:44.5	25	3.77284427	0.00944400	3.84464993	0.01982000	7.49386318	0.01453800	7.51195988	0.01585300	0
643	05:52:12.12	+32:37:57.6	21	5.59952306	0.08085600	5.33088258	0.00820300	5.58946338	0.00835400	5.54958350	0.01156200	1
645	05:52:12.16	+32:33:13.4	23	6.38932562	0.02913800	6.47579351	0.01364100	6.43559624	0.00793700	6.54391659	0.00857200	1
646	05:52:12.26	+32:41:36.7	20	14.74270142	0.06234500	14.52923867	0.05194000	14.39477094	0.05067200	14.39477094	0.05338600	1
647	05:52:12.29	+32:31:01.6	24	14.20242009	0.15905200	14.18299134	0.13062700	13.74427751	0.08494000	13.86683014	0.09732000	1
650	05:52:12.43	+32:34:55.1	22	8.62184338	0.03347600	8.30972482	0.01684800	8.44509910	0.01827000	8.42223125	0.02093600	1
651	05:52:12.53	+32:33:18.1	23	2.32983528	0.03561500	2.31543794	0.03200400	2.38650174	0.01890700	5.23359392	0.00731600	0
654	05:52:12.72	+32:27:53.3	25	12.19886314	0.08301300	12.09917542	0.07962700	12.58882036	0.06399700	12.58882036	2.31319400	1
658	05:52:13.05	+32:39:13.0	21	15.78680231	0.15839000	15.74286799	0.11343900	15.35440458	0.10754400	15.35440458	7.28032300	1
661	05:52:13.32	+32:40:46.3	20	16.86021680	2.78861400	16.10932159	0.14703100	17.36856505	0.13323900	16.71526061	3.69542800	0
662	05:52:13.37	+32:41:50.5	20	0.54761201	0.00015400	0.54736148	0.00015700	0.54765057	0.00014900	0.54793997	0.00013900	1
663	05:52:13.52	+32:33:16.9	23	6.29238076	0.01989300	6.29238076	0.00782100	6.29238076	0.00724600	6.30513642	0.01116300	1
664	05:52:13.63	+32:31:52.9	23	6.13477337	0.00942200	6.05946628	0.00777300	6.13113339	0.05487000	6.05946628	0.00839700	1
666	05:52:13.81	+32:27:35.6	25	6.85933870	0.02773300	6.95751094	0.01884600	13.88083989	1.56364100	19.80070210	0.08755800	0
669	05:52:13.99	+32:22:36.7	27	0.49118800	0.00013000	0.49087948	0.00013700	0.49150001	0.00016700	0.49142236	0.00018300	1
670	05:52:14.05	+32:36:08.3	22	5.54920607	0.00855800	5.58106944	0.01151400	5.61127548	0.01195200	5.51183767	0.02141600	1
673	05:52:14.33	+32:23:56.0	26	10.95320423	0.05851900	11.34881430	0.07053300	11.47440059	0.06839000	11.34881430	0.07342500	1
675	05:52:14.41	+32:23:45.8	26	5.92967976	0.04810900	5.98098443	0.00585300	11.98501252	0.02204500	17.86737507	2.64966400	0
676	05:52:14.47	+32:40:49.2	20	11.41335535	0.03235100	11.34881430	0.03536200	11.39036983	0.02632500	11.39036983	0.02706100	1
680	05:52:14.77	+32:33:27.7	23	0.98272673	0.00130100	0.98263328	0.00192000	1.96321917	0.00500200	2.95293568	0.00280500	0
685	05:52:15.31	+32:37:34.3	21	10.35948124	0.07169500	10.24688931	0.02443400	10.11365276	0.04040500	10.14663601	0.03231800	1
686	05:52:15.37	+32:26:59.9	25	8.79598842	0.01449500	8.76007136	0.01557100	17.52014272	0.04347600	17.36846863	2.70289400	0
689	05:52:15.57	+32:32:52.2	23	7.00942677	0.01730900	6.96156650	0.00688500	6.97718621	0.00588200	6.97718621	0.00851500	1
691	05:52:15.83	+32:36:09.6	22	15.28417690	0.09109900	15.00400386	0.09781700	2.00240134	0.00184000	0.49882604	0.00004100	0
697	05:52:16.11	+32:23:31.9	26	9.05197148	0.02255700	9.17342967	0.02365700	9.01393799	0.01929100	8.96199942	0.01631000	1
702	05:52:17.40	+32:29:53.8	24	7.44430082	0.05432400	7.39112598	0.01957100	7.51640233	0.01905800	7.49824633	0.02545700	1
703	05:52:17.55	+32:24:22.3	26	0.90568471	0.00022700	0.90424988	0.00017600	0.90556607	0.00014200	0.90556607	0.00014500	1
705	05:52:18.29	+32:42:08.9	11	7.94561941	0.02216500	1.01256795	0.00030200	15.86287608	5.83501000	15.62385736	0.04420100	0
707	05:52:18.47	+32:42:25.6	11	14.23665904	0.19164500	14.32846614	0.16190500	14.13316674	0.08745300	14.00589824	0.26112600	1
708	05:52:18.74	+32:38:37.3	12	7.30985783	0.03514000	7.14941393	0.01289600	7.18242900	0.01277500	7.18242900	0.01624100	1
710	05:52:19.05	+32:35:09.2	13	5.48626120	0.01627700	5.48528410	0.01450400	5.45641930	0.01049000	5.45641930	0.01158100	1

Table 1—Continued

ID	RA (J2000)	DEC (J2000)	Chip	Period[a] (days)	σ_P (days)	$P_{N=1}$[b] (days)	$\sigma_{P_{N=1}}$ (days)	$P_{N=2}$[b] (days)	$\sigma_{P_{N=2}}$ (days)	$P_{N=3}$[b] (days)	$\sigma_{P_{N=3}}$ (days)	Clean[c]
711	05:52:19.06	+32:39:14.4	12	9.10629391	0.00653200	4.56718544	0.00351700	4.57390090	0.00332500	4.57390090	0.00350100	1
713	05:52:19.26	+32:30:36.8	15	9.18968981	0.02829300	9.22785524	0.02914600	17.56470920	0.08361100	17.66445202	0.10373300	0
714	05:52:19.41	+32:44:13.7	10	9.89013672	0.04419700	9.79730377	0.04308200	9.89076571	0.03385900	9.89076571	0.03512800	1
719	05:52:19.80	+32:28:58.0	15	2.11966202	0.00096700	2.12320661	0.00068000	2.12031218	0.00072800	2.12175841	0.00087900	1
722	05:52:19.93	+32:22:15.2	18	5.33773559	0.00532900	5.30133656	0.00826200	5.41205402	0.01442000	5.42148959	0.01982800	1
724	05:52:20.05	+32:29:26.0	15	10.63490598	0.06295500	5.67544244	0.01063000	10.54120637	0.04464900	10.40023404	0.03386700	0
727	05:52:20.18	+32:24:12.0	17	13.55429194	0.29034100	13.40245584	0.11964500	13.46045002	0.10739100	13.40245584	0.13286600	1
730	05:52:20.21	+32:36:38.9	13	1.25255037	0.00052100	1.25376198	0.00027600	1.25376198	0.00032100	1.25376198	0.00028400	1
736	05:52:20.47	+32:40:29.2	11	8.81220963	0.02446000	8.73549565	0.02500200	17.56470920	0.06341200	18.39568303	2.35038600	0
745	05:52:20.95	+32:29:22.9	15	10.98802543	0.08938400	11.02697625	0.02762200	11.02697625	0.03212500	10.98802543	0.03303900	1
746	05:52:20.96	+32:22:08.9	18	1.20040842	0.00045000	1.20176304	0.00052700	1.20129878	0.00039300	1.20176304	0.00066300	1
747	05:52:21.01	+32:27:28.0	16	9.42496591	0.06582200	9.50996637	0.02019000	19.01993274	0.06010700	9.50996637	0.02150000	0
748	05:52:21.09	+32:30:16.6	15	12.96129167	0.10008200	12.84886411	0.10878000	12.79600987	0.11831300	12.90215678	0.11780300	1
751	05:52:21.38	+32:28:04.4	16	3.89496025	0.08134200	1.97618322	0.00144300	4.03412009	0.00405600	5.92403352	0.00545000	0
756	05:52:21.68	+32:23:50.1	17	0.76779218	0.00028100	0.76767849	0.00023900	0.76748908	0.00023600	0.76748908	0.00024700	1
758	05:52:21.87	+32:34:44.8	13	12.61951359	0.10442800	12.74353690	0.07812800	12.38828240	0.06577200	12.58882036	0.07966400	1
763	05:52:22.06	+32:27:15.2	16	10.61675768	0.12395900	9.77903175	0.05549100	9.06648208	0.44554200	9.65759081	0.04220500	1
767	05:52:22.20	+32:25:53.8	17	0.68071806	0.00024800	0.68079409	0.00029400	0.67797291	0.00016700	0.67797291	0.00017200	1
768	05:52:22.22	+32:29:26.8	15	6.52140461	0.00815300	6.52003773	0.01037000	6.60307790	0.00823600	6.61712402	0.00731000	1
771	05:52:22.44	+32:22:10.6	18	1.25820676	0.00065300	1.26122778	0.00075200	1.26481872	0.00097500	1.26430447	0.00068600	1
772	05:52:22.50	+32:44:03.9	10	6.69633584	0.02469600	6.68223769	0.02376800	6.66791288	0.01798900	6.68223769	0.02860300	1
773	05:52:22.62	+32:36:44.1	13	17.65933829	0.35167600	17.36846863	0.13267700	17.46598896	6.86592300	17.46598896	4.87001500	1
774	05:52:22.81	+32:35:56.8	13	4.07480485	0.01181000	4.05515063	0.00309700	4.05515063	0.00312900	4.06044386	0.00360600	1
777	05:52:22.93	+32:44:49.5	10	6.92318376	0.03677600	6.98223938	0.02741200	6.82894529	0.01150100	6.82894529	0.01117100	1
778	05:52:22.95	+32:21:55.5	18	7.16791831	0.01457000	7.12276788	0.01140000	14.35801090	0.03315200	14.42461267	0.06749200	0
779	05:52:23.18	+32:24:02.8	17	3.51095937	0.00342800	6.71714532	0.02995100	3.51056314	0.00216100	3.52648226	0.00375200	0
780	05:52:23.20	+32:33:02.9	14	9.12046141	0.02464700	8.82302413	0.02499600	8.97574647	0.01232300	8.97574647	0.01350300	1
783	05:52:23.34	+32:29:08.8	15	6.46112784	0.08556200	6.56129509	0.02664800	6.52003773	0.03086800	6.54748474	0.05422100	1
784	05:52:23.34	+32:26:28.1	16	16.50244032	0.09583800	15.94418247	0.09900300	15.94418247	0.17238700	15.86287608	7.38253600	1
785	05:52:23.40	+32:37:56.6	12	7.85433657	0.01600800	7.83356837	0.01634200	7.77483129	0.01030900	7.77483129	0.01012000	1
789	05:52:23.71	+32:38:11.2	12	1.46248707	0.00097800	1.46241832	0.00102900	1.46173112	0.00114800	1.46035867	0.00093900	1
790	05:52:23.76	+32:33:44.4	14	7.57127248	0.13201500	7.43201156	0.02431600	7.54007949	0.01811000	7.54007949	0.01631600	1
793	05:52:24.19	+32:32:02.7	14	0.62898272	0.00019600	0.62934787	0.00021300	1.25844118	0.00044300	1.88718087	0.00078600	0
799	05:52:24.38	+32:32:10.9	14	8.29670133	0.01930800	8.30489550	0.01824800	8.48611134	0.01094400	8.46302804	0.01092500	1

Table 1—Continued

ID	RA (J2000)	DEC (J2000)	Chip	Period[a] (days)	σ_P (days)	$P_{N=1}$[b] (days)	$\sigma_{P_{N=1}}$ (days)	$P_{N=2}$[b] (days)	$\sigma_{P_{N=2}}$ (days)	$P_{N=3}$[b] (days)	$\sigma_{P_{N=3}}$ (days)	Clean[c]
800	05:52:24.43	+32:26:39.9	16	2.07311563	0.00533400	2.07090740	0.00401800	2.07782379	0.00258200	2.07921262	0.00983100	1
802	05:52:24.61	+32:39:47.1	12	8.11242665	0.00775500	8.27096517	0.01008900	8.03593387	0.01158100	8.03593387	0.01274900	1
803	05:52:24.62	+32:29:31.8	15	8.44154681	0.02820200	8.52015886	0.03671200	9.14645692	0.12743400	8.42782444	0.01674700	1
808	05:52:24.99	+32:26:55.5	16	8.89663950	0.07722300	8.91065597	0.01514600	8.93625395	0.01682800	8.93625395	0.01487200	1
809	05:52:25.02	+32:26:29.4	16	5.53015111	0.09354700	6.05078778	0.26121900	5.98098443	0.01290700	17.17675317	0.10438100	0
810	05:52:25.08	+32:34:02.4	14	2.27152547	0.00100800	2.27326816	0.00088000	2.26499348	0.00065400	2.26995104	0.00077000	1
812	05:52:25.24	+32:34:46.9	13	6.55505962	0.01107300	6.47928269	0.01194900	6.58907755	0.01114400	6.50638693	0.03727600	1
813	05:52:25.31	+32:23:49.3	17	13.61361050	0.16963600	13.69753413	0.14013900	13.75811588	0.16986700	13.75811588	0.13838400	1
815	05:52:25.36	+32:28:15.6	16	6.65179087	0.02059000	6.65962321	0.01120000	6.64539628	0.00612300	6.64539628	0.00786800	1
817	05:52:25.39	+32:38:12.1	12	7.58802293	0.06619200	7.42235743	0.01991100	14.80585435	0.03794100	14.91589547	1.55129900	0
818	05:52:25.39	+32:29:49.6	15	9.92251994	0.03266200	10.09642973	0.03607400	9.93519642	0.05631400	10.29695465	0.02875800	1
819	05:52:25.85	+32:33:59.2	14	5.12158919	0.00506400	5.13723395	0.00414100	5.13723395	0.00427600	5.07853517	0.00315600	1
821	05:52:25.94	+32:28:09.7	16	6.85782628	0.01316600	6.49281987	0.01349400	6.88057952	0.00953400	6.88057952	0.00865300	1
822	05:52:26.02	+32:43:29.4	10	10.58587619	0.03227700	10.56251019	0.02844700	10.56251019	0.02114700	10.56251019	0.02354300	1
825	05:52:26.20	+32:36:22.9	13	6.81424597	0.01735600	7.24936577	0.01776200	6.85026040	0.12305900	6.85026040	0.13545100	1
827	05:52:26.24	+32:40:44.6	11	6.76682619	0.04257800	6.65962321	0.01164800	6.65962321	0.01797700	6.80531612	0.02866000	1
828	05:52:26.40	+32:29:33.4	15	1.31642404	0.00033200	1.31636833	0.00031500	2.63373973	0.00112300	2.63373973	0.00119900	0
830	05:52:26.63	+32:32:07.9	14	6.27270766	0.01209300	6.29008148	0.01242500	6.34136315	0.00705400	6.35431448	0.00800700	1
832	05:52:26.78	+32:36:09.6	13	7.26801425	0.46466100	7.23251074	0.01487000	14.39470479	0.30114700	7.30040554	0.01242000	0
834	05:52:26.93	+32:29:44.9	15	1.77653341	0.00122800	2.27208385	0.00202200	3.55469089	0.00257500	3.55469089	0.00290900	0
835	05:52:26.94	+32:22:38.1	18	7.16544080	0.01816600	7.12276788	0.00828400	7.17205129	0.00735200	7.17205129	0.00700800	1
838	05:52:27.16	+32:29:59.8	15	11.41126192	0.20081900	10.75997925	0.03156900	11.30756089	0.02874900	11.39036983	0.02852600	1
841	05:52:27.47	+32:27:12.4	16	6.15007908	0.00544000	6.13431276	0.00604100	6.14643351	0.00559500	6.14643351	0.00491200	1
842	05:52:27.53	+32:37:55.0	12	15.67108312	0.17146800	15.31614968	0.11906800	14.87666188	0.07650800	14.87666188	5.48481200	1
845	05:52:27.83	+32:29:53.1	15	6.87146013	0.04427700	6.98878904	0.01208900	6.94199955	0.00921100	6.94199955	0.01027700	1
850	05:52:28.40	+32:27:50.0	16	10.48789616	0.11699500	10.50560621	0.03512800	10.43512244	0.01871500	10.43512244	0.01973900	1
852	05:52:28.58	+32:31:15.1	15	10.63490598	0.03749200	10.36557814	0.02188800	10.12930641	0.01491700	10.12930641	0.01623800	1
853	05:52:28.71	+32:45:21.7	10	0.70925733	0.00033500	0.70893725	0.00027500	0.70780798	0.00030100	0.70861423	0.00029900	1
854	05:52:28.84	+32:40:47.9	11	16.45007932	0.24896300	15.39193469	0.08197800	16.53753323	0.12796400	16.71526061	0.12991000	1
857	05:52:28.89	+32:30:31.9	15	11.14949821	0.05080800	10.64946936	0.04850400	10.83493556	0.08832500	10.72288866	0.04660900	1
859	05:52:28.96	+32:38:04.9	12	3.23358628	0.00191600	3.23998542	0.00278200	6.48672714	0.00867000	3.24336357	0.00284000	0
860	05:52:29.19	+32:27:20.3	16	7.78455956	0.00709300	7.75544752	0.01388100	7.79431220	0.01341300	7.77483129	0.01952300	1
862	05:52:29.28	+32:45:30.8	10	12.90481683	0.97374100	12.51790084	0.13178600	12.17491780	0.12445400	12.12744853	0.11260800	1
864	05:52:29.38	+32:27:00.5	16	3.70322619	0.00384200	3.72942093	0.00393300	7.45794773	0.00990900	7.45794773	0.00973900	0

Table 1—Continued

ID	RA (J2000)	DEC (J2000)	Chip	Period[a] (days)	σ_P (days)	$P_{N=1}$[b] (days)	$\sigma_{P_{N=1}}$ (days)	$P_{N=2}$[b] (days)	$\sigma_{P_{N=2}}$ (days)	$P_{N=3}$[b] (days)	$\sigma_{P_{N=3}}$ (days)	Clean[c]
865	05:52:29.41	+32:24:27.7	17	3.84251745	0.02083800	3.83045191	0.01181400	3.83517445	0.01270500	3.82998030	0.01193400	1
867	05:52:29.44	+32:38:48.6	12	0.66546369	0.00032800	1.96619051	0.00292800	4.07641200	0.00518300	4.10871747	0.00447800	0
868	05:52:29.47	+32:23:34.3	17	10.83871080	0.11274400	10.98802543	0.11015500	10.83493556	0.14977000	10.47024571	0.27576100	1
869	05:52:29.52	+32:25:28.8	17	7.13465596	0.01090100	7.05216504	0.01042500	14.32846614	0.03133200	14.32846614	0.03172400	0
870	05:52:29.61	+32:40:58.7	11	9.38374057	0.03350400	9.39507702	0.03483500	18.50511600	0.10529500	18.50511600	0.14086700	0
871	05:52:29.62	+32:29:43.8	15	11.54038212	0.03882200	11.51688264	0.04040200	11.60279746	0.02949800	11.64623736	0.02636600	1
873	05:52:29.67	+32:45:08.2	10	7.91462595	0.01501900	7.86499444	0.02377000	8.02737690	0.11865400	15.91184776	0.85223700	0
875	05:52:29.88	+32:35:53.9	13	0.67514055	0.00018900	0.67490604	0.00024600	0.67637351	0.00013700	0.67652061	0.00013500	1
876	05:52:29.92	+32:36:10.0	13	7.56677824	0.00974100	7.73614117	0.01108900	7.62240254	0.00885800	7.60377046	0.00904400	1
878	05:52:30.07	+32:25:24.9	17	8.31740642	0.04839000	8.49688610	0.06376800	8.45071991	0.02401200	15.94418247	3.95806200	0
880	05:52:30.14	+32:31:29.6	15	7.53198547	0.03020900	7.38710520	0.02577900	7.47587118	0.03020600	7.64114468	0.01341300	1
882	05:52:30.40	+32:36:31.3	13	13.01002547	0.19391600	12.58882036	0.06629700	12.79595765	0.04479500	12.90210368	0.03944900	1
886	05:52:30.70	+32:40:56.3	11	1.17604960	0.00037000	1.17513883	0.00028200	1.17513883	0.00027000	1.17513883	0.00027300	1
888	05:52:30.82	+32:32:47.0	14	7.24847518	0.02759000	6.90425183	0.02090700	7.25862166	0.00836800	7.22491002	0.00871000	1
889	05:52:30.83	+32:39:18.9	12	5.02132365	0.01011800	5.00838834	0.01437000	10.09642973	0.03643200	10.03131248	0.02789400	0
890	05:52:30.84	+32:29:05.8	15	1.70216689	0.00141500	1.69974865	0.00144600	3.40303030	0.00303000	3.40303030	0.00322700	0
891	05:52:30.90	+32:37:51.1	12	5.02944220	0.01774000	4.94469878	0.00557800	5.01646509	0.00336400	5.03269697	0.00814600	1
892	05:52:31.06	+32:39:52.4	12	7.63364417	0.01389800	7.62242098	0.01518900	15.46847340	0.03753300	15.62385736	2.88674200	0
893	05:52:31.13	+32:34:04.0	14	2.24396899	0.00354700	2.25841699	0.00376700	2.24537791	0.00150400	2.23409161	0.00165200	1
901	05:52:31.39	+32:37:46.4	12	3.30873797	0.00245700	3.31950699	0.00201200	3.31950699	0.00131400	3.31950699	0.00160400	1
902	05:52:31.40	+32:41:23.8	11	7.17497405	0.01631900	7.10045652	0.01386300	6.89583241	0.01066200	14.52923867	0.03352100	0
903	05:52:31.46	+32:33:30.1	14	1.81414752	0.00121200	3.42036103	0.00740000	1.79880263	0.00123600	1.80192803	0.00085400	0
904	05:52:31.49	+32:34:03.8	14	7.40547688	0.11260900	7.29264937	0.02596600	7.34429337	0.01124200	7.30978315	0.01422700	1
907	05:52:31.66	+32:30:03.3	15	4.46941092	0.01123500	4.46876886	0.01218600	4.44323668	0.00656200	4.43689916	0.00758500	1
910	05:52:31.89	+32:41:22.3	11	17.36371755	0.45180300	18.50511600	0.13662100	17.66445202	0.13516000	17.56470920	0.14577300	1
912	05:52:32.08	+32:43:20.8	10	7.79560902	0.03345700	7.67102693	0.02914200	8.26192095	0.01553500	8.21826252	0.01232000	1
915	05:52:32.25	+32:41:46.1	11	8.76256338	0.03483300	8.80971396	0.03529500	8.24903209	0.02856600	8.31518311	0.02344800	1
917	05:52:32.38	+32:26:11.8	16	8.48761255	0.02839900	8.63846154	0.01416400	8.52015886	0.01226200	8.52015886	0.01160000	1
920	05:52:32.43	+32:36:40.1	13	7.80504904	0.00855700	7.99460834	0.01522500	7.89317992	0.01481300	16.10923869	0.02748700	0
921	05:52:32.46	+32:29:25.1	15	12.46777555	0.07094500	12.64002438	0.06792200	12.58887090	0.07756100	12.90215678	0.21538100	1
922	05:52:32.48	+32:30:23.1	15	6.22142000	0.01552900	6.23263875	0.01185900	7.11670098	0.01419000	12.33919080	0.03471300	0
924	05:52:32.57	+32:21:13.1	18	11.89161759	0.05200500	11.84270698	0.08335100	10.96571691	0.02521800	11.00452261	0.02694600	1
933	05:52:33.02	+32:30:24.8	15	8.17102706	0.13174700	8.16245080	0.01280800	16.54193034	0.03650200	16.19318063	0.04446500	0
939	05:52:33.36	+32:38:32.0	12	13.84691743	0.22092300	13.63748356	0.06203400	13.75811588	0.06572800	13.75811588	0.05215700	1

Table 1—Continued

ID	RA (J2000)	DEC (J2000)	Chip	Period[a] (days)	σ_P (days)	$P_{N=1}$[b] (days)	$\sigma_{P_{N=1}}$ (days)	$P_{N=2}$[b] (days)	$\sigma_{P_{N=2}}$ (days)	$P_{N=3}$[b] (days)	$\sigma_{P_{N=3}}$ (days)	Clean[c]
941	05:52:33.43	+32:36:40.0	13	7.06474077	0.07584400	7.19259938	0.02177600	14.21917266	0.04656700	14.17920965	3.26590900	0
942	05:52:33.62	+32:31:05.6	15	8.48414019	0.05299900	8.45071991	0.01699700	8.45071991	0.01384600	8.42782444	0.01517700	1
944	05:52:33.68	+32:39:08.8	12	11.67245779	0.04563600	11.55968042	0.05804400	12.05234405	0.34589400	12.24207005	0.73192100	1
951	05:52:33.92	+32:38:21.2	12	9.20328402	0.04203400	9.20056196	0.03896700	18.28753674	0.05782300	17.86737507	0.06619800	0
952	05:52:33.98	+32:31:50.4	14	8.49886090	0.02834600	8.53265776	0.01618800	17.03588129	0.04529900	17.03588129	0.03930200	0
953	05:52:34.07	+32:40:50.3	11	8.77244783	0.00955400	8.66251740	0.02290300	8.73549565	0.02242400	8.83473445	0.01516900	1
956	05:52:34.25	+32:24:51.5	17	14.95533654	0.22390200	14.66624234	0.19593800	14.59741905	4.91942500	14.32846614	0.10877100	1
958	05:52:34.32	+32:33:03.3	14	6.40177572	0.00982100	6.44647660	0.01382400	6.40665321	0.01957400	19.49046545	0.40808700	0
961	05:52:34.53	+32:28:25.6	16	7.30985783	0.01899800	7.24938243	0.01043700	7.24938243	0.01265900	7.24938243	0.01214400	1
962	05:52:34.69	+32:27:09.9	16	15.95235897	0.08826500	15.94418247	0.09289700	15.86287608	5.84648200	15.78239472	0.19206100	1
968	05:52:35.08	+32:41:21.6	11	8.21743495	0.01147500	8.24903209	0.01788600	16.49806417	0.03674600	16.19318063	0.03785500	0
970	05:52:35.34	+32:29:05.3	15	3.98808974	0.00516800	3.97230239	0.00432300	3.12602753	0.00227500	8.03593387	0.01979500	0
971	05:52:35.34	+32:29:58.8	15	3.23022845	0.00282400	3.23325018	0.00311300	3.23325018	0.00459900	3.21986337	0.00340900	1
972	05:52:35.44	+32:28:37.3	16	17.91367694	1.71151800	19.80082750	0.13358100	17.36856505	2.87278900	17.27212660	2.08079000	0
974	05:52:35.49	+32:33:58.4	14	0.82867572	0.00042600	0.83019482	0.00041000	0.83108186	0.00026700	2.49324559	0.00131600	0
975	05:52:35.54	+32:27:42.4	16	5.65069936	0.01422900	5.61398664	0.00941800	11.10571225	0.02857900	11.10571225	1.03521000	0
978	05:52:35.85	+32:32:36.8	14	9.81470978	0.01301300	9.79524289	0.02001700	9.64343985	0.02203600	9.82617882	0.01808400	1
980	05:52:35.93	+32:31:08.4	15	4.59145387	0.01222400	4.60777663	0.01304100	4.60096140	0.01383800	4.60096140	0.00983000	1
983	05:52:36.09	+32:38:56.9	12	13.40823276	0.12281700	13.69753413	0.15767000	14.00589824	0.07605900	13.94311968	0.06772300	1
986	05:52:36.24	+32:29:37.1	15	4.39676325	0.00741900	12.09922209	0.43617000	8.54355946	0.01895300	8.56708896	0.01588300	0
987	05:52:36.25	+32:36:22.5	13	11.96426962	0.32467400	11.10567295	0.16668100	12.38828240	0.05562700	12.09917542	0.04289700	0
990	05:52:36.35	+32:41:27.6	11	6.86539395	0.01878400	7.03621353	0.01078600	6.92654197	0.00900100	6.94199955	0.01066900	1
991	05:52:36.37	+32:26:15.6	16	3.62279159	0.00651600	3.61668411	0.00225000	3.60829370	0.00221700	3.60829370	0.00214100	1
992	05:52:36.46	+32:22:57.5	18	6.21310290	0.00882200	6.19972487	0.00904500	12.21485584	0.02678900	12.26302548	0.02473200	0
993	05:52:36.50	+32:36:53.0	13	7.31757888	0.10017000	7.18241265	0.01094000	7.47585346	0.01705800	7.47585346	0.01351200	1
996	05:52:36.63	+32:25:53.1	17	8.58126897	0.00815400	8.59074841	0.01543300	17.56470920	0.04831400	17.46608647	0.78116600	0
1000	05:52:37.01	+32:37:59.6	12	9.71641418	0.01356300	9.77903175	0.01607000	9.71793190	0.01432200	9.71793190	0.01475500	1
1004	05:52:37.32	+32:31:51.6	14	7.81370988	0.01321600	3.99069174	0.00601300	3.94514918	0.00444500	3.92029409	0.00674700	1
1005	05:52:37.45	+32:33:06.8	14	7.40547688	0.02531000	7.46768836	0.01113300	7.48565551	0.01027900	7.48565551	0.00942700	1
1006	05:52:37.48	+32:36:09.5	13	11.40494480	0.12680600	10.94931063	0.04017100	11.06616519	0.04985400	11.06616519	0.07800500	1
1007	05:52:37.53	+32:27:29.7	16	3.79586333	0.00414900	3.79771701	0.00444200	7.45794773	0.01022800	7.44011002	0.01028600	0
1008	05:52:37.56	+32:35:17.0	13	8.87377329	0.00701100	4.43057352	0.00732200	4.45595995	0.00560600	4.44958611	0.00405900	1
1010	05:52:37.67	+32:21:12.4	18	12.58054050	0.09223800	12.61115257	0.04226300	12.56021488	0.03914300	12.56021488	0.03599600	1
1012	05:52:37.71	+32:32:19.5	14	3.31337913	0.01143800	3.32176313	0.00525300	3.33243683	0.00310100	10.04832542	0.01544200	0

Table 1—Continued

ID	RA (J2000)	DEC (J2000)	Chip	Period[a] (days)	σ_P (days)	$P_{N=1}$[b] (days)	$\sigma_{P_{N=1}}$ (days)	$P_{N=2}$[b] (days)	$\sigma_{P_{N=2}}$ (days)	$P_{N=3}$[b] (days)	$\sigma_{P_{N=3}}$ (days)	Clean[c]
1013	05:52:37.74	+32:31:55.9	14	10.36740667	0.03175700	9.92983207	0.02544000	9.92983207	0.03174500	9.95462169	0.03600400	1
1014	05:52:37.75	+32:40:31.8	11	5.51544326	0.00960900	5.56378108	0.00700000	5.55384753	0.00561000	16.36354550	0.03617500	0
1015	05:52:37.85	+32:30:05.5	15	10.59686595	0.17246900	5.36236856	0.00859500	10.83493556	0.02289500	10.79732732	0.02932900	0
1018	05:52:37.96	+32:34:15.4	14	1.41945297	0.00031700	1.41944001	0.00040300	1.42138709	0.00040700	1.42203731	0.00034200	1
1021	05:52:38.24	+32:21:57.4	18	6.56738754	0.01128700	6.53866437	0.01258300	13.03402632	0.03427600	19.98751768	0.07978400	0
1024	05:52:38.30	+32:41:37.5	11	2.06280504	0.00325400	2.06130144	0.00363600	2.05993643	0.00198100	4.13603244	0.00943100	0
1025	05:52:38.35	+32:27:18.2	16	4.10654785	0.00686800	4.07107708	0.01082800	4.11960005	0.00646400	4.09250099	0.00933500	1
1027	05:52:38.42	+32:23:05.2	18	7.48413478	0.01511800	3.75753160	0.00590200	7.42906493	0.00957400	7.42906493	0.00726100	0
1030	05:52:38.65	+32:43:27.5	10	14.77647506	0.10635700	14.50227527	0.09270400	14.77787913	0.12380800	14.77787913	0.14634500	1
1032	05:52:38.80	+32:44:54.2	10	17.88333237	0.80560200	15.99366516	0.11444900	17.72537041	0.11896100	18.57205636	0.17239100	0
1033	05:52:38.86	+32:42:43.2	11	8.32965591	0.03050000	8.38240366	0.02838100	8.33746985	0.02567000	8.35987638	0.02687600	1
1035	05:52:38.89	+32:28:08.1	16	7.86327098	0.14624500	3.87337816	0.00292100	7.89319970	0.01086800	7.89319970	0.01111200	0
1037	05:52:38.98	+32:30:58.2	15	12.67091650	0.08738400	12.53812979	0.09407300	12.48779607	0.08698700	12.43786485	0.09550000	1
1039	05:52:39.01	+32:25:22.5	17	7.72847205	0.01895600	7.64114468	0.01944400	7.97413484	0.01808600	7.99462863	0.01858100	1
1040	05:52:39.03	+32:32:05.1	14	6.21630969	0.02205200	2.28160351	0.00278600	6.02222674	0.01525600	3.59007073	0.00296900	1
1041	05:52:39.10	+32:35:18.7	13	8.92599742	0.02087200	8.93622857	0.01972500	8.98786799	0.10571500	8.93622857	0.03532000	1
1043	05:52:39.14	+32:38:47.1	12	6.78971952	0.02452300	6.86539395	0.00954600	6.83522303	0.00660400	6.83522303	0.00656700	1
1044	05:52:39.28	+32:36:58.9	13	11.89564092	0.06546200	12.05229774	0.09333500	11.51684037	0.05162100	11.51684037	0.05265900	1
1051	05:52:39.84	+32:37:00.8	13	7.93548495	0.03695700	7.97411465	0.04364800	2.27540621	0.00242800	2.27208226	0.00169600	0
1053	05:52:40.05	+32:33:51.9	14	6.83794066	0.01771700	6.78381920	0.02361500	13.60828850	5.23971600	13.97503930	0.73060200	0
1056	05:52:40.24	+32:25:44.9	17	0.89698813	0.00008500	0.89694934	0.00009300	0.89694934	0.00008500	0.89694934	0.00008500	1
1058	05:52:40.29	+32:28:19.1	16	13.94937220	0.00581000	1.07521690	0.00064100	16.27791732	1.49661700	16.80556456	1.49528500	0
1060	05:52:40.43	+32:37:28.8	12	8.21743495	0.03979600	8.18392528	0.01446100	8.11983816	0.01252400	8.09869826	0.01046100	1
1061	05:52:40.46	+32:29:08.3	15	8.79850092	0.01341700	9.04013368	0.01379300	8.96199942	0.00904000	9.01393799	0.01231900	1
1062	05:52:40.48	+32:30:39.8	15	2.15363473	0.00088800	2.15259152	0.00125800	2.15259152	0.00079900	2.15408213	0.00090400	1
1064	05:52:40.49	+32:43:12.1	10	0.78918741	0.00025100	0.78935764	0.00018800	0.78935764	0.00014700	0.78855717	0.00015200	1
1066	05:52:40.66	+32:28:41.9	16	6.78379675	0.02196900	6.76094327	0.00971000	6.79046060	0.00961500	6.79046060	0.00941500	1
1069	05:52:41.03	+32:40:25.2	11	9.21691852	0.03940800	9.22785524	0.03560100	9.80987070	0.06258800	17.46608647	0.08092400	0
1070	05:52:41.04	+32:38:27.2	12	8.21743495	0.17226000	8.42782444	0.01499800	8.14108872	0.02892900	8.07766814	0.04333200	1
1072	05:52:41.37	+32:43:15.0	10	5.24103255	0.02143900	5.22342984	0.00949700	10.49125742	0.01981500	15.67028951	1.43463200	0
1073	05:52:41.41	+32:30:49.4	15	0.78207668	0.00021700	0.78156579	0.00026000	1.56624037	0.00052300	2.34399066	0.00085600	0
1074	05:52:41.43	+32:22:29.6	18	1.47266881	0.00048100	1.47057950	0.00043300	1.47546380	0.00048700	1.47546380	0.00050700	1
1080	05:52:41.73	+32:40:28.3	11	8.62887656	0.02747300	8.80971396	0.03558200	17.97059503	0.06460100	17.56470920	0.05488100	0
1081	05:52:41.83	+32:28:37.8	16	7.82568553	0.02187600	7.79431220	0.02323700	7.62242098	0.01897800	7.64114468	0.01614600	1

Table 1—Continued

ID	RA (J2000)	DEC (J2000)	Chip	Period[a] (days)	σ_P (days)	$P_{N=1}$[b] (days)	$\sigma_{P_{N=1}}$ (days)	$P_{N=2}$[b] (days)	$\sigma_{P_{N=2}}$ (days)	$P_{N=3}$[b] (days)	$\sigma_{P_{N=3}}$ (days)	Clean[c]
1084	05:52:41.92	+32:27:31.5	16	4.05304235	0.00773000	4.03412009	0.00764800	4.03935852	0.00619900	7.93346085	0.01105200	0
1085	05:52:41.92	+32:29:36.7	15	8.21743495	0.01906500	8.47374013	0.01754000	8.09869826	0.01306800	8.14108872	0.04636400	1
1086	05:52:42.14	+32:45:24.5	10	0.63543630	0.00022200	0.63550122	0.00013100	0.63550122	0.00011100	0.63550122	0.00012000	1
1097	05:52:42.85	+32:21:17.9	18	3.51719544	0.00705400	3.53137478	0.00289400	7.06274955	0.00852600	7.05473808	0.00798900	0
1100	05:52:42.98	+32:30:05.9	15	7.86525917	0.02035600	7.85334511	0.02199500	15.78239472	0.05910500	7.83356837	0.01979300	0
1102	05:52:43.15	+32:44:57.8	10	6.81100114	0.04217300	6.82894529	0.01316600	6.75479500	0.01363200	6.68223769	0.01311500	1
1104	05:52:43.26	+32:26:57.1	16	10.70628119	0.04092400	10.68605290	0.02503900	10.72288866	0.01839500	10.83493556	0.02522000	1
1105	05:52:43.29	+32:27:53.1	16	8.93882184	0.02673000	8.93625395	0.02555800	9.31071535	0.05919400	9.39507702	0.05513800	1
1107	05:52:43.49	+32:25:48.7	17	3.24708768	0.00316400	3.24674877	0.00432600	3.27408694	0.00215000	3.27408694	0.00169600	1
1109	05:52:43.83	+32:32:45.2	14	8.13976663	0.02567900	8.08897642	0.02293500	7.92416015	0.01642800	17.12124153	0.08990000	0
1110	05:52:43.95	+32:28:05.3	16	18.01743411	7.65468400	16.89684954	0.21455800	18.72793498	0.17741900	17.56470920	0.53109800	0
1111	05:52:43.96	+32:34:58.5	13	12.10393035	0.04947000	12.00578192	0.06370100	12.29039040	0.05745600	12.29039040	0.05163600	1
1112	05:52:44.01	+32:43:35.6	10	1.43173671	0.00091000	1.43043302	0.00089400	1.43043302	0.00065900	1.43043302	0.00072400	1
1113	05:52:44.23	+32:29:34.6	15	0.51753735	0.00059800	0.51801136	0.00037000	0.51740823	0.00031900	0.51758041	0.00036700	1
1117	05:52:44.55	+32:27:59.4	16	7.99668380	0.01277600	7.99462863	0.01334900	16.36354550	0.04171200	16.53753323	0.04489400	1
1120	05:52:44.66	+32:29:30.8	15	1.73845810	0.00053900	1.73870102	0.00047200	1.73967340	0.00050400	1.73967340	0.00047000	1
1122	05:52:44.72	+32:33:50.0	14	7.33788443	0.02110900	7.25862166	0.01879300	7.12562811	0.02693700	14.72334193	0.03472000	0
1124	05:52:44.79	+32:36:40.1	13	0.76646793	0.00030900	0.76767832	0.00041500	1.53003225	0.00078500	1.52852861	0.00067400	0
1126	05:52:44.94	+32:37:55.5	12	5.97065259	0.01780200	5.94668323	0.01980900	11.86840900	0.04761200	11.82329913	0.05560500	0
1127	05:52:44.97	+32:31:00.3	15	12.12752437	0.05056200	12.24207005	0.05373100	12.09922209	0.04638400	12.09922209	0.04025600	1
1130	05:52:45.04	+32:25:29.4	17	0.76130003	0.00024300	0.76110445	0.00016400	0.76129072	0.00013500	0.76110445	0.00013500	1
1131	05:52:45.44	+32:31:57.0	14	3.29582945	0.00448900	3.28320442	0.00490200	3.28667272	0.00468800	3.28667272	0.01303600	1
1135	05:52:45.97	+32:25:34.0	17	1.69428649	0.00057000	1.70067793	0.00066500	1.70814892	0.00050700	1.70721146	0.00082200	1
1136	05:52:45.98	+32:36:31.3	13	9.73618185	0.02097000	9.77900132	0.01654000	9.62767091	0.01390900	9.62767091	0.01405000	1
1137	05:52:45.99	+32:29:35.1	15	6.35357435	0.02304800	6.46582831	0.01283500	6.25771475	0.00822200	6.29570937	0.00749600	1
1138	05:52:46.01	+32:22:43.0	18	10.15630675	0.02421100	10.31122090	0.04400500	10.07731545	0.01685900	10.07731545	0.02200900	1
1142	05:52:46.23	+32:20:45.3	18	8.05610881	0.02710500	7.98207814	0.02182700	7.84118715	0.04569100	12.92567129	4.52075100	0
1145	05:52:46.63	+32:35:27.6	13	14.84825823	0.08174100	14.73564834	0.09082800	14.66617366	0.09323000	14.66617366	0.07764300	1
1146	05:52:46.75	+32:36:13.8	13	1.40090462	0.00143300	1.39675304	0.00058400	1.40115702	0.00056000	1.40115702	0.00074800	1
1147	05:52:46.87	+32:31:24.5	15	15.91156010	0.13646200	15.16679668	0.13925100	15.54577711	6.00351400	14.87666188	2.97466700	1
1149	05:52:46.97	+32:29:45.4	15	0.62071436	0.00016900	0.62051625	0.00017000	0.62051625	0.00015000	0.62064005	0.00016500	1
1151	05:52:47.08	+32:27:42.1	16	6.39405961	0.01909700	6.42575914	0.01992900	6.83522303	0.01218600	6.82023679	0.00861900	1
1159	05:52:51.26	+32:24:44.4	8	0.70944648	0.00010200	0.70970546	0.00009300	0.70938177	0.00008700	0.70938177	0.00008400	1
1162	05:52:51.48	+32:32:22.3	5	8.75639343	0.06754900	9.05075383	0.01746000	8.99837375	0.01655100	9.02448778	0.01850500	1

Table 1—Continued

ID	RA (J2000)	DEC (J2000)	Chip	Period[a] (days)	σ_P (days)	$P_{N=1}$[b] (days)	$\sigma_{P_{N=1}}$ (days)	$P_{N=2}$[b] (days)	$\sigma_{P_{N=2}}$ (days)	$P_{N=3}$[b] (days)	$\sigma_{P_{N=3}}$ (days)	Clean[c]
1163	05:52:51.60	+32:38:22.8	3	1.20626217	0.00019900	1.20658970	0.00023600	1.20612186	0.00022900	1.20612186	0.00024400	1
1165	05:52:51.66	+32:21:48.0	9	5.93081030	0.01436200	5.93533677	0.01740800	5.89038061	0.01397700	5.43735361	0.10932700	1
1169	05:52:52.04	+32:29:48.4	6	5.09117840	0.01418500	5.04903425	0.01244000	5.15786768	0.00602100	5.15786768	0.00601100	0
1174	05:52:52.26	+32:36:01.6	4	9.66059006	0.02285000	9.74838609	0.01569500	9.68766739	0.01537000	9.71793190	0.01728600	1
1179	05:52:52.88	+32:32:41.9	5	16.44625555	0.53898700	16.84720988	0.29040600	18.66765518	0.36513300	18.55625970	5.73182600	0
1180	05:52:52.92	+32:38:51.2	3	14.46162547	0.54946200	14.32840061	0.08204000	14.32840061	0.07394100	14.19760795	0.14524100	1
1186	05:52:53.93	+32:24:57.9	8	11.91842912	0.06178400	11.77853086	0.10261700	12.05234405	0.18058000	11.82329913	0.34534700	1
1188	05:52:54.10	+32:34:44.9	4	1.43977691	0.00096300	1.43542522	0.00064000	1.44074383	0.00057200	1.44074383	0.00056900	1
1191	05:52:54.54	+32:31:05.5	6	14.67316038	0.11021900	14.26276937	0.07967800	14.52923867	0.08693400	14.39477094	0.09813900	1
1192	05:52:54.56	+32:22:13.4	9	17.13889807	0.08217600	16.80556456	0.13049700	16.98913162	4.33521400	17.17675317	1.82654000	1
1196	05:52:54.75	+32:21:50.0	9	5.59480216	0.00941800	5.60387318	0.00989200	11.18558073	0.02908900	5.62413668	0.00617400	0
1199	05:52:55.05	+32:25:55.7	8	0.44851993	0.00008900	0.44828724	0.00009900	0.44841649	0.00007900	0.44848113	0.00008700	1
1202	05:52:55.18	+32:29:27.6	6	13.07021008	0.06563200	13.06472071	0.06778900	13.11982286	0.06239700	13.11982286	0.10011900	1
1203	05:52:55.35	+32:35:35.6	4	14.10433008	0.10558200	14.06924469	0.08850500	14.26276937	0.05143300	14.32846614	0.04011400	1
1208	05:52:55.83	+32:33:44.3	5	10.33177620	0.01752900	10.41482350	0.02223600	10.31122090	0.01603300	10.31122090	0.01680200	1
1210	05:52:55.94	+32:35:38.3	4	8.17102706	0.05197700	8.22721502	0.01564300	8.18392528	0.01347700	8.20551306	0.01243700	1
1213	05:52:56.10	+32:41:16.3	2	0.77035909	0.00031300	0.77053083	0.00038800	0.77053083	0.00032400	0.77034001	0.00031900	1
1218	05:52:56.63	+32:44:54.8	1	14.46841907	0.06847100	14.39470479	0.05832800	14.80578436	0.15459900	14.66617366	0.31234800	1
1219	05:52:56.75	+32:28:00.2	7	9.35473083	0.04838600	9.29935422	0.05553700	9.02940084	0.03783500	9.29935422	0.05117400	1
1221	05:52:56.86	+32:33:00.5	5	9.45184802	0.01416800	9.43521452	0.01365500	9.35010524	0.01378200	9.35010524	0.01428000	1
1223	05:52:56.97	+32:33:27.9	5	9.06605831	0.02004100	9.18441137	0.02096200	9.18441137	0.01551900	9.21161799	0.01937800	1
1225	05:52:57.08	+32:25:07.4	8	10.21579639	0.03915500	10.19570633	0.04076000	10.22923380	0.03294400	10.19570633	0.03580600	1
1233	05:52:57.61	+32:34:05.3	5	1.62045753	0.00106300	1.62165751	0.00089800	1.62165751	0.00117900	4.86203133	0.00484200	0
1235	05:52:57.75	+32:35:16.1	4	11.30550609	0.29239300	11.95966936	0.03855000	12.38833134	0.04036800	12.43786485	0.54271200	1
1239	05:52:58.35	+32:23:25.7	8	6.88210177	0.02982800	6.88057952	0.02462600	6.71714532	0.01268200	10.26298251	0.43483500	0
1242	05:52:58.65	+32:39:49.6	3	11.31167309	0.03552800	11.10567295	0.03738900	10.98798697	0.03621100	11.51684037	0.09473800	1
1243	05:52:58.72	+32:32:57.6	5	10.66778045	0.03905100	10.44982190	0.04993100	10.96571691	0.07733300	18.89450723	0.12340700	0
1248	05:52:59.54	+32:42:14.0	2	17.91367694	4.00844800	19.19006786	0.36875500	19.67558507	6.43179800	19.80082750	10.52750700	1
1249	05:52:59.61	+32:26:45.7	7	13.34956223	0.15115300	13.67350097	0.13874100	13.26530194	0.06158000	13.26530194	0.06312400	1
1250	05:52:59.66	+32:27:34.6	7	0.65359277	0.00009800	0.65352686	0.00012400	1.30445548	0.00023700	1.30445548	0.00025600	0
1253	05:52:59.99	+32:35:15.2	4	1.95950236	0.00105200	1.95629835	0.00152700	1.95752942	0.00124500	1.95752942	0.00151100	1
1255	05:53:00.30	+32:34:23.1	5	5.43522976	0.01145900	0.84695363	0.00032800	5.42148959	0.00791600	5.43095812	0.00663000	0
1259	05:53:00.49	+32:34:11.5	5	12.07634175	0.03701600	12.21485584	0.04989800	12.21485584	0.05683000	12.36051355	0.15979100	1
1262	05:53:00.56	+32:40:50.6	2	6.56960929	0.01936700	6.67391118	0.01987900	13.23143343	0.12990300	12.48779607	1.52893300	0

Table 1—Continued

ID	RA (J2000)	DEC (J2000)	Chip	Period[a] (days)	σ_P (days)	$P_{N=1}$[b] (days)	$\sigma_{P_{N=1}}$ (days)	$P_{N=2}$[b] (days)	$\sigma_{P_{N=2}}$ (days)	$P_{N=3}$[b] (days)	$\sigma_{P_{N=3}}$ (days)	Clean[c]
1264	05:53:00.82	+32:27:43.6	7	1.23333571	0.00033900	5.22342984	0.00806500	1.23406970	0.00020000	1.23211434	0.00026200	0
1265	05:53:00.86	+32:35:30.2	4	11.87293893	0.04989400	11.55968042	0.05100000	11.64623736	0.04622900	11.86840900	0.03631900	1
1269	05:53:01.04	+32:31:19.5	6	1.29421481	0.00026100	1.29499605	0.00020800	1.29499605	0.00032100	1.29445716	0.00036400	1
1273	05:53:01.49	+32:34:47.6	4	8.45071991	0.01115600	8.93625395	0.13369400	8.52015886	0.01218100	8.54355946	0.01234900	1
1276	05:53:01.59	+32:25:21.7	8	8.76997463	0.14368800	8.98789367	0.02413000	8.47374013	0.05448400	19.55191703	0.05205300	0
1277	05:53:01.67	+32:34:59.6	4	10.26636964	0.03848500	10.22923380	0.03466400	10.79732732	0.02772900	10.75997925	0.03451700	1
1278	05:53:02.41	+32:39:04.7	3	12.29529684	0.10244200	12.38828240	0.14900000	12.43781552	0.15660100	13.01002547	0.42236300	1
1284	05:53:03.21	+32:33:32.2	5	11.30866972	0.09252000	11.40823978	0.02700400	11.36653995	0.02302900	11.36653995	0.02382500	1
1285	05:53:03.30	+32:21:19.6	9	5.14081970	0.00778600	5.16643415	0.00491000	5.13233790	0.00459000	5.13233790	0.00433400	1
1289	05:53:03.69	+32:36:46.1	4	18.03310145	0.14689800	17.86737507	2.69735500	17.97059503	0.23702200	17.66445202	0.18670100	1
1291	05:53:03.72	+32:29:39.3	6	2.46100475	0.00118100	2.46666402	0.00161500	4.90570888	0.00416000	2.42059762	0.00103200	0
1293	05:53:03.89	+32:28:07.9	7	8.18538947	0.01995000	8.06902563	0.02541300	15.51500399	0.08814500	15.59278123	3.81998000	0
1296	05:53:04.19	+32:45:33.8	1	8.11134808	0.09627100	8.22719353	0.01280200	16.49802095	0.03863800	16.44999286	0.04069100	0
1298	05:53:04.67	+32:42:45.4	2	12.27104536	0.08357800	12.79600987	0.07342400	12.95589338	0.07285200	13.01007946	0.07946500	1
1299	05:53:04.68	+32:33:24.3	5	5.73737638	0.00947200	5.72069981	0.00654300	5.71019501	0.00701100	5.73124332	0.00675700	1
1300	05:53:04.71	+32:25:39.6	8	0.62164468	0.00016500	0.62125981	0.00021900	0.62138391	0.00026400	0.62138391	0.00034000	1
1301	05:53:04.76	+32:23:00.6	9	1.33736457	0.00103900	1.34018784	0.00145100	1.34018784	0.00401200	4.01848598	0.00460200	0
1302	05:53:04.87	+32:27:57.5	7	4.31706870	0.00953800	4.34735842	0.00645700	6.54170102	0.01590000	13.04280443	0.02651300	0
1309	05:53:05.19	+32:29:35.9	6	1.64357383	0.00044200	1.64405158	0.00040500	1.64405158	0.00046000	1.64405158	0.00046100	1
1313	05:53:05.62	+32:32:58.9	5	14.91442686	0.13955700	14.49183521	0.11623800	15.05304483	0.14444500	15.27486983	0.11820100	1
1314	05:53:05.66	+32:35:46.0	4	5.26569614	0.00528200	2.66077324	0.00380000	5.26257824	0.00709400	4.86732906	0.00394900	0
1320	05:53:06.12	+32:35:48.2	4	3.15168186	0.00260900	3.13864393	0.00288200	6.32129648	0.00829600	6.24515158	0.01247600	0
1328	05:53:06.69	+32:24:29.9	8	7.69977723	0.05399600	7.81389098	0.25530000	15.54577711	0.11843700	15.46847340	3.79248900	0
1331	05:53:06.87	+32:31:52.9	5	1.38824018	0.00096700	1.38850052	0.00125600	2.78000501	0.00222700	4.16520400	0.00433000	0
1332	05:53:06.99	+32:33:19.0	5	10.17624845	0.06732900	10.73851095	0.06823400	9.98028757	0.01709300	9.98028757	0.01365400	1
1333	05:53:07.07	+32:22:51.9	9	7.78455956	0.00444300	8.18392528	0.01936700	7.91327906	0.01407900	7.89319970	0.02726600	1
1334	05:53:07.20	+32:26:34.0	7	6.89678049	0.01012400	6.82894529	0.00855800	6.92010323	0.02399500	6.98223938	0.04793900	1
1335	05:53:07.38	+32:36:57.9	4	13.70356828	0.42851600	14.19767230	0.32782400	14.26276937	2.88977200	15.62385736	6.73529800	0
1336	05:53:07.44	+32:36:07.7	4	2.22583092	0.00072000	2.22814268	0.00077800	2.22654785	0.00065400	2.22654785	0.00068700	1
1338	05:53:07.66	+32:23:45.7	8	7.87421845	0.06490000	8.01522803	0.01470600	7.91327906	0.01896700	7.91327906	0.01838000	1
1340	05:53:07.75	+32:30:23.5	6	0.58008578	0.00012700	0.57958860	0.00017200	0.58012905	0.00015100	0.58023726	0.00014700	1
1343	05:53:07.80	+32:35:08.9	4	11.18960432	0.22128800	10.75997925	0.07464200	17.66445202	1.89745600	10.68605290	0.57006400	0
1349	05:53:08.27	+32:35:13.9	4	7.86029059	0.00717600	7.73616016	0.01428300	15.51089504	0.03555600	15.62778196	0.07594500	0
1350	05:53:08.39	+32:33:49.3	5	5.91043658	0.00371300	5.99648656	0.00855400	5.87193247	0.00369300	5.88304136	0.00539400	1

Table 1—Continued

ID	RA (J2000)	DEC (J2000)	Chip	Period[a] (days)	σ_P (days)	$P_{N=1}$[b] (days)	$\sigma_{P_{N=1}}$ (days)	$P_{N=2}$[b] (days)	$\sigma_{P_{N=2}}$ (days)	$P_{N=3}$[b] (days)	$\sigma_{P_{N=3}}$ (days)	Clean[c]
1352	05:53:08.84	+32:30:55.9	6	2.14724236	0.00069700	2.14961647	0.00061800	2.14664964	0.00042900	2.14664964	0.00045000	1
1355	05:53:09.16	+32:21:31.6	9	9.85649556	0.05738900	9.50996637	0.01780700	9.80987070	0.01780100	9.87213583	0.01838600	1
1360	05:53:09.61	+32:35:58.4	4	9.41213313	0.02070100	9.33866707	0.02729200	8.88520423	0.11785500	18.84136887	0.06340100	0
1364	05:53:09.98	+32:44:01.3	1	16.03863914	0.47784400	16.89675830	0.19628600	16.53744584	0.20458900	16.53744584	6.26335800	1
1367	05:53:10.31	+32:31:27.5	6	10.61675768	0.03682800	10.47024571	0.05076300	10.61313545	0.05326800	10.61313545	0.07975000	1
1373	05:53:10.69	+32:40:57.8	2	15.55355000	0.18733500	15.09320718	0.15851800	14.52923867	0.20888600	14.73571767	0.19598300	1
1374	05:53:10.75	+32:34:01.6	5	2.36836101	0.00194300	2.36731528	0.00206900	2.36012842	0.00138900	2.36012842	0.00145500	1
1377	05:53:10.91	+32:28:40.0	7	0.57627568	0.00009400	0.57659830	0.00011800	0.57638461	0.00009500	0.57638461	0.00009800	1
1378	05:53:10.96	+32:34:18.7	5	7.31632591	0.00839300	7.27269283	0.01399500	7.28974167	0.01029100	7.23883328	0.02466400	1
1383	05:53:11.44	+32:29:09.4	6	7.56679640	0.05283400	3.79771701	0.01008700	7.62242098	0.01594400	7.64114468	0.01184300	0
1385	05:53:11.64	+32:39:30.1	3	6.43238972	0.06710900	6.52002427	0.01520700	6.36005672	0.01309100	6.36005672	0.01175500	1
1386	05:53:11.87	+32:22:40.5	9	2.46685964	0.00155000	2.46470961	0.00152800	2.46666402	0.00156100	7.39999207	0.00930400	0
1392	05:53:12.48	+32:43:58.2	1	15.20750375	0.12996900	15.02025630	0.05353600	15.02025630	0.05472800	15.02025630	0.06181700	1
1394	05:53:12.58	+32:33:40.1	5	9.59534066	0.07881000	9.66993594	0.01712000	9.70009982	0.01879800	9.73045247	0.01673900	1
1395	05:53:12.59	+32:29:13.9	6	7.52287787	0.00935400	7.58524750	0.01474300	15.02032834	0.03755800	7.58524750	0.01485400	1
1398	05:53:12.78	+32:21:59.6	9	8.44957219	0.07113900	8.71103332	0.01976700	8.45071991	0.01440500	8.45071991	0.01629500	1
1399	05:53:12.84	+32:27:39.2	7	6.40167943	0.07609000	6.48712772	0.01023900	12.81390788	0.02916100	19.66236911	0.04488700	0
1404	05:53:13.10	+32:35:19.6	4	2.01601426	0.00062100	2.01849977	0.00103500	2.01981040	0.00064700	2.02375252	0.00068800	1
1408	05:53:13.28	+32:31:52.7	5	1.97941311	0.00096600	1.97742436	0.00099500	3.95339063	0.00241000	5.92790042	0.00407900	0
1419	05:53:14.47	+32:41:27.7	2	10.40197291	0.04093100	10.40023404	0.02415000	10.43512244	0.01959500	10.40023404	0.02169900	1
1420	05:53:14.54	+32:29:25.7	6	10.58064626	0.36859600	11.10571225	0.05109100	19.55191703	0.11558500	19.80082750	0.83906700	0
1424	05:53:15.32	+32:33:14.7	5	2.90758111	0.00173400	2.90193733	0.00272400	2.92651659	0.00180900	2.91554126	0.00174800	1
1425	05:53:15.52	+32:31:34.3	6	8.09027308	0.02360600	8.01522803	0.01978500	8.11983816	0.01960100	16.10932159	0.11776500	0
1435	05:53:16.39	+32:30:44.3	6	8.39597841	0.04932800	7.36960436	0.01924500	14.32846614	0.04490000	14.13316674	0.09710500	0
1439	05:53:16.72	+32:29:58.5	6	5.60488288	0.17807700	5.68581612	0.01310000	11.43223080	0.31579900	13.51894828	0.04058700	0
1440	05:53:16.87	+32:44:51.3	1	13.67038642	0.06915900	13.69747425	0.05656900	13.75805547	0.05582000	13.75805547	0.05276500	1
1442	05:53:16.95	+32:26:52.7	7	7.83488161	0.03119900	7.86499444	0.04268500	8.26192095	0.58732700	8.06902563	0.33981400	1
1443	05:53:17.08	+32:42:48.8	2	9.21009622	0.01879700	9.09298451	0.01621100	9.17342967	0.01554900	9.17342967	0.01569300	1
1446	05:53:17.41	+32:33:39.1	5	4.45829104	0.00604500	2.26886282	0.03703900	4.38857715	0.00295500	4.38239240	0.00300700	0
1450	05:53:17.77	+32:34:15.1	5	8.09532710	0.13173500	8.12812484	0.01821400	16.08804387	0.04406100	16.48986107	0.06300800	0
1451	05:53:17.87	+32:26:50.9	7	5.83026804	0.01135500	5.80870994	0.01163800	11.54240760	0.03696000	16.86062446	0.06189900	0

[a]The period from Paper II.

[b]The period from the multi-harmonic AoV algorithm, with the specified value of N.

[c]A flag that is either 1 or 0. Stars with a value of 1 were included in the clean sample of stars in §5.

Table 2. Candidate Cluster Members with Measured Rotation Periods: Magnitudes

ID	$<r>$[a] (mag)	RMS_r[b] (mag)	g[c] (mag)	r[c] (mag)	i[c] (mag)	B[d] (mag)	V[d] (mag)	I[e] (mag)	$A_{r,N=1}$[f] (mag)	min $A_{r,N=1}$[g] (mag)	$A_{r,N=2}$[f] (mag)	min $A_{r,N=2}$[g] (mag)	$A_{r,N=3}$[f] (mag)	min $A_{r,N=3}$[g]
25	16.743	0.016	17.548	16.732	16.401	18.064	17.076	15.966	0.027	0.020	0.031	0.024	0.032	0.024
26	17.341	0.005	18.365	17.344	16.881	18.879	17.735	16.438	0.013	0.006	0.013	0.006	0.014	0.006
43	16.423	0.007	17.198	16.421	16.074	17.707	16.763	15.637	0.011	0.008	0.013	0.010	0.013	0.009
47	18.930	0.021	20.303	18.923	18.131	21.125	19.645	17.673	0.051	0.015	0.059	0.012	0.059	0.012
57	16.972	0.005	17.823	16.974	16.576	18.347	17.325	16.137	0.009	0.005	0.010	0.005	0.011	0.006
58	16.743	0.006	17.566	16.742	16.311	18.089	17.099	15.871	0.012	0.005	0.014	0.005	0.015	0.005
61	19.725	0.019	21.366	19.721	18.584	21.958	20.305	18.110	0.045	0.014	0.046	0.014	0.049	0.015
71	17.444	0.006	18.439	17.445	16.991	19.042	17.877	16.550	0.012	0.006	0.016	0.007	0.016	0.006
73	17.172	0.012	18.088	17.170	16.780	18.600	17.537	16.341	0.025	0.013	0.029	0.015	0.028	0.014
78	20.032	0.032	21.658	20.017	18.910	22.306	20.707	18.437	0.076	0.018	0.085	0.022	0.086	0.022
81	18.322	0.006	19.642	18.319	17.731	20.258	18.864	17.283	0.014	0.006	0.015	0.006	0.015	0.006
84	17.675	0.012	18.737	17.670	17.204	19.287	18.091	16.762	0.034	0.007	0.033	0.007	0.036	0.008
86	18.084	0.021	19.221	18.086	17.499	19.733	18.461	17.051	0.062	0.011	0.062	0.010	0.060	0.010
91	20.552	0.024	22.242	20.553	19.301	22.916	21.242	18.822	0.035	0.025	0.055	0.038	0.054	0.038
94	20.548	0.018	22.150	20.550	19.309	22.846	21.183	18.829	0.019	0.018	0.023	0.023	0.026	0.025
98	19.297	0.054	20.905	19.281	18.484	21.500	19.951	18.025	0.164	0.015	0.167	0.015	0.166	0.014
99	18.046	0.010	19.248	18.043	17.503	19.918	18.620	17.057	0.025	0.009	0.029	0.009	0.031	0.009
103	16.965	0.005	17.831	16.962	16.606	18.282	17.276	16.169	0.013	0.005	0.013	0.004	0.016	0.005
104	17.968	0.006	19.157	17.971	17.468	19.679	18.443	17.024	0.012	0.006	0.015	0.007	0.014	0.007
105	16.973	0.007	17.867	16.973	16.582	18.383	17.338	16.144	0.017	0.006	0.018	0.005	0.018	0.005
106	17.633	0.008	18.745	17.634	17.127	19.240	18.041	16.683	0.022	0.007	0.023	0.007	0.024	0.007
115	18.150	0.005	19.406	18.154	17.614	19.958	18.644	17.168	0.009	0.006	0.010	0.006	0.010	0.006
122	17.937	0.005	19.208	17.936	17.390	19.799	18.504	16.943	0.007	0.006	0.010	0.008	0.011	0.008
123	17.035	0.011	17.936	17.036	16.644	18.399	17.365	16.205	0.019	0.012	0.025	0.016	0.025	0.016
124	19.696	0.019	21.264	19.688	18.731	21.920	20.339	18.265	0.047	0.018	0.050	0.019	0.051	0.019
127	16.665	0.004	17.472	16.664	16.298	17.968	16.996	15.861	0.010	0.005	0.011	0.006	0.011	0.005
133	18.047	0.005	19.258	18.046	17.535	19.797	18.531	17.090	0.011	0.005	0.013	0.006	0.014	0.006
139	17.647	0.007	18.737	17.648	17.199	19.285	18.109	16.757	0.018	0.006	0.019	0.006	0.019	0.006
140	15.569	0.003	16.177	15.569	15.307	16.532	15.791	14.875	0.007	0.004	0.008	0.005	0.008	0.005
142	17.209	0.016	18.173	17.212	16.695	18.743	17.660	16.250	0.044	0.009	0.046	0.007	0.045	0.006
143	19.864	0.019	21.454	19.857	18.825	22.109	20.495	18.355	0.038	0.012	0.039	0.012	0.039	0.012
144	20.903	0.031	22.586	20.899	19.502	23.478	21.613	19.015	0.050	0.031	0.060	0.037	0.059	0.036
145	20.703	0.021	22.389	20.699	19.412	23.126	21.375	18.930	0.033	0.024	0.036	0.026	0.036	0.027
151	16.811	0.012	17.682	16.816	16.439	18.115	17.116	16.000	0.029	0.009	0.031	0.010	0.032	0.010

Table 2—Continued

ID	$<r>$[a] (mag)	RMS_r[b] (mag)	g[c] (mag)	r[c] (mag)	i[c] (mag)	B[d] (mag)	V[d] (mag)	I[e] (mag)	$A_{r,N=1}$[f] (mag)	min $A_{r,N=1}$[g] (mag)	$A_{r,N=2}$[f] (mag)	min $A_{r,N=2}$[g] (mag)	$A_{r,N=3}$[f]	min $A_{r,N=3}$[g]
153	20.025	0.017	21.722	20.029	19.088	22.238	20.645	18.623	0.041	0.016	0.042	0.017	0.040	0.015
157	17.687	0.009	18.853	17.688	17.110	19.311	18.094	16.663	0.020	0.007	0.025	0.008	0.026	0.007
160	16.737	0.008	17.538	16.742	16.403	17.955	17.000	15.967	0.019	0.006	0.021	0.007	0.021	0.006
161	16.351	0.009	17.098	16.352	16.051	17.514	16.627	15.616	0.015	0.013	0.015	0.013	0.019	0.017
163	17.483	0.006	18.532	17.482	17.032	19.065	17.894	16.591	0.012	0.007	0.015	0.009	0.016	0.009
164	16.986	0.009	17.852	16.989	16.592	18.369	17.341	16.153	0.021	0.005	0.021	0.005	0.024	0.006
165	20.448	0.027	22.126	20.454	19.166	22.828	21.112	18.684	0.061	0.022	0.061	0.022	0.059	0.021
169	20.814	0.034	22.412	20.835	19.505	23.042	21.441	19.022	0.069	0.028	0.077	0.030	0.078	0.031
171	15.952	0.005	16.649	15.953	15.631	17.061	16.207	15.195	0.010	0.003	0.012	0.004	0.013	0.004
174	18.091	0.007	19.358	18.094	17.464	19.839	18.539	17.014	0.013	0.006	0.021	0.008	0.021	0.008
182	18.076	0.006	19.354	18.077	17.538	19.885	18.574	17.093	0.014	0.005	0.015	0.006	0.021	0.008
183	21.154	0.030	22.851	21.141	19.637	23.504	21.792	19.145	0.035	0.034	0.045	0.043	0.044	0.042
187	18.057	0.009	19.430	18.059	17.519	19.851	18.535	17.073	0.018	0.008	0.025	0.002	0.024	0.002
192	16.755	0.004	17.601	16.756	16.392	18.077	17.094	15.955	0.008	0.004	0.009	0.005	0.010	0.005
194	18.471	0.008	19.900	18.469	17.845	20.428	18.992	17.395	0.014	0.007	0.020	0.009	0.020	0.009
198	18.014	0.005	19.265	18.015	17.504	19.830	18.573	17.059	0.012	0.006	0.013	0.006	0.013	0.006
208	18.570	0.005	20.027	18.570	17.910	20.580	19.144	17.458	0.008	0.007	0.008	0.007	0.009	0.008
209	19.461	0.009	21.105	19.463	18.566	21.705	20.094	18.104	0.014	0.014	0.015	0.014	0.019	0.018
211	16.178	0.004	16.877	16.175	15.867	17.414	16.548	15.432	0.008	0.004	0.008	0.004	0.008	0.004
214	18.184	0.007	19.467	18.184	17.619	20.119	18.789	17.172	0.020	0.007	0.022	0.007	0.022	0.008
216	15.141	0.004	15.666	15.141	14.885	16.043	15.359	14.453	0.007	0.004	0.007	0.004	0.010	0.006
218	17.097	0.006	18.038	17.096	16.681	18.482	17.430	16.241	0.016	0.006	0.019	0.006	0.019	0.006
220	20.227	0.035	21.845	20.242	18.993	22.503	20.900	18.514	0.088	0.019	0.088	0.019	0.094	0.020
223	17.212	0.010	18.186	17.216	16.768	18.615	17.529	16.327	0.025	0.006	0.024	0.005	0.025	0.006
229	16.124	0.007	16.881	16.130	15.801	16.972	16.159	15.366	0.014	0.010	0.019	0.012	0.024	0.015
232	19.151	0.021	20.702	19.161	18.337	21.397	19.863	17.878	0.044	0.017	0.062	0.014	0.059	0.012
233	19.728	0.013	21.428	19.724	18.706	22.090	20.428	18.238	0.027	0.013	0.034	0.016	0.034	0.016
234	16.723	0.006	17.559	16.724	16.356	18.081	17.115	15.918	0.010	0.005	0.013	0.007	0.017	0.008
237	19.335	0.009	20.996	19.334	18.490	21.566	19.987	18.029	0.014	0.009	0.016	0.010	0.016	0.011
240	19.758	0.010	21.404	19.757	18.798	22.067	20.434	18.332	0.012	0.012	0.013	0.012	0.014	0.013
241	18.578	0.010	19.984	18.575	17.900	20.556	19.157	17.448	0.027	0.007	0.028	0.007	0.030	0.008
248	17.683	0.004	18.794	17.682	17.165	19.332	18.123	16.720	0.008	0.005	0.008	0.005	0.011	0.007
249	15.506	0.003	16.131	15.506	15.221	16.460	15.726	14.787	0.004	0.004	0.004	0.004	0.005	0.005
251	16.903	0.012	17.772	16.904	16.528	18.234	17.240	16.090	0.018	0.016	0.021	0.017	0.019	0.016

Table 2—Continued

ID	$<r>$[a] (mag)	RMS_r[b] (mag)	g[c] (mag)	r[c] (mag)	i[c] (mag)	B[d] (mag)	V[d] (mag)	I[e] (mag)	$A_{r,N=1}$[f] (mag)	min $A_{r,N=1}$[g] (mag)	$A_{r,N=2}$[f] (mag)	min $A_{r,N=2}$[g] (mag)	$A_{r,N=3}$[f]	min $A_{r,N=3}$[g]
253	17.292	0.006	18.295	17.291	16.860	18.791	17.666	16.419	0.013	0.007	0.019	0.008	0.019	0.008
257	16.127	0.004	16.856	16.127	15.765	17.210	16.367	15.328	0.008	0.004	0.009	0.004	0.011	0.005
258	17.066	0.003	18.000	17.067	16.680	18.438	17.413	16.242	0.005	0.004	0.005	0.004	0.005	0.004
261	18.320	0.012	19.734	18.319	17.616	20.332	18.954	17.163	0.032	0.006	0.031	0.006	0.035	0.007
262	17.916	0.024	19.195	17.911	17.424	19.610	18.358	16.981	0.068	0.009	0.068	0.009	0.075	0.009
269	17.327	0.014	18.311	17.324	16.892	18.821	17.719	16.452	0.035	0.003	0.035	0.003	0.035	0.003
286	21.249	0.045	22.884	21.253	19.767	23.662	21.907	19.276	0.070	0.049	0.083	0.059	0.088	0.062
287	18.231	0.006	19.608	18.235	17.653	20.111	18.745	17.206	0.011	0.005	0.013	0.006	0.012	0.006
288	18.535	0.036	19.880	18.538	17.855	20.457	19.114	17.402	0.106	0.017	0.107	0.014	0.105	0.014
290	16.416	0.005	17.197	16.412	16.061	17.614	16.711	15.625	0.010	0.007	0.012	0.006	0.012	0.006
292	15.609	0.005	16.241	15.607	15.306	16.564	15.818	14.871	0.010	0.006	0.010	0.006	0.012	0.006
294	19.185	0.015	20.773	19.180	18.324	21.359	19.773	17.863	0.033	0.015	0.031	0.014	0.034	0.015
295	17.777	0.005	19.014	17.778	17.211	19.490	18.242	16.764	0.009	0.006	0.014	0.008	0.014	0.008
298	17.783	0.005	18.949	17.784	17.262	19.411	18.221	16.817	0.008	0.006	0.009	0.007	0.011	0.008
299	18.706	0.006	20.233	18.705	18.030	20.748	19.289	17.578	0.009	0.007	0.011	0.008	0.016	0.010
300	16.025	0.005	16.706	16.023	15.690	17.076	16.258	15.254	0.008	0.000	0.010	0.006	0.012	0.008
303	18.149	0.020	19.483	18.144	17.586	20.010	18.696	17.140	0.060	0.011	0.063	0.010	0.064	0.011
305	20.137	0.025	22.001	20.140	19.025	22.462	20.783	18.552	0.048	0.022	0.050	0.023	0.049	0.023
307	20.322	0.030	22.029	20.332	19.143	22.579	21.002	18.666	0.065	0.022	0.070	0.025	0.068	0.023
311	18.253	0.035	19.564	18.272	17.637	20.125	18.801	17.187	0.103	0.015	0.100	0.012	0.103	0.012
314	15.507	0.007	16.127	15.510	15.267	16.531	15.779	14.836	0.011	0.009	0.013	0.010	0.016	0.012
315	20.247	0.016	21.925	20.245	19.195	22.622	20.921	18.724	0.020	0.017	0.022	0.019	0.023	0.020
318	19.245	0.011	20.909	19.251	18.331	21.535	19.945	17.867	0.017	0.011	0.017	0.011	0.021	0.014
319	15.952	0.005	16.535	15.952	15.639	16.987	16.178	15.204	0.008	0.006	0.011	0.007	0.011	0.007
320	16.040	0.009	16.689	16.040	15.737	17.129	16.294	15.302	0.014	0.010	0.014	0.010	0.015	0.010
321	20.817	0.026	22.459	20.830	19.455	23.149	21.452	18.969	0.033	0.031	0.040	0.038	0.040	0.038
322	18.302	0.007	19.643	18.302	17.722	20.229	18.850	17.274	0.009	0.008	0.014	0.013	0.014	0.012
324	20.560	0.021	22.255	20.558	19.249	23.122	21.379	18.767	0.028	-0.028	0.029	-0.029	0.027	-0.027
326	19.977	0.031	21.624	19.981	18.861	22.244	20.592	18.388	0.077	0.025	0.081	0.023	0.083	0.024
327	16.229	0.005	16.879	16.230	15.900	17.328	16.456	15.464	0.010	0.004	0.011	0.004	0.012	0.004
328	16.566	0.005	17.344	16.564	16.172	17.849	16.899	15.733	0.009	0.002	0.011	0.000	0.018	0.003
332	20.549	0.026	22.226	20.556	19.259	22.925	21.212	18.776	0.061	0.023	0.063	0.024	0.060	0.023
334	17.772	0.010	18.876	17.772	17.286	19.422	18.211	16.842	0.021	0.008	0.033	0.011	0.033	0.011
335	17.557	0.010	18.663	17.559	17.093	19.096	17.941	16.650	0.021	0.009	0.024	0.009	0.024	0.008

Table 2—Continued

ID	$<r>$[a] (mag)	RMS_r[b] (mag)	g[c] (mag)	r[c] (mag)	i[c] (mag)	B[d] (mag)	V[d] (mag)	I[e] (mag)	$A_{r,N=1}$[f] (mag)	min $A_{r,N=1}$[g] (mag)	$A_{r,N=2}$[f] (mag)	min $A_{r,N=2}$[g] (mag)	$A_{r,N=3}$[f]	min $A_{r,N=3}$[g]
340	20.670	0.025	22.415	20.663	19.425	23.089	21.383	18.946	0.044	0.024	0.045	0.025	0.045	0.024
345	18.002	0.007	19.247	18.007	17.519	19.795	18.503	17.075	0.012	0.006	0.013	0.006	0.013	0.006
348	17.970	0.007	19.184	17.972	17.458	19.745	18.486	17.013	0.015	0.008	0.020	0.008	0.020	0.008
350	17.751	0.006	18.891	17.755	17.280	19.384	18.182	16.837	0.011	0.006	0.014	0.007	0.015	0.008
357	19.865	0.013	21.605	19.871	18.870	22.237	20.597	18.402	0.019	0.015	0.021	0.016	0.021	0.016
359	16.366	0.004	17.075	16.365	15.999	17.560	16.655	15.562	0.005	0.005	0.008	0.007	0.008	0.008
361	17.642	0.006	18.714	17.643	17.169	19.184	18.016	16.726	0.008	0.007	0.010	0.008	0.011	0.009
362	18.434	0.014	19.793	18.436	17.836	20.373	19.000	17.387	0.033	0.008	0.046	0.013	0.053	0.014
363	16.159	0.005	16.904	16.156	15.857	17.340	16.479	15.423	0.014	0.005	0.016	0.005	0.016	0.005
364	17.233	0.012	18.213	17.234	16.772	18.636	17.555	16.330	0.027	0.011	0.033	0.014	0.043	0.017
366	19.112	0.008	20.693	19.116	18.340	21.325	19.757	17.883	0.009	0.009	0.010	0.009	0.011	0.010
368	20.312	0.027	22.000	20.307	19.113	22.734	21.043	18.636	0.060	0.018	0.060	0.018	0.066	0.020
369	18.890	0.008	20.378	18.888	18.149	20.981	19.546	17.693	0.013	0.008	0.023	0.013	0.022	0.013
370	20.417	0.024	22.183	20.425	19.208	22.862	21.172	18.730	0.049	0.026	0.053	0.028	0.051	0.026
373	16.185	0.007	16.933	16.182	15.878	17.380	16.507	15.444	0.012	0.006	0.016	0.007	0.021	0.011
374	17.687	0.010	18.811	17.688	17.198	19.314	18.125	16.754	0.031	0.007	0.032	0.007	0.035	0.008
377	20.822	0.025	22.572	20.823	19.542	23.304	21.585	19.061	0.037	0.030	0.042	0.034	0.041	0.033
378	17.828	0.005	18.968	17.829	17.332	19.496	18.281	16.888	0.009	0.005	0.013	0.007	0.014	0.008
380	17.539	0.006	18.617	17.535	17.068	19.068	17.924	16.625	0.013	0.006	0.014	0.006	0.015	0.006
381	17.398	0.007	18.400	17.403	16.916	18.929	17.772	16.472	0.015	0.009	0.020	0.010	0.019	0.010
387	17.284	0.006	18.209	17.288	16.826	18.724	17.631	16.383	0.011	0.006	0.014	0.007	0.015	0.007
388	20.684	0.022	22.322	20.676	19.259	23.139	21.423	18.771	0.029	0.025	0.030	0.026	0.033	0.029
389	18.076	0.017	19.271	18.083	17.499	19.918	18.630	17.051	0.048	0.008	0.046	0.007	0.048	0.007
394	18.066	0.007	19.395	18.069	17.431	19.956	18.603	16.980	0.014	0.006	0.014	0.006	0.014	0.006
396	16.794	0.005	17.628	16.795	16.407	18.131	17.128	15.969	0.009	0.006	0.013	0.008	0.013	0.008
399	15.729	0.006	16.383	15.730	15.413	16.723	15.947	14.978	0.013	0.005	0.014	0.005	0.014	0.005
402	16.364	0.006	17.136	16.366	16.010	17.629	16.694	15.573	0.017	0.005	0.017	0.004	0.017	0.004
404	18.149	0.032	19.460	18.142	17.645	19.860	18.593	17.201	0.086	0.014	0.089	0.013	0.087	0.013
406	21.343	0.039	23.061	21.356	19.867	23.779	22.045	19.376	0.061	0.053	0.076	0.066	0.077	0.066
409	18.080	0.006	19.352	18.081	17.471	19.886	18.594	17.022	0.010	0.007	0.014	0.009	0.016	0.010
410	17.516	0.010	18.577	17.511	17.031	19.170	18.000	16.588	0.026	0.007	0.031	0.009	0.030	0.008
413	18.210	0.007	19.523	18.217	17.621	20.123	18.757	17.172	0.013	0.007	0.017	0.008	0.017	0.009
414	19.286	0.012	20.901	19.283	18.431	21.503	19.912	17.970	0.022	0.000	0.027	0.019	0.035	0.016
415	17.176	0.009	18.179	17.176	16.796	18.634	17.553	16.358	0.019	0.009	0.024	0.012	0.024	0.011

Table 2—Continued

ID	$<r>$[a] (mag)	RMS_r[b] (mag)	g[c] (mag)	r[c] (mag)	i[c] (mag)	B[d] (mag)	V[d] (mag)	I[e] (mag)	$A_{r,N=1}$[f] (mag)	min $A_{r,N=1}$[g] (mag)	$A_{r,N=2}$[f] (mag)	min $A_{r,N=2}$[g] (mag)	$A_{r,N=3}$[f]	min $A_{r,N=3}$[g]
416	19.511	0.042	21.107	19.483	18.554	21.690	20.121	18.089	0.117	0.014	0.118	0.013	0.120	0.013
417	17.341	0.009	18.320	17.346	16.902	18.844	17.736	16.460	0.023	0.008	0.026	0.006	0.024	0.006
418	19.220	0.008	20.862	19.221	18.329	21.496	19.886	17.867	0.010	0.010	0.015	0.014	0.016	0.015
420	18.768	0.035	20.130	18.794	18.064	21.958	20.380	17.609	0.096	-0.096	0.099	-0.099	0.098	-0.098
421	20.991	0.029	22.704	20.985	19.626	23.437	21.715	19.141	0.028	-0.028	0.027	-0.027	0.029	-0.029
422	16.902	0.012	17.722	16.902	16.511	18.230	17.210	16.072	0.034	0.007	0.034	0.006	0.035	0.006
424	16.031	0.006	16.689	16.034	15.728	17.131	16.309	15.293	0.010	0.007	0.010	0.007	0.011	0.007
426	15.762	0.009	16.353	15.764	15.440	16.773	15.991	15.005	0.021	0.007	0.027	0.010	0.028	0.010
428	20.207	0.020	21.923	20.213	19.073	22.597	20.933	18.598	0.040	0.019	0.054	0.024	0.053	0.024
430	15.892	0.005	16.554	15.890	15.595	16.914	16.114	15.161	0.010	0.005	0.010	0.004	0.012	0.005
432	16.605	0.005	17.389	16.604	16.269	17.876	16.936	15.833	0.009	0.006	0.011	0.007	0.010	0.006
434	18.507	0.021	19.910	18.497	17.868	20.408	18.997	17.418	0.060	0.007	0.063	0.007	0.062	0.007
438	18.984	0.018	20.553	18.990	18.256	21.038	19.559	17.801	0.035	0.019	0.037	0.017	0.045	0.024
442	16.733	0.008	17.505	16.731	16.334	18.010	17.036	15.896	0.021	0.010	0.021	0.004	0.023	0.005
448	17.266	0.011	18.217	17.267	16.825	18.728	17.630	16.383	0.019	0.013	0.020	0.014	0.020	0.013
450	16.091	0.005	16.775	16.091	15.764	17.249	16.393	15.328	0.013	0.004	0.014	0.004	0.014	0.004
453	21.361	0.038	23.041	21.360	19.876	23.709	22.010	19.385	0.023	-0.023	0.034	-0.034	0.036	-0.036
454	17.393	0.009	18.404	17.391	16.945	18.926	17.804	16.504	0.011	0.011	0.012	0.012	0.018	0.018
463	18.683	0.006	20.155	18.688	17.978	20.718	19.266	17.524	0.010	0.009	0.013	0.012	0.013	0.012
464	16.233	0.003	16.926	16.235	15.889	17.442	16.560	15.452	0.004	0.003	0.007	0.006	0.006	0.005
467	20.481	0.021	22.172	20.490	19.220	22.716	21.109	18.739	0.037	0.025	0.053	0.033	0.053	0.033
468	20.574	0.040	22.253	20.581	19.203	23.014	21.259	18.718	0.105	0.025	0.106	0.026	0.106	0.026
469	16.403	0.005	17.110	16.407	16.040	17.594	16.696	15.602	0.009	0.006	0.011	0.006	0.010	0.006
470	16.168	0.004	16.895	16.168	15.842	17.339	16.480	15.407	0.007	0.004	0.008	0.005	0.010	0.006
471	15.595	0.004	16.162	15.595	15.278	16.568	15.817	14.843	0.008	0.004	0.009	0.004	0.009	0.004
472	21.191	0.028	22.939	21.187	19.781	23.587	21.890	19.293	0.024	-0.024	0.025	-0.025	0.022	-0.022
476	21.456	0.044	23.169	21.481	19.933	23.840	22.089	19.439	0.063	0.054	0.067	0.056	0.067	0.057
478	17.945	0.009	19.158	17.944	17.421	19.691	18.443	16.976	0.020	0.009	0.020	0.008	0.021	0.008
480	18.503	0.010	19.927	18.509	17.795	20.471	19.070	17.340	0.025	0.012	0.030	0.013	0.032	0.014
481	19.148	0.032	20.640	19.161	18.321	21.354	19.821	17.861	0.080	0.025	0.085	0.024	0.091	0.024
482	15.217	0.003	15.711	15.217	14.941	16.149	15.447	14.508	0.005	0.004	0.005	0.004	0.006	0.004
483	15.475	0.003	16.027	15.477	15.187	16.467	15.725	14.753	0.006	0.004	0.009	0.007	0.010	0.007
486	16.697	0.005	17.566	16.703	16.276	18.034	17.046	15.836	0.010	0.006	0.013	0.000	0.018	0.000
487	17.938	0.009	19.195	17.944	17.398	19.677	18.405	16.951	0.015	0.010	0.020	0.012	0.021	0.012

Table 2—Continued

ID	$<r>$[a] (mag)	RMS_r[b] (mag)	g[c] (mag)	r[c] (mag)	i[c] (mag)	B[d] (mag)	V[d] (mag)	I[e] (mag)	$A_{r,N=1}$[f] (mag)	min $A_{r,N=1}$[g] (mag)	$A_{r,N=2}$[f] (mag)	min $A_{r,N=2}$[g] (mag)	$A_{r,N=3}$[f]	min $A_{r,N=3}$[g]
489	20.841	0.030	22.501	20.856	19.415	23.284	21.557	18.926	0.061	0.034	0.069	0.038	0.073	0.040
491	17.816	0.008	18.956	17.817	17.271	19.544	18.278	16.825	0.021	0.007	0.023	0.006	0.022	0.006
493	16.663	0.005	17.471	16.664	16.270	17.933	16.961	15.831	0.010	0.006	0.011	0.006	0.012	0.007
494	18.972	0.008	20.553	18.971	18.125	21.160	19.614	17.664	0.011	0.011	0.012	0.011	0.011	0.011
495	17.199	0.009	18.086	17.199	16.807	18.685	17.607	16.368	0.022	0.008	0.023	0.008	0.026	0.009
499	17.871	0.005	19.090	17.873	17.384	19.615	18.380	16.941	0.008	0.006	0.011	0.007	0.012	0.008
500	16.132	0.006	16.828	16.131	15.793	17.299	16.430	15.357	0.013	0.005	0.016	0.006	0.016	0.006
501	20.346	0.030	22.056	20.344	19.170	22.707	21.025	18.694	0.065	0.021	0.069	0.019	0.065	0.020
502	17.746	0.008	18.896	17.748	17.253	19.394	18.193	16.809	0.020	0.008	0.021	0.008	0.024	0.010
503	20.245	0.019	22.028	20.234	19.151	22.565	20.933	18.680	0.037	0.020	0.038	0.020	0.044	0.023
505	17.739	0.008	18.901	17.737	17.221	19.354	18.142	16.776	0.016	0.009	0.017	0.009	0.018	0.010
506	21.853	0.056	23.537	21.850	20.162	24.194	22.458	19.662	0.090	0.060	0.093	0.063	0.097	0.066
517	17.856	0.011	18.967	17.855	17.328	19.586	18.356	16.883	0.030	0.007	0.032	0.007	0.032	0.007
519	19.779	0.013	21.465	19.780	18.646	22.151	20.487	18.172	0.022	0.015	0.025	0.017	0.024	0.016
521	18.700	0.006	20.211	18.701	17.994	20.770	19.319	17.541	0.009	0.008	0.011	0.009	0.011	0.009
522	17.383	0.006	18.405	17.383	16.969	18.921	17.804	16.529	0.010	0.007	0.015	0.011	0.015	0.010
524	21.645	0.040	23.353	21.640	20.042	24.031	22.327	19.546	0.029	-0.029	0.033	-0.033	0.033	-0.033
527	21.538	0.050	23.184	21.541	19.968	23.951	22.194	19.472	0.066	0.060	0.078	0.071	0.086	0.079
528	18.793	0.006	20.317	18.797	18.110	20.847	19.391	17.657	0.010	0.008	0.012	0.010	0.012	0.010
529	20.233	0.017	21.957	20.235	19.064	22.646	20.970	18.588	0.031	0.021	0.038	0.026	0.038	0.026
531	21.352	0.042	23.152	21.351	19.878	23.985	22.154	19.388	0.053	0.048	0.054	0.049	0.061	0.055
539	21.355	0.040	23.049	21.364	19.803	23.651	21.882	19.308	0.055	0.050	0.059	0.054	0.065	0.060
546	16.451	0.006	17.247	16.453	16.077	17.676	16.743	15.639	0.012	0.005	0.012	0.005	0.012	0.005
548	20.304	0.018	21.956	20.312	19.077	22.872	21.119	18.598	0.032	0.026	0.036	0.028	0.036	0.028
550	17.252	0.014	18.231	17.256	16.812	18.785	17.655	16.370	0.039	0.008	0.038	0.006	0.039	0.006
552	15.989	0.007	16.645	15.987	15.667	17.079	16.256	15.232	0.016	0.007	0.016	0.006	0.016	0.006
553	17.805	0.007	18.935	17.808	17.286	19.462	18.255	16.841	0.016	0.006	0.019	0.007	0.020	0.007
555	18.319	0.020	19.649	18.284	17.655	20.178	18.838	17.205	0.049	0.016	0.052	0.015	0.050	0.015
556	16.978	0.014	17.899	16.984	16.538	18.351	17.340	16.097	0.041	0.011	0.041	0.010	0.043	0.011
558	16.729	0.007	17.575	16.729	16.367	18.088	17.118	15.930	0.014	0.007	0.016	0.007	0.019	0.009
561	18.592	0.009	19.997	18.595	17.875	20.503	19.096	17.420	0.020	0.010	0.023	0.012	0.022	0.011
563	19.840	0.023	21.532	19.839	18.723	22.057	20.489	18.249	0.039	0.026	0.044	0.028	0.046	0.029
564	17.065	0.006	17.959	17.062	16.625	18.447	17.411	16.184	0.009	0.007	0.012	0.008	0.023	0.013
565	17.352	0.006	18.370	17.351	16.900	18.868	17.748	16.459	0.013	0.006	0.015	0.006	0.016	0.006

Table 2—Continued

ID	$<r>$[a] (mag)	RMS_r[b] (mag)	g[c] (mag)	r[c] (mag)	i[c] (mag)	B[d] (mag)	V[d] (mag)	I[e] (mag)	$A_{r,N=1}$[f] (mag)	min $A_{r,N=1}$[g] (mag)	$A_{r,N=2}$[f] (mag)	min $A_{r,N=2}$[g] (mag)	$A_{r,N=3}$[f]	min $A_{r,N=3}$[g]
567	22.014	0.064	23.663	22.007	20.368	24.327	22.600	19.869	0.087	0.064	0.136	0.095	0.312	0.226
571	18.202	0.007	19.531	18.205	17.637	20.052	18.695	17.189	0.010	0.009	0.017	0.013	0.020	0.017
572	17.881	0.007	19.019	17.882	17.350	19.636	18.373	16.904	0.014	0.006	0.016	0.007	0.016	0.007
573	17.055	0.012	17.955	17.054	16.617	18.475	17.411	16.176	0.031	0.008	0.032	0.007	0.033	0.007
576	19.353	0.009	21.012	19.356	18.483	21.630	20.013	18.021	0.013	0.009	0.013	0.010	0.013	0.010
579	18.367	0.016	19.646	18.371	17.675	20.209	18.874	17.221	0.045	0.008	0.045	0.006	0.047	0.006
580	16.753	0.006	17.568	16.751	16.337	18.056	17.065	15.897	0.012	0.007	0.013	0.007	0.012	0.007
582	20.380	0.028	22.085	20.373	19.166	22.743	21.031	18.689	0.070	0.026	0.077	0.023	0.079	0.026
586	15.962	0.004	16.611	15.961	15.609	17.088	16.259	15.172	0.007	0.005	0.008	0.007	0.011	0.009
587	16.568	0.022	17.378	16.572	16.051	17.892	16.906	15.606	0.057	0.013	0.053	0.011	0.053	0.011
589	16.930	0.009	17.869	16.927	16.528	18.274	17.261	16.089	0.023	0.007	0.029	0.007	0.030	0.007
592	17.094	0.005	17.994	17.093	16.663	18.517	17.471	16.223	0.010	0.005	0.013	0.007	0.014	0.007
594	17.839	0.006	19.055	17.838	17.317	19.567	18.306	16.872	0.012	0.007	0.018	0.008	0.018	0.008
596	16.761	0.013	17.641	16.768	16.400	18.109	17.116	15.963	0.034	0.008	0.034	0.008	0.036	0.008
598	15.748	0.006	16.325	15.745	15.427	16.789	15.992	14.992	0.012	0.007	0.015	0.008	0.019	0.009
600	16.744	0.009	17.601	16.750	16.333	18.043	17.050	15.893	0.023	0.006	0.024	0.006	0.025	0.006
602	17.858	0.007	19.004	17.863	17.326	19.540	18.282	16.880	0.012	0.000	0.018	0.012	0.017	0.011
603	18.004	0.008	19.190	18.005	17.488	19.635	18.402	17.043	0.015	0.005	0.023	0.007	0.025	0.007
604	18.892	0.018	20.403	18.888	18.130	20.907	19.435	17.674	0.034	0.025	0.036	0.025	0.035	0.024
606	16.337	0.007	17.068	16.337	15.989	17.481	16.580	15.552	0.018	0.006	0.020	0.006	0.020	0.006
607	16.423	0.003	17.251	16.424	16.033	17.632	16.701	15.594	0.004	0.003	0.004	0.004	0.005	0.005
608	16.442	0.006	17.180	16.443	16.101	17.658	16.734	15.664	0.017	-0.017	0.019	-0.019	0.018	-0.018
611	17.576	0.011	18.677	17.582	17.069	19.169	17.984	16.624	0.030	0.009	0.033	0.010	0.033	0.010
612	17.263	0.005	18.227	17.262	16.849	18.730	17.644	16.410	0.009	0.007	0.010	0.006	0.010	0.006
614	16.489	0.005	17.221	16.490	16.105	17.679	16.755	15.666	0.009	0.007	0.012	0.009	0.010	0.006
619	19.336	0.009	20.969	19.345	18.350	21.656	20.014	17.882	0.011	0.010	0.011	0.010	0.011	0.010
620	17.819	0.004	18.930	17.822	17.259	19.479	18.260	16.812	0.008	0.007	0.009	0.007	0.009	0.008
622	17.970	0.005	19.150	17.970	17.401	19.739	18.459	16.953	0.007	0.003	0.012	0.012	0.019	0.019
623	20.132	0.018	21.905	20.124	18.981	22.596	20.873	18.506	0.027	0.020	0.032	0.020	0.049	0.034
625	20.230	0.022	21.948	20.240	19.081	22.405	20.810	18.606	0.032	0.031	0.041	0.000	0.053	0.006
626	15.790	0.005	16.472	15.792	15.455	16.827	16.014	15.018	0.008	0.005	0.009	0.006	0.010	0.006
627	20.881	0.032	22.552	20.891	19.517	23.200	21.492	19.031	0.068	0.040	0.070	0.042	0.067	0.040
629	18.901	0.011	20.519	18.906	18.147	21.081	19.552	17.691	0.025	0.009	0.027	0.009	0.032	0.011
633	18.268	0.006	19.571	18.269	17.690	20.187	18.839	17.242	0.009	0.007	0.009	0.007	0.013	0.007

Table 2—Continued

ID	$<r>$[a] (mag)	RMS_r[b] (mag)	g[c] (mag)	r[c] (mag)	i[c] (mag)	B[d] (mag)	V[d] (mag)	I[e] (mag)	$A_{r,N=1}$[f] (mag)	min $A_{r,N=1}$[g] (mag)	$A_{r,N=2}$[f] (mag)	min $A_{r,N=2}$[g] (mag)	$A_{r,N=3}$[f]	min $A_{r,N=3}$[g]
634	19.895	0.034	21.604	19.881	18.882	22.418	20.726	18.415	0.089	0.019	0.097	0.019	0.100	0.019
635	17.066	0.009	17.927	17.070	16.596	18.461	17.407	16.153	0.023	0.006	0.023	0.006	0.026	0.006
638	19.150	0.007	20.839	19.155	18.340	21.351	19.749	17.881	0.010	0.009	0.010	0.009	0.012	0.011
639	17.393	0.004	18.457	17.397	16.914	18.943	17.782	16.471	0.006	0.004	0.009	0.006	0.010	0.007
643	15.863	0.005	16.499	15.865	15.532	16.974	16.141	15.096	0.011	0.007	0.012	0.005	0.012	0.006
645	20.271	0.023	22.016	20.266	19.108	22.695	21.002	18.632	0.046	0.028	0.051	0.026	0.057	0.030
646	20.556	0.020	22.320	20.562	19.323	22.929	21.263	18.844	0.042	0.026	0.040	0.025	0.040	0.025
647	19.499	0.010	21.143	19.501	18.581	21.844	20.173	18.116	0.015	0.011	0.016	0.012	0.016	0.012
650	17.328	0.011	18.302	17.325	16.879	18.860	17.751	16.438	0.028	0.007	0.029	0.007	0.029	0.007
651	15.546	0.003	16.088	15.546	15.253	16.521	15.777	14.819	0.005	0.004	0.007	0.006	0.007	0.006
654	19.188	0.009	20.849	19.183	18.358	21.437	19.832	17.898	0.014	0.009	0.017	0.011	0.017	0.011
658	20.173	0.020	21.852	20.183	19.075	22.489	20.883	18.602	0.035	0.019	0.036	0.021	0.037	0.021
661	16.911	0.004	17.785	16.910	16.497	18.242	17.236	16.058	0.007	0.004	0.008	0.004	0.010	0.005
662	20.466	0.018	22.200	20.470	19.197	22.913	21.240	18.716	0.026	0.020	0.027	0.021	0.031	0.024
663	16.698	0.009	17.482	16.694	16.325	17.987	17.029	15.887	0.025	0.006	0.024	0.005	0.023	0.005
664	17.812	0.016	18.877	17.810	17.273	19.410	18.198	16.827	0.036	0.017	0.036	0.017	0.044	0.019
666	15.954	0.004	16.682	15.953	15.592	17.088	16.236	15.155	0.007	0.005	0.008	0.006	0.011	0.008
669	20.887	0.033	22.542	20.880	19.576	23.175	21.481	19.093	0.050	0.035	0.051	0.035	0.050	0.035
670	15.848	0.006	16.507	15.851	15.533	16.944	16.130	15.097	0.011	0.006	0.011	0.006	0.013	0.007
673	18.239	0.006	19.521	18.238	17.624	20.103	18.744	17.175	0.010	0.006	0.010	0.006	0.011	0.007
675	16.685	0.009	17.475	16.688	16.289	17.934	16.957	15.850	0.025	0.006	0.026	0.006	0.026	0.006
676	18.134	0.007	19.460	18.138	17.491	19.981	18.637	17.040	0.015	0.006	0.016	0.006	0.016	0.006
680	17.291	0.004	18.203	17.291	16.814	18.741	17.644	16.371	0.004	0.004	0.005	0.005	0.008	0.008
685	17.778	0.010	18.931	17.774	17.273	19.452	18.243	16.829	0.024	0.010	0.023	0.009	0.024	0.009
686	17.636	0.011	18.784	17.640	17.107	19.280	18.073	16.661	0.030	0.007	0.032	0.007	0.033	0.008
689	17.815	0.034	19.005	17.819	17.504	19.592	18.376	17.069	0.099	0.011	0.110	0.011	0.108	0.010
691	19.950	0.028	21.457	19.954	18.859	22.023	20.453	18.387	0.050	0.040	0.083	0.015	0.097	0.000
697	19.193	0.012	20.760	19.194	18.368	22.913	21.536	17.908	0.027	0.015	0.028	0.015	0.028	0.015
702	17.340	0.011	18.323	17.345	16.779	18.811	17.692	16.331	0.025	0.009	0.027	0.010	0.027	0.010
703	20.276	0.035	21.963	20.272	19.052	22.582	20.903	18.574	0.091	0.031	0.107	0.029	0.108	0.029
705	15.800	0.008	16.482	15.797	15.428	16.912	16.080	14.990	0.013	0.001	0.018	0.013	0.022	0.016
707	20.264	0.033	21.918	20.249	19.104	22.453	20.818	18.629	0.046	0.038	0.046	0.037	0.054	0.044
708	16.928	0.008	17.790	16.926	16.529	18.238	17.247	16.089	0.018	0.008	0.020	0.009	0.020	0.009
710	16.067	0.004	16.742	16.067	15.758	17.200	16.376	15.323	0.006	0.005	0.007	0.006	0.006	0.006

Table 2—Continued

ID	$<r>$[a] (mag)	RMS_r[b] (mag)	g[c] (mag)	r[c] (mag)	i[c] (mag)	B[d] (mag)	V[d] (mag)	I[e] (mag)	$A_{r,N=1}$[f] (mag)	min $A_{r,N=1}$[g] (mag)	$A_{r,N=2}$[f] (mag)	min $A_{r,N=2}$[g] (mag)	$A_{r,N=3}$[f]	min $A_{r,N=3}$[g]
711	18.643	0.046	19.985	18.647	17.870	20.626	19.233	17.413	0.126	0.020	0.126	0.014	0.126	0.014
713	17.923	0.009	19.082	17.925	17.357	19.667	18.397	16.910	0.014	0.013	0.020	0.019	0.021	0.019
714	17.914	0.008	19.101	17.913	17.385	19.578	18.351	16.940	0.013	0.008	0.014	0.009	0.014	0.009
719	19.567	0.033	21.271	19.574	18.630	21.866	20.230	18.165	0.086	0.018	0.085	0.015	0.088	0.015
722	15.937	0.004	16.573	15.939	15.578	16.962	16.142	15.141	0.010	0.005	0.010	0.004	0.010	0.004
724	18.392	0.008	19.764	18.398	17.747	20.339	18.956	17.296	0.013	0.000	0.024	0.020	0.023	0.019
727	20.842	0.023	22.565	20.833	19.494	23.161	21.487	19.010	0.034	0.028	0.035	0.029	0.033	0.028
730	19.594	0.029	21.258	19.578	18.667	21.532	20.003	18.204	0.078	0.015	0.084	0.016	0.086	0.017
736	17.602	0.009	18.651	17.600	17.118	19.188	18.011	16.675	0.016	0.010	0.019	0.011	0.021	0.011
745	18.548	0.009	19.999	18.552	17.875	20.546	19.107	17.423	0.022	0.009	0.021	0.008	0.020	0.008
746	20.410	0.022	22.047	20.410	19.173	22.616	20.957	18.694	0.044	0.022	0.046	0.023	0.046	0.022
747	17.918	0.007	19.110	17.918	17.379	19.644	18.390	16.933	0.017	0.007	0.018	0.007	0.020	0.008
748	21.014	0.028	22.759	21.012	19.648	23.558	21.826	19.163	0.036	0.027	0.036	0.028	0.041	0.032
751	18.944	0.018	20.441	18.949	18.203	21.444	19.812	17.748	0.037	0.010	0.046	0.010	0.050	0.011
756	20.955	0.026	22.686	20.950	19.542	23.276	21.525	19.055	0.045	0.032	0.045	0.032	0.044	0.031
758	18.660	0.007	20.191	18.661	17.984	20.736	19.280	17.532	0.010	0.009	0.010	0.009	0.011	0.010
763	17.584	0.005	18.656	17.583	17.101	19.198	18.012	16.658	0.010	0.006	0.013	0.005	0.013	0.007
767	20.897	0.036	22.699	20.877	19.535	23.342	21.577	19.051	0.068	0.063	0.089	0.081	0.086	0.078
768	16.491	0.007	17.264	16.494	16.115	17.715	16.775	15.677	0.015	0.007	0.017	0.007	0.018	0.007
771	19.617	0.012	21.213	19.612	18.637	21.920	20.304	18.170	0.021	0.014	0.024	0.015	0.024	0.015
772	20.898	0.027	22.515	20.912	19.528	23.214	21.565	19.042	0.047	0.034	0.048	0.034	0.049	0.034
773	20.314	0.020	22.041	20.308	19.227	22.606	20.943	18.756	0.038	0.019	0.038	0.019	0.037	0.019
774	19.436	0.020	21.105	19.429	18.550	21.820	20.221	18.088	0.052	0.011	0.053	0.011	0.050	0.010
777	16.753	0.008	17.596	16.752	16.404	18.057	17.065	15.967	0.019	0.008	0.019	0.007	0.020	0.007
778	16.236	0.005	16.987	16.236	15.816	17.424	16.507	15.376	0.012	0.005	0.013	0.005	0.012	0.005
779	19.403	0.011	21.059	19.407	18.468	21.722	20.104	18.003	0.019	0.005	0.032	0.017	0.026	0.014
780	17.489	0.010	18.529	17.485	16.995	19.072	17.932	16.552	0.022	0.007	0.033	0.009	0.033	0.009
783	22.125	0.066	23.854	22.144	20.429	24.756	22.794	19.927	0.081	0.080	0.080	0.079	0.082	0.081
784	20.501	0.022	22.272	20.490	19.331	22.954	21.224	18.856	0.041	0.021	0.041	0.021	0.043	0.021
785	19.414	0.015	21.055	19.419	18.491	21.586	20.028	18.027	0.041	0.013	0.042	0.012	0.043	0.012
789	21.214	0.035	22.906	21.223	19.712	23.574	21.935	19.220	0.051	0.044	0.051	0.044	0.054	0.046
790	19.780	0.026	21.535	19.766	18.773	22.190	20.563	18.305	0.063	0.016	0.066	0.017	0.069	0.018
793	20.900	0.032	22.596	20.901	19.465	23.270	21.640	18.977	0.044	0.036	0.047	0.038	0.052	0.042
799	17.236	0.007	18.213	17.231	16.794	18.717	17.633	16.354	0.014	0.008	0.019	0.009	0.020	0.009

Table 2—Continued

ID	$<r>$[a] (mag)	RMS_r[b] (mag)	g[c] (mag)	r[c] (mag)	i[c] (mag)	B[d] (mag)	V[d] (mag)	I[e] (mag)	$A_{r,N=1}$[f] (mag)	min $A_{r,N=1}$[g] (mag)	$A_{r,N=2}$[f] (mag)	min $A_{r,N=2}$[g] (mag)	$A_{r,N=3}$[f]	min $A_{r,N=3}$[g]
800	20.920	0.025	22.671	20.913	19.565	23.428	21.663	19.081	0.031	0.026	0.037	0.032	0.037	0.032
802	17.002	0.012	17.868	17.006	16.605	18.377	17.359	16.166	0.031	0.007	0.031	0.006	0.031	0.006
803	17.511	0.006	18.569	17.511	17.001	19.100	17.937	16.557	0.013	0.008	0.019	0.007	0.018	0.009
808	17.578	0.007	18.661	17.578	17.116	19.209	17.996	16.674	0.017	0.006	0.017	0.006	0.018	0.006
809	16.339	0.008	17.081	16.335	16.003	17.540	16.621	15.567	0.016	0.005	0.019	0.006	0.023	0.011
810	19.703	0.043	21.431	19.713	18.738	22.026	20.426	18.271	0.110	0.018	0.134	0.018	0.133	0.018
812	16.409	0.005	17.179	16.407	16.063	17.633	16.739	15.627	0.012	0.004	0.016	0.004	0.016	0.004
813	20.348	0.014	22.123	20.354	19.213	22.787	21.059	18.738	0.017	0.017	0.018	0.017	0.017	0.017
815	19.056	0.019	20.643	19.065	18.267	21.306	19.754	17.809	0.051	0.014	0.048	0.009	0.048	0.009
817	17.008	0.005	17.877	17.009	16.593	18.341	17.334	16.154	0.012	0.004	0.015	0.006	0.015	0.006
818	17.656	0.006	18.747	17.659	17.105	19.265	18.058	16.659	0.012	0.006	0.011	0.006	0.012	0.006
819	18.314	0.022	19.735	18.306	17.715	20.211	18.881	17.266	0.065	0.010	0.064	0.010	0.064	0.009
821	17.142	0.008	18.107	17.136	16.707	18.606	17.525	16.267	0.017	0.008	0.027	0.007	0.030	0.008
822	18.063	0.010	19.388	18.069	17.525	19.774	18.510	17.079	0.024	0.006	0.026	0.006	0.026	0.006
825	16.284	0.006	17.046	16.286	15.917	17.485	16.600	15.479	0.009	0.000	0.024	0.000	0.024	0.001
827	15.773	0.007	16.363	15.774	15.428	16.769	15.991	14.991	0.014	0.008	0.016	0.009	0.018	0.009
828	18.913	0.015	20.389	18.908	18.144	21.101	19.637	17.688	0.034	0.017	0.048	0.018	0.045	0.016
830	16.855	0.006	17.727	16.856	16.436	18.276	17.260	15.995	0.015	0.007	0.016	0.006	0.016	0.006
832	15.918	0.003	16.590	15.916	15.600	17.015	16.213	15.165	0.005	0.004	0.007	0.006	0.007	0.006
834	20.678	0.024	22.454	20.680	19.345	23.042	21.351	18.861	0.043	0.028	0.057	0.036	0.057	0.036
835	19.591	0.030	21.294	19.591	18.636	21.770	20.129	18.170	0.081	0.015	0.080	0.013	0.082	0.013
838	18.494	0.009	19.908	18.491	17.818	20.459	19.034	17.366	0.019	0.007	0.024	0.008	0.025	0.008
841	19.581	0.041	21.265	19.559	18.680	21.917	20.279	18.218	0.107	0.012	0.118	0.012	0.121	0.012
842	21.234	0.034	22.985	21.234	19.782	23.824	21.991	19.293	0.045	0.044	0.048	0.047	0.048	0.047
845	16.371	0.006	17.122	16.370	16.004	17.561	16.654	15.567	0.012	0.007	0.018	0.009	0.020	0.010
850	16.037	0.006	16.756	16.040	15.705	17.188	16.318	15.269	0.013	0.004	0.015	0.004	0.015	0.004
852	17.881	0.010	19.077	17.893	17.372	19.622	18.364	16.927	0.023	0.014	0.025	0.013	0.025	0.014
853	20.984	0.028	22.677	20.975	19.500	23.309	21.642	19.009	0.035	0.034	0.042	0.041	0.043	0.043
854	16.473	0.006	17.230	16.475	16.080	17.663	16.751	15.641	0.014	0.005	0.015	0.005	0.014	0.004
857	17.684	0.006	18.791	17.690	17.181	19.249	18.061	16.737	0.008	0.006	0.010	0.007	0.012	0.008
859	16.429	0.005	17.194	16.427	16.052	17.625	16.718	15.614	0.012	0.006	0.013	0.006	0.013	0.006
860	18.097	0.014	19.331	18.090	17.526	19.876	18.544	17.079	0.034	0.011	0.040	0.010	0.040	0.010
862	21.652	0.046	23.340	21.645	20.161	23.892	22.222	19.670	0.045	-0.045	0.051	-0.051	0.062	-0.062
864	16.776	0.005	17.610	16.776	16.405	18.100	17.097	15.967	0.011	0.005	0.016	0.007	0.016	0.006

Table 2—Continued

ID	$<r>$[a] (mag)	RMS_r[b] (mag)	g[c] (mag)	r[c] (mag)	i[c] (mag)	B[d] (mag)	V[d] (mag)	I[e] (mag)	$A_{r,N=1}$[f] (mag)	min $A_{r,N=1}$[g] (mag)	$A_{r,N=2}$[f] (mag)	min $A_{r,N=2}$[g] (mag)	$A_{r,N=3}$[f] (mag)	min $A_{r,N=3}$[g] (mag)
865	22.150	0.061	23.984	22.139	20.446	24.686	22.835	19.945	0.060	-0.060	0.063	-0.063	0.065	-0.065
867	15.521	0.004	16.118	15.521	15.229	16.518	15.766	14.795	0.005	0.005	0.007	0.006	0.008	0.007
868	21.112	0.027	22.901	21.117	19.734	23.596	21.789	19.248	0.032	0.032	0.033	0.033	0.035	0.035
869	16.460	0.006	17.282	16.457	16.105	17.636	16.698	15.668	0.013	0.005	0.017	0.006	0.018	0.006
870	17.287	0.003	18.266	17.286	16.786	18.759	17.660	16.342	0.006	0.004	0.009	0.006	0.009	0.006
871	18.257	0.007	19.613	18.261	17.670	20.142	18.780	17.222	0.016	0.007	0.020	0.008	0.021	0.008
873	17.118	0.006	18.047	17.119	16.717	18.482	17.442	16.278	0.014	0.006	0.014	0.005	0.019	0.007
875	20.692	0.031	22.453	20.693	19.392	23.027	21.389	18.910	0.046	0.026	0.070	0.036	0.072	0.037
876	16.867	0.010	17.733	16.862	16.473	18.196	17.198	16.035	0.030	0.008	0.032	0.007	0.030	0.006
878	17.745	0.004	18.921	17.746	17.228	19.397	18.163	16.783	0.007	0.004	0.008	0.005	0.011	0.006
880	16.807	0.010	17.685	16.810	16.402	18.150	17.146	15.963	0.015	0.011	0.016	0.012	0.022	0.017
882	18.978	0.008	20.620	18.976	18.209	21.172	19.636	17.753	0.015	0.008	0.016	0.008	0.017	0.009
886	19.984	0.024	21.716	19.971	18.870	22.285	20.658	18.397	0.060	0.017	0.057	0.014	0.059	0.014
888	16.839	0.007	17.720	16.835	16.438	18.238	17.232	15.998	0.015	0.007	0.019	0.006	0.018	0.005
889	18.405	0.005	19.840	18.408	17.787	20.387	19.000	17.337	0.006	0.006	0.007	0.007	0.009	0.009
890	21.988	0.062	23.650	22.001	20.218	24.610	22.639	19.713	0.086	0.080	0.099	0.093	0.104	0.097
891	16.071	0.010	16.755	16.072	15.713	17.167	16.325	15.275	0.025	0.013	0.028	0.009	0.027	0.009
892	16.803	0.006	17.672	16.803	16.404	18.163	17.151	15.965	0.012	0.008	0.014	0.009	0.014	0.009
893	20.642	0.027	22.448	20.632	19.392	23.118	21.413	18.913	0.039	0.030	0.057	0.044	0.056	0.043
901	19.293	0.029	20.843	19.306	18.392	21.226	19.716	17.929	0.078	0.013	0.092	0.016	0.092	0.016
902	17.436	0.008	18.513	17.435	16.948	18.868	17.730	16.505	0.018	0.007	0.021	0.006	0.027	0.009
903	15.462	0.004	16.082	15.460	15.169	16.486	15.730	14.736	0.007	0.003	0.008	0.007	0.007	0.007
904	16.731	0.005	17.584	16.731	16.375	18.074	17.096	15.937	0.008	0.005	0.014	0.006	0.014	0.006
907	20.955	0.028	22.692	20.945	19.474	23.289	21.555	18.984	0.045	0.027	0.052	0.031	0.054	0.032
910	20.885	0.024	22.656	20.889	19.548	23.144	21.487	19.064	0.040	0.033	0.045	0.038	0.046	0.038
912	17.625	0.008	18.714	17.626	17.145	19.214	18.048	16.702	0.014	0.009	0.019	0.009	0.021	0.011
915	17.168	0.004	18.099	17.170	16.729	18.585	17.523	16.288	0.006	0.005	0.008	0.006	0.009	0.007
917	19.239	0.024	20.803	19.233	18.342	21.324	19.750	17.880	0.060	0.016	0.069	0.016	0.069	0.016
920	17.871	0.011	19.085	17.874	17.390	19.569	18.338	16.947	0.025	0.009	0.024	0.008	0.041	0.011
921	19.253	0.007	20.928	19.259	18.415	21.524	19.917	17.955	0.012	0.010	0.013	0.011	0.013	0.011
922	16.535	0.006	17.304	16.540	16.146	17.777	16.840	15.707	0.010	0.008	0.017	0.010	0.019	0.014
924	18.508	0.007	19.850	18.505	17.846	20.439	19.021	17.394	0.013	0.006	0.016	0.007	0.016	0.007
933	17.049	0.009	17.944	17.049	16.605	18.407	17.365	16.164	0.023	0.007	0.027	0.008	0.029	0.008
939	19.730	0.015	21.434	19.723	18.736	22.104	20.435	18.269	0.034	0.015	0.036	0.016	0.036	0.016

Table 2—Continued

ID	$<r>$[a] (mag)	RMS_r[b] (mag)	g[c] (mag)	r[c] (mag)	i[c] (mag)	B[d] (mag)	V[d] (mag)	I[e] (mag)	$A_{r,N=1}$[f] (mag)	min $A_{r,N=1}$[g] (mag)	$A_{r,N=2}$[f] (mag)	min $A_{r,N=2}$[g] (mag)	$A_{r,N=3}$[f]	min $A_{r,N=3}$[g]
941	16.855	0.012	17.789	16.862	16.527	18.173	17.164	16.091	0.027	0.024	0.035	0.030	0.029	0.025
942	17.190	0.010	18.134	17.196	16.750	18.603	17.524	16.309	0.022	0.008	0.027	0.009	0.027	0.009
944	18.765	0.007	20.336	18.769	18.062	20.841	19.385	17.609	0.009	0.009	0.010	0.009	0.011	0.010
951	17.591	0.005	18.718	17.593	17.166	19.214	18.040	16.726	0.010	0.006	0.013	0.008	0.014	0.008
952	17.705	0.008	18.843	17.707	17.210	19.368	18.157	16.767	0.017	0.006	0.019	0.006	0.018	0.006
953	17.428	0.004	18.439	17.427	16.951	18.929	17.809	16.508	0.007	0.004	0.007	0.004	0.011	0.006
956	20.078	0.014	21.802	20.081	19.027	22.446	20.736	18.557	0.018	0.016	0.018	0.016	0.021	0.018
958	16.361	0.005	17.102	16.358	16.020	17.543	16.660	15.583	0.009	0.006	0.009	0.006	0.014	0.008
961	15.712	0.008	16.339	15.716	15.398	16.783	15.968	14.963	0.021	0.007	0.023	0.008	0.023	0.008
962	19.584	0.009	21.280	19.582	18.700	21.872	20.226	18.238	0.016	0.012	0.016	0.012	0.016	0.012
968	17.063	0.007	17.952	17.066	16.624	18.413	17.387	16.183	0.018	0.005	0.020	0.005	0.019	0.004
970	17.094	0.005	18.064	17.095	16.689	18.506	17.427	16.250	0.007	0.006	0.011	0.005	0.011	0.009
971	15.636	0.004	16.256	15.637	15.333	16.640	15.873	14.899	0.008	0.004	0.008	0.004	0.009	0.004
972	17.804	0.008	18.976	17.809	17.269	19.437	18.223	16.823	0.016	0.006	0.015	0.006	0.016	0.006
974	20.926	0.037	22.729	20.929	19.593	23.348	21.651	19.108	0.071	0.053	0.066	0.047	0.086	0.062
975	18.348	0.005	19.725	18.344	17.762	20.279	18.915	17.314	0.009	0.007	0.011	0.008	0.011	0.008
978	18.117	0.011	19.406	18.113	17.541	19.951	18.667	17.094	0.028	0.005	0.028	0.005	0.028	0.005
980	21.561	0.040	23.295	21.571	19.948	24.066	22.255	19.451	0.044	0.042	0.044	0.043	0.050	0.049
983	19.486	0.010	21.199	19.493	18.582	21.778	20.155	18.119	0.012	0.010	0.017	0.013	0.017	0.014
986	17.289	0.005	18.272	17.294	16.852	18.768	17.667	16.411	0.007	0.000	0.010	0.007	0.011	0.008
987	18.839	0.007	20.412	18.840	18.110	20.981	19.507	17.655	0.009	0.008	0.016	0.014	0.018	0.015
990	18.280	0.011	19.549	18.278	17.577	20.114	18.770	17.123	0.027	0.009	0.030	0.008	0.033	0.009
991	19.226	0.018	20.771	19.229	18.400	21.399	19.852	17.941	0.046	0.011	0.047	0.011	0.050	0.012
992	16.703	0.006	17.508	16.706	16.312	17.928	16.965	15.873	0.013	0.006	0.016	0.007	0.016	0.007
993	17.121	0.014	18.098	17.128	16.668	18.581	17.510	16.226	0.035	0.011	0.039	0.009	0.040	0.009
996	17.359	0.012	18.396	17.353	16.902	18.885	17.748	16.460	0.034	0.007	0.038	0.007	0.038	0.008
1000	17.705	0.009	18.862	17.708	17.189	19.335	18.144	16.745	0.028	0.008	0.028	0.006	0.029	0.006
1004	15.472	0.005	16.074	15.469	15.211	16.454	15.703	14.779	0.008	0.005	0.010	0.005	0.009	0.005
1005	17.014	0.011	17.994	17.017	16.654	18.436	17.401	16.216	0.031	0.006	0.033	0.006	0.035	0.006
1006	18.714	0.008	20.249	18.720	18.037	20.756	19.312	17.584	0.015	0.007	0.018	0.008	0.018	0.008
1007	16.700	0.004	17.506	16.701	16.335	17.997	17.030	15.898	0.006	0.004	0.011	0.007	0.011	0.006
1008	15.948	0.005	16.640	15.952	15.605	17.064	16.234	15.169	0.011	0.004	0.012	0.004	0.013	0.004
1010	18.952	0.009	20.438	18.955	18.200	21.054	19.521	17.744	0.022	0.010	0.022	0.010	0.024	0.011
1012	16.319	0.004	17.089	16.316	15.975	17.528	16.629	15.538	0.008	0.005	0.009	0.006	0.011	0.007

Table 2—Continued

ID	$<r>$[a] (mag)	RMS_r[b] (mag)	g[c] (mag)	r[c] (mag)	i[c] (mag)	B[d] (mag)	V[d] (mag)	I[e] (mag)	$A_{r,N=1}$[f] (mag)	min $A_{r,N=1}$[g] (mag)	$A_{r,N=2}$[f] (mag)	min $A_{r,N=2}$[g] (mag)	$A_{r,N=3}$[f]	min $A_{r,N=3}$[g]
1013	17.272	0.016	18.291	17.258	16.820	18.702	17.615	16.378	0.039	0.018	0.042	0.019	0.043	0.020
1014	16.432	0.005	17.136	16.436	16.045	17.560	16.691	15.606	0.012	0.006	0.011	0.005	0.014	0.005
1015	18.851	0.010	20.307	18.864	18.074	20.830	19.399	17.616	0.019	0.008	0.021	0.009	0.024	0.010
1018	16.583	0.021	17.476	16.569	16.230	17.814	16.878	15.794	0.055	0.013	0.057	0.012	0.055	0.012
1021	16.232	0.004	16.892	16.234	15.877	17.326	16.464	15.440	0.007	0.004	0.009	0.005	0.009	0.005
1024	19.477	0.012	21.047	19.483	18.499	21.627	20.087	18.032	0.020	0.012	0.022	0.013	0.024	0.013
1025	15.761	0.004	16.398	15.760	15.476	16.848	16.037	15.043	0.006	0.003	0.007	0.003	0.008	0.004
1027	16.874	0.008	17.700	16.875	16.443	18.144	17.141	16.002	0.015	0.008	0.022	0.012	0.019	0.010
1030	20.157	0.015	21.835	20.157	19.059	22.494	20.811	18.586	0.026	0.018	0.029	0.020	0.030	0.020
1032	18.046	0.006	19.306	18.044	17.482	19.800	18.526	17.035	0.010	0.007	0.013	0.008	0.013	0.008
1033	20.678	0.026	22.346	20.692	19.373	23.033	21.508	18.890	0.047	0.031	0.051	0.034	0.048	0.031
1035	17.210	0.008	18.164	17.208	16.807	18.679	17.601	16.368	0.017	0.006	0.020	0.005	0.020	0.005
1037	21.804	0.048	23.611	21.802	20.238	24.347	22.496	19.743	0.058	0.057	0.059	0.058	0.061	0.060
1039	17.598	0.004	18.688	17.598	17.146	19.200	18.024	16.705	0.008	0.005	0.010	0.006	0.010	0.005
1040	15.322	0.003	15.887	15.321	15.088	16.291	15.564	14.656	0.004	0.004	0.005	0.005	0.005	0.005
1041	17.521	0.005	18.630	17.518	17.005	19.114	17.961	16.561	0.010	0.004	0.011	0.004	0.011	0.004
1043	16.894	0.011	17.681	16.899	16.500	18.239	17.237	16.061	0.028	0.006	0.026	0.006	0.027	0.006
1044	18.872	0.007	20.458	18.872	18.154	21.002	19.508	17.700	0.008	0.007	0.011	0.009	0.011	0.009
1051	15.389	0.004	16.011	15.389	15.102	16.389	15.651	14.668	0.006	0.006	0.007	0.007	0.007	0.007
1053	19.205	0.009	20.902	19.210	18.439	21.474	19.876	17.982	0.010	0.009	0.012	0.011	0.015	0.013
1056	18.203	0.039	19.388	18.208	17.516	19.782	18.508	17.063	0.108	0.014	0.109	0.010	0.108	0.010
1058	18.283	0.005	19.605	18.285	17.701	20.112	18.795	17.253	0.008	0.007	0.009	0.008	0.008	0.007
1060	16.950	0.012	17.852	16.942	16.523	18.338	17.316	16.083	0.027	0.012	0.029	0.013	0.034	0.015
1061	17.404	0.015	18.485	17.409	16.993	18.934	17.806	16.553	0.039	0.008	0.046	0.010	0.047	0.009
1062	19.669	0.019	21.339	19.682	18.705	22.017	20.384	18.238	0.039	0.016	0.060	0.021	0.060	0.022
1064	20.787	0.032	22.494	20.788	19.454	23.041	21.417	18.970	0.071	0.031	0.077	0.033	0.080	0.034
1066	20.838	0.037	22.558	20.853	19.420	23.242	21.491	18.932	0.087	0.038	0.094	0.036	0.089	0.034
1069	18.378	0.009	19.840	18.379	17.776	20.194	18.864	17.327	0.014	0.010	0.018	0.013	0.022	0.015
1070	17.221	0.007	18.183	17.224	16.767	18.659	17.585	16.326	0.018	0.006	0.021	0.006	0.023	0.007
1072	16.031	0.004	16.732	16.030	15.732	17.108	16.272	15.298	0.008	0.004	0.008	0.005	0.008	0.005
1073	20.986	0.038	22.693	20.987	19.500	23.451	21.687	19.009	0.079	0.051	0.097	0.061	0.117	0.073
1074	19.554	0.022	21.123	19.567	18.571	21.631	20.059	18.103	0.044	0.018	0.067	0.017	0.067	0.017
1080	16.120	0.004	16.761	16.118	15.743	17.233	16.380	15.305	0.007	0.004	0.012	0.007	0.014	0.008
1081	16.350	0.007	17.092	16.350	16.021	17.560	16.660	15.585	0.015	0.009	0.017	0.010	0.017	0.010

Table 2—Continued

ID	$<r>$[a] (mag)	RMS_r[b] (mag)	g[c] (mag)	r[c] (mag)	i[c] (mag)	B[d] (mag)	V[d] (mag)	I[e] (mag)	$A_{r,N=1}$[f] (mag)	min $A_{r,N=1}$[g] (mag)	$A_{r,N=2}$[f] (mag)	min $A_{r,N=2}$[g] (mag)	$A_{r,N=3}$[f]	min $A_{r,N=3}$[g]
1084	15.607	0.004	16.202	15.607	15.332	16.579	15.799	14.898	0.007	0.004	0.007	0.004	0.010	0.006
1085	16.929	0.006	17.777	16.931	16.535	18.248	17.249	16.096	0.013	0.006	0.018	0.008	0.017	0.007
1086	21.069	0.037	22.802	21.067	19.721	23.425	21.743	19.236	0.078	0.040	0.078	0.040	0.075	0.038
1097	20.516	0.027	22.171	20.508	19.246	22.812	21.102	18.765	0.055	0.020	0.059	0.021	0.059	0.021
1100	17.022	0.005	17.947	17.022	16.594	18.446	17.384	16.154	0.009	0.005	0.010	0.006	0.009	0.005
1102	16.425	0.010	17.203	16.420	16.066	17.631	16.704	15.629	0.024	0.009	0.027	0.009	0.027	0.009
1104	18.043	0.009	19.276	18.037	17.511	19.805	18.510	17.066	0.025	0.006	0.028	0.006	0.028	0.006
1105	17.798	0.007	18.956	17.797	17.286	19.506	18.260	16.842	0.014	0.006	0.016	0.006	0.017	0.006
1107	15.609	0.006	16.241	15.611	15.334	16.575	15.801	14.901	0.011	0.005	0.014	0.006	0.015	0.006
1109	16.320	0.005	17.080	16.322	16.041	17.529	16.654	15.607	0.010	0.005	0.013	0.006	0.012	0.005
1110	19.435	0.008	21.073	19.434	18.579	21.668	20.059	18.118	0.008	-0.008	0.010	-0.010	0.012	-0.012
1111	19.151	0.009	20.887	19.145	18.311	21.363	19.811	17.851	0.014	0.009	0.015	0.010	0.016	0.011
1112	20.717	0.024	22.434	20.710	19.406	23.105	21.411	18.924	0.043	0.031	0.043	0.029	0.042	0.028
1113	22.069	0.058	23.758	22.081	20.378	24.557	22.769	19.877	0.044	-0.044	0.050	-0.050	0.051	-0.051
1117	17.504	0.008	18.529	17.503	17.056	19.054	17.911	16.615	0.018	0.007	0.024	0.010	0.028	0.010
1120	18.861	0.029	20.402	18.855	18.053	20.874	19.425	17.595	0.092	0.015	0.090	0.013	0.099	0.015
1122	16.440	0.006	17.222	16.439	16.151	17.662	16.761	15.718	0.011	0.006	0.013	0.006	0.016	0.008
1124	20.274	0.017	22.016	20.276	19.048	22.732	21.044	18.569	0.020	0.019	0.030	0.028	0.030	0.028
1126	18.536	0.008	20.010	18.534	17.834	20.552	19.110	17.380	0.013	0.010	0.016	0.012	0.016	0.013
1127	18.494	0.011	19.887	18.497	17.861	20.429	19.024	17.411	0.020	0.014	0.022	0.015	0.022	0.015
1130	20.638	0.033	22.318	20.641	19.326	22.999	21.273	18.843	0.073	0.025	0.079	0.026	0.078	0.025
1131	15.619	0.005	16.238	15.618	15.378	16.644	15.875	14.947	0.007	0.007	0.007	0.007	0.009	0.009
1135	17.022	0.011	17.971	17.027	16.557	18.321	17.299	16.114	0.025	0.010	0.033	0.011	0.034	0.011
1136	17.568	0.010	18.659	17.563	17.097	19.310	18.119	16.655	0.023	0.011	0.025	0.009	0.025	0.009
1137	16.025	0.008	16.689	16.023	15.737	17.100	16.273	15.303	0.017	0.007	0.020	0.007	0.020	0.007
1138	17.987	0.008	19.109	17.991	17.414	19.626	18.406	16.966	0.019	0.012	0.022	0.012	0.022	0.012
1142	16.515	0.008	17.247	16.512	16.146	17.712	16.766	15.708	0.013	0.011	0.013	0.011	0.019	0.012
1145	19.945	0.012	21.693	19.943	18.933	22.243	20.616	18.465	0.021	0.018	0.021	0.018	0.020	0.017
1146	20.433	0.028	22.188	20.415	19.196	22.788	21.124	18.718	0.054	0.025	0.065	0.028	0.065	0.028
1147	19.862	0.019	21.530	19.866	18.821	22.174	20.512	18.351	0.030	0.018	0.030	0.018	0.033	0.020
1149	21.561	0.047	23.295	21.577	20.062	23.950	22.177	19.570	0.075	0.056	0.079	0.059	0.080	0.060
1151	16.453	0.012	17.208	16.445	16.125	17.666	16.741	15.690	0.018	0.013	0.021	0.013	0.023	0.014
1159	20.386	0.035	22.077	20.379	19.173	22.717	21.070	18.695	0.089	0.021	0.092	0.020	0.090	0.020
1162	17.577	0.006	18.661	17.577	17.020	19.077	17.918	16.573	0.015	0.007	0.014	0.007	0.015	0.007

Table 2—Continued

ID	$<r>$[a] (mag)	RMS_r[b] (mag)	g[c] (mag)	r[c] (mag)	i[c] (mag)	B[d] (mag)	V[d] (mag)	I[e] (mag)	$A_{r,N=1}$[f] (mag)	min $A_{r,N=1}$[g] (mag)	$A_{r,N=2}$[f] (mag)	min $A_{r,N=2}$[g] (mag)	$A_{r,N=3}$[f]	min $A_{r,N=3}$[g]
1163	19.233	0.054	20.976	19.233	18.443	21.244	19.772	17.986	0.143	0.017	0.141	0.015	0.142	0.015
1165	19.519	0.023	21.142	19.518	18.466	21.635	20.006	17.996	0.038	0.024	0.042	0.027	0.059	0.031
1169	17.070	0.013	17.933	17.069	16.585	18.382	17.372	16.142	0.023	0.016	0.034	0.022	0.034	0.022
1174	18.499	0.011	19.984	18.493	17.799	20.499	19.079	17.346	0.026	0.012	0.028	0.010	0.030	0.010
1179	19.764	0.010	21.532	19.764	18.723	22.131	20.463	18.253	0.011	-0.011	0.014	-0.014	0.014	-0.014
1180	19.245	0.012	20.998	19.238	18.380	21.541	19.928	17.919	0.023	0.009	0.023	0.009	0.022	0.009
1186	18.904	0.006	20.455	18.906	18.160	21.026	19.506	17.704	0.007	0.006	0.008	0.008	0.009	0.008
1188	20.844	0.031	22.664	20.828	19.503	23.273	21.533	19.019	0.048	0.024	0.072	0.037	0.073	0.038
1191	19.773	0.013	21.465	19.768	18.744	22.528	20.788	18.275	0.022	0.015	0.023	0.016	0.023	0.016
1192	20.414	0.019	22.078	20.405	19.230	22.764	21.054	18.754	0.035	0.019	0.034	0.019	0.035	0.019
1196	16.405	0.004	17.141	16.406	16.018	17.566	16.652	15.579	0.008	0.005	0.009	0.005	0.011	0.005
1199	21.650	0.051	23.340	21.665	19.955	24.016	22.267	19.453	0.062	0.059	0.073	0.070	0.073	0.071
1202	19.245	0.010	20.863	19.249	18.371	21.464	19.868	17.909	0.017	0.010	0.016	0.010	0.015	0.010
1203	19.956	0.018	21.726	19.962	18.915	22.335	20.660	18.444	0.037	0.012	0.040	0.014	0.041	0.013
1208	18.152	0.009	19.493	18.155	17.544	19.953	18.631	17.095	0.024	0.008	0.026	0.006	0.026	0.006
1210	17.277	0.009	18.328	17.272	16.848	18.764	17.648	16.407	0.023	0.006	0.024	0.004	0.025	0.004
1213	20.714	0.020	22.431	20.715	19.332	22.978	21.280	18.846	0.029	0.023	0.031	0.025	0.031	0.025
1218	20.868	0.027	22.509	20.858	19.525	23.160	21.511	19.042	0.052	0.036	0.062	0.039	0.061	0.039
1219	21.438	0.037	23.122	21.426	19.894	23.754	22.069	19.401	0.055	0.051	0.055	0.051	0.059	0.054
1221	18.305	0.014	19.673	18.314	17.681	20.117	18.773	17.231	0.038	0.009	0.038	0.007	0.038	0.007
1223	17.666	0.005	18.805	17.664	17.097	19.260	18.063	16.650	0.011	0.006	0.012	0.006	0.012	0.005
1225	18.091	0.005	19.358	18.091	17.525	19.878	18.569	17.078	0.009	0.004	0.009	0.004	0.009	0.005
1233	20.872	0.032	22.669	20.857	19.506	23.281	21.539	19.022	0.065	0.031	0.064	0.030	0.068	0.030
1235	18.630	0.007	20.164	18.634	17.953	20.660	19.188	17.500	0.015	0.006	0.017	0.006	0.017	0.006
1239	16.766	0.007	17.600	16.764	16.355	18.049	17.068	15.916	0.011	0.009	0.013	0.010	0.019	0.011
1242	19.095	0.011	20.668	19.088	18.388	21.116	19.635	17.935	0.020	0.010	0.020	0.010	0.024	0.011
1243	18.548	0.005	20.033	18.547	17.869	20.477	19.041	17.417	0.009	0.008	0.012	0.010	0.014	0.011
1248	20.393	0.016	22.198	20.399	19.328	22.697	21.030	18.857	0.020	0.017	0.020	0.016	0.019	0.016
1249	19.543	0.009	21.240	19.549	18.637	21.845	20.183	18.174	0.011	0.009	0.012	0.010	0.012	0.010
1250	19.550	0.017	21.139	19.546	18.575	21.916	20.328	18.109	0.037	0.015	0.051	0.014	0.052	0.015
1253	20.230	0.023	21.981	20.235	19.043	22.573	20.859	18.566	0.057	0.026	0.072	0.030	0.071	0.029
1255	16.078	0.005	16.787	16.078	15.732	17.151	16.294	15.296	0.007	0.004	0.014	0.009	0.014	0.009
1259	19.425	0.010	21.008	19.425	18.588	21.477	19.973	18.128	0.020	0.010	0.020	0.010	0.021	0.011
1262	19.017	0.007	20.660	19.019	18.229	21.124	19.585	17.772	0.011	0.010	0.016	0.014	0.020	0.017

Table 2—Continued

ID	$<r>$[a] (mag)	RMS_r[b] (mag)	g[c] (mag)	r[c] (mag)	i[c] (mag)	B[d] (mag)	V[d] (mag)	I[e] (mag)	$A_{r,N=1}$[f] (mag)	min $A_{r,N=1}$[g] (mag)	$A_{r,N=2}$[f] (mag)	min $A_{r,N=2}$[g] (mag)	$A_{r,N=3}$[f]	min $A_{r,N=3}$[g]
1264	20.803	0.043	22.602	20.805	19.483	23.184	21.438	19.000	0.093	0.030	0.131	0.040	0.132	0.039
1265	18.720	0.007	20.278	18.715	18.000	20.795	19.305	17.546	0.014	0.006	0.016	0.007	0.017	0.007
1269	19.472	0.024	21.017	19.477	18.500	22.158	20.505	18.034	0.060	0.015	0.061	0.015	0.062	0.015
1273	17.249	0.009	18.290	17.253	16.817	18.740	17.625	16.377	0.025	0.006	0.029	0.007	0.029	0.006
1276	17.834	0.005	18.998	17.833	17.320	19.529	18.285	16.876	0.012	0.006	0.014	0.006	0.023	0.011
1277	18.097	0.005	19.415	18.095	17.529	19.922	18.590	17.081	0.008	0.006	0.012	0.008	0.012	0.008
1278	19.686	0.010	21.467	19.685	18.734	21.998	20.338	18.269	0.014	0.012	0.016	0.013	0.018	0.015
1284	18.507	0.010	19.932	18.498	17.829	20.447	19.031	17.377	0.024	0.005	0.024	0.005	0.025	0.005
1285	18.242	0.022	19.427	18.251	17.572	19.860	18.568	17.119	0.061	0.009	0.069	0.012	0.075	0.012
1289	20.112	0.014	21.806	20.116	18.944	22.502	20.803	18.467	0.019	0.015	0.023	0.017	0.024	0.018
1291	18.373	0.009	19.604	18.372	17.705	20.210	18.880	17.253	0.020	0.010	0.021	0.010	0.027	0.011
1293	17.314	0.004	18.336	17.313	16.943	18.843	17.709	16.506	0.007	0.005	0.009	0.006	0.010	0.007
1296	18.615	0.021	20.020	18.622	17.967	20.635	19.166	17.516	0.061	0.016	0.063	0.014	0.070	0.016
1298	18.940	0.007	20.603	18.940	18.163	21.074	19.524	17.706	0.012	0.009	0.012	0.008	0.012	0.009
1299	18.655	0.016	20.071	18.665	17.866	20.391	18.991	17.408	0.045	0.013	0.044	0.010	0.045	0.010
1300	20.903	0.024	22.658	20.900	19.550	23.288	21.572	19.066	0.033	0.029	0.033	0.029	0.033	0.029
1301	21.170	0.032	22.824	21.172	19.597	23.636	21.879	19.102	0.037	0.036	0.041	0.040	0.052	0.051
1302	16.986	0.005	17.890	16.984	16.556	18.385	17.337	16.116	0.008	0.006	0.013	0.003	0.016	0.010
1309	20.104	0.047	21.816	20.087	18.981	22.302	20.629	18.509	0.134	0.018	0.133	0.018	0.131	0.017
1313	19.969	0.012	21.692	19.965	18.870	22.298	20.588	18.398	0.019	0.016	0.021	0.018	0.023	0.019
1314	15.865	0.003	16.548	15.865	15.562	16.932	16.098	15.127	0.005	0.003	0.010	0.006	0.010	0.005
1320	18.911	0.011	20.433	18.913	18.168	20.868	19.386	17.712	0.021	0.013	0.029	0.017	0.034	0.019
1328	17.977	0.004	19.123	17.975	17.407	19.645	18.418	16.960	0.006	0.006	0.007	0.007	0.007	0.007
1331	20.016	0.015	21.717	20.017	18.867	22.539	20.827	18.392	0.022	0.015	0.026	0.017	0.027	0.018
1332	17.960	0.007	19.221	17.961	17.385	19.698	18.406	16.938	0.013	0.000	0.021	0.008	0.021	0.008
1333	17.645	0.010	18.739	17.646	17.135	19.242	18.031	16.691	0.021	0.009	0.030	0.010	0.030	0.010
1334	16.683	0.008	17.467	16.682	16.290	17.926	16.968	15.851	0.019	0.006	0.022	0.006	0.022	0.004
1335	19.823	0.011	21.479	19.819	18.828	22.205	20.483	18.360	0.012	0.012	0.012	0.012	0.013	0.013
1336	19.881	0.036	21.556	19.864	18.802	22.266	20.578	18.332	0.114	0.016	0.117	0.015	0.121	0.016
1338	17.524	0.005	18.582	17.526	16.968	19.079	17.891	16.521	0.011	0.005	0.011	0.004	0.011	0.005
1340	21.343	0.040	23.026	21.335	19.977	23.811	21.979	19.492	0.071	0.045	0.073	0.046	0.074	0.047
1343	17.818	0.005	19.006	17.815	17.294	19.535	18.273	16.850	0.010	0.006	0.011	0.001	0.013	0.006
1349	17.120	0.004	18.104	17.121	16.724	18.579	17.489	16.284	0.011	0.004	0.012	0.004	0.012	0.004
1350	18.185	0.019	19.449	18.179	17.566	19.949	18.647	17.117	0.045	0.017	0.060	0.011	0.059	0.011

Table 2—Continued

ID	$<r>$[a] (mag)	RMS_r[b] (mag)	g[c] (mag)	r[c] (mag)	i[c] (mag)	B[d] (mag)	V[d] (mag)	I[e] (mag)	$A_{r,N=1}$[f] (mag)	min $A_{r,N=1}$[g] (mag)	$A_{r,N=2}$[f] (mag)	min $A_{r,N=2}$[g] (mag)	$A_{r,N=3}$[f]	min $A_{r,N=3}$[g]
1352	19.381	0.032	20.947	19.397	18.473	21.521	19.959	18.009	0.091	0.020	0.097	0.016	0.093	0.015
1355	18.561	0.012	19.945	18.559	17.893	20.529	19.100	17.441	0.029	0.008	0.035	0.008	0.035	0.008
1360	17.427	0.006	18.479	17.425	16.968	18.978	17.816	16.527	0.012	0.005	0.017	0.006	0.017	0.007
1364	20.396	0.016	22.068	20.390	19.226	22.730	21.026	18.751	0.018	-0.018	0.020	-0.020	0.019	-0.019
1367	18.366	0.009	19.714	18.364	17.737	20.299	18.888	17.287	0.014	0.012	0.016	0.013	0.019	0.015
1373	19.525	0.008	21.228	19.520	18.602	21.783	20.140	18.139	0.011	0.010	0.011	0.010	0.011	0.011
1374	21.633	0.058	23.432	21.624	20.047	24.026	22.249	19.552	0.119	0.060	0.129	0.063	0.124	0.061
1377	21.225	0.038	22.902	21.232	19.740	23.616	21.844	19.249	0.068	0.037	0.080	0.043	0.080	0.043
1378	18.288	0.016	19.579	18.289	17.626	19.955	18.641	17.174	0.038	0.009	0.042	0.010	0.046	0.011
1383	17.309	0.007	18.227	17.308	16.840	18.798	17.683	16.398	0.010	0.009	0.021	0.019	0.026	0.023
1385	20.434	0.024	22.237	20.434	19.219	22.831	21.141	18.741	0.049	0.020	0.052	0.021	0.051	0.021
1386	21.343	0.047	23.034	21.366	19.926	23.684	21.949	19.437	0.101	0.046	0.100	0.045	0.110	0.050
1392	21.005	0.040	22.672	20.995	19.578	23.381	21.601	19.091	0.092	0.033	0.093	0.035	0.091	0.033
1394	18.116	0.007	19.362	18.115	17.503	19.901	18.577	17.054	0.022	0.007	0.022	0.007	0.021	0.006
1395	17.013	0.007	17.865	17.014	16.577	18.430	17.371	16.137	0.016	0.007	0.019	0.008	0.018	0.007
1398	17.285	0.007	18.242	17.284	16.808	18.758	17.637	16.365	0.016	0.007	0.022	0.009	0.023	0.009
1399	16.073	0.006	16.758	16.071	15.696	17.196	16.326	15.258	0.016	0.004	0.016	0.004	0.021	0.006
1404	19.758	0.055	21.336	19.765	18.669	22.073	20.406	18.196	0.138	0.015	0.144	0.013	0.149	0.013
1408	19.665	0.030	21.282	19.648	18.628	21.842	20.221	18.159	0.059	0.019	0.062	0.020	0.075	0.024
1419	18.160	0.009	19.504	18.163	17.575	19.952	18.606	17.127	0.024	0.005	0.026	0.005	0.026	0.005
1420	18.362	0.009	19.638	18.354	17.747	20.252	18.868	17.298	0.016	0.011	0.023	0.013	0.023	0.013
1424	19.119	0.014	20.644	19.122	18.266	21.221	19.699	17.805	0.027	0.009	0.041	0.012	0.037	0.011
1425	16.391	0.008	17.092	16.388	16.068	17.616	16.681	15.633	0.013	0.009	0.015	0.011	0.013	0.009
1435	16.936	0.006	17.732	16.934	16.568	18.326	17.278	16.131	0.010	0.007	0.016	0.009	0.020	0.009
1439	16.431	0.010	17.090	16.433	16.079	17.635	16.700	15.643	0.019	0.014	0.021	0.015	0.045	0.012
1440	19.480	0.012	21.085	19.476	18.561	21.710	20.084	18.098	0.025	0.015	0.026	0.015	0.024	0.014
1442	17.597	0.007	18.667	17.598	17.118	19.174	17.985	16.675	0.011	0.008	0.016	0.010	0.015	0.010
1443	17.527	0.016	18.587	17.520	17.034	19.032	17.881	16.591	0.043	0.011	0.043	0.008	0.042	0.008
1446	18.408	0.014	19.693	18.401	17.703	20.288	18.939	17.250	0.031	0.000	0.046	0.016	0.047	0.016
1450	17.703	0.009	18.822	17.701	17.188	19.315	18.099	16.744	0.019	0.009	0.023	0.010	0.026	0.011
1451	16.566	0.005	17.345	16.565	16.177	17.811	16.869	15.739	0.008	0.007	0.010	0.009	0.009	0.008

[a]The flux averaged r magnitude of the light curve.

[b]The root-mean-square of the light curve.

[c]The magnitude of the source in the photometric catalog (Paper I)

[d]Value from Kalirai et al. (2001)

[e]Value transformed from r and i

[f]Peak-to-peak amplitude in r-band for the multi-harmonic AoV model with specified N.

[g]Minimum peak-to-peak amplitude in r-band that the light curve could have had and still have been detected as a variable. Entries with no value correspond to light curves that would be selected as variable even when $A_{r,N} = 0.0$. The model does not adequately describe the light curve in these cases.

Table 3. Candidate Cluster Members with Measured Rotation Periods: Spectroscopic Parameters

ID	T_{eff} (K)	σT_{eff} (K)	$v \sin i$ (km/s)	$\sigma v \sin i$[a] (km/s)	RV (km/s)	σRV (km/s)
25	5384	123	7.53	1.20	8.65	0.190
26	5057	122	11.94	1.81	9.38	0.322
71	4991	133	8.06	1.54	8.68	0.108
99	4785	378	10.94	19.02	7.60	0.758
103	5216	127	3.65	1.78	8.90	0.237
104	4773	1506	12.04	418.07	48.85	15.984
174	4741	584	8.72	35.15	-1.76	0.805
216	6521	287	48.36	3.19	9.02	0.242
223	5009	201	4.64	4.56	10.72	0.314
258	5244	163	7.92	2.52	2.35	0.335
292	6245	124	9.41	1.33	7.59	0.080
335	4916	151	9.42	1.81	9.06	0.285
364	5112	186	5.12	3.53	8.44	0.405
380	4973	254	6.18	7.29	9.95	0.374
389	4744	502	6.50	12.79	9.93	0.529
396	5350	131	7.52	1.23	9.08	0.307
404	4727	336	12.39	19.01	9.74	0.332
413	4751	407	6.08	29.18	5.36	0.846
432	5416	113	3.05	1.54	7.89	0.141
483	6167	129	23.82	0.26	10.52	0.217
522	5030	163	6.53	3.68	8.58	0.368
550	5137	152	2.95	1.66	10.06	0.292
552	5840	121	6.60	1.14	7.12	0.126
561	4639	1359	7.97	64.42	10.46	0.941
620	4804	171	6.35	3.52	9.46	0.564
622	4800	216	7.86	6.38	10.79	0.234
661	5164	153	5.62	1.58	-20.74	0.293
664	4889	186	5.76	2.89	8.66	0.362
713	4833	567	5.69	24.02	11.46	0.835
745	4541	463	10.24	32.09	10.32	1.184
821	5246	126	6.78	1.61	9.34	0.479
867	6185	134	12.64	1.07	10.48	0.179
912	4961	249	8.19	8.15	9.16	0.080
970	5142	145	4.61	2.72	8.98	0.239

Table 3—Continued

ID	T_{eff} (K)	σT_{eff} (K)	$v \sin i$ (km/s)	$\sigma v \sin i$[a] (km/s)	RV (km/s)	σRV (km/s)
971	5927	123	6.58	0.52	9.16	0.205
1007	5397	139	4.69	1.49	10.88	0.338
1008	5828	141	5.41	1.30	9.25	0.310
1032	4666	601	7.11	29.51	-4.25	0.519
1169	5315	162	7.74	2.13	-15.75	11.090
1328	4996	1522	11.78	85.95	-25.67	1.298
1367	4689	1276	6.17	27.64	11.31	1.050

[a]In cases where $\sigma v \sin i$ exceeds $v \sin i$, the values for $\sigma v \sin i$ should be taken as an upper limit on $v \sin i$.

Table 4. Color Uncertainty as a Function of Absolute Magnitude

$M_V(mag)$	$\sigma(B-V)_0$ (mag)	$\sigma(V-I_C)_0$ (mag)	$\sigma(g-r)$ (mag)	$\sigma(g-i)$ (mag)
4.0	0.012	0.027	0.032	0.034
5.0	0.017	0.046	0.035	0.049
6.0	0.016	0.036	0.034	0.046
7.0	0.022	0.045	0.046	0.062
8.0	0.035	0.062	0.066	0.073
9.0	0.039	0.107	0.069	0.094
10.0	0.066	0.147	0.059	0.102
11.0	0.075	0.069	0.061	0.060

Table 5. Parameters from Fitting equations 3 and 4.

Parameter	Value	Bootstrap Error	Monte Carlo Error
a_{lin}	10.81 days/mag	0.35	0.14
b_{lin}	-1.36 days	0.35	0.12
a_{bpl}	4.752 days	0.031	0.021
b_{bpl}	-20.9	4.0	2.0

Table 6. Spread in Period about the Main Period-Color Band as a Function of Color.

$(B-V)_0$	# Points	RMS[a] linear (days)	χ^2[b] linear	significance[c] linear	RMS[d] B.P.L. (days)	χ^2[e] B.P.L.	significance[f] B.P.L.
0.60	33	1.07	10.77	39.51	9.28	5.11	16.62
0.80	51	0.54	1.69	3.46	2.58	1.65	3.25
1.00	61	0.77	2.22	6.73	4.34	2.34	7.38
1.20	35	0.72	2.90	7.92	5.52	2.71	7.11
1.40	57	1.36	1.57	3.03	3.03	1.80	4.24
1.60	7	0.69	2.72	3.21	2.79	1.93	1.73

[a]Standard deviation of the period residuals of stars within 0.1 mag of $(B-V)_0$ for a linear fit between period and $(B-V)_0$.

[b]χ^2 per degree of freedom of the period residuals of stars within 0.1 mag of $(B-V)_0$ for a linear fit between period and $(B-V)_0$

[c]Significance in σ of χ^2 for the linear model.

[d]Standard deviation of the period residuals of stars within 0.1 mag of $(B-V)_0$ for a broken power-law fit between period and $(B-V)_0$.

[e]χ^2 per degree of freedom of the period residuals of stars within 0.1 mag of $(B-V)_0$ for a broken power-law fit between period and $(B-V)_0$

[f]Significance in σ of χ^2 for the broken power-law model.

Table 7. Parameters for models displayed in figures 27 and 28

Color Range (mag)	Mass Range[a] ($M_\odot$)	$P_{0,10}$[b] (days)	$P_{0,90}$[b] (days)	P_{sat}[b] (days)	$\omega_{sat}/\omega_\odot$	K[b] (10^{47} g cm^2 s)	χ^2	D.O.F.[c]	C.L.[d]
$(B-V)_0$, using data from all available clusters and the Sun[e]									
$[0.5, 0.7]$	$[0.99, 1.21]$	0.64(0.06)	2.71(0.50)	4.26(0.18)	5.82	3.25(0.18)	2.39	4	0.43
$[0.7, 0.9]$	$[0.86, 0.99]$	0.13(0.04)	3.18(0.84)	2.28(0.27)	10.89	3.65(0.18)	12.21	4	2.41
$[0.9, 1.1]$	$[0.76, 0.86]$	0.16(0.05)	5.06(1.01)	2.85(0.32)	8.70	3.24(0.27)	21.75	4	3.69
$[1.1, 1.3]$	$[0.68, 0.76]$	0.24(0.05)	4.48(0.74)	5.06(1.27)	4.90	3.16(0.36)	1.19	2	0.59
$[1.3, 1.5]$	$[0.53, 0.68]$	0.32(0.05)	6.76(0.74)	12.15(1.85)	2.04	5.35(1.09)	0.31	2	0.18
$(B-V)_0$, using data from M37, the Hyades, and the Sun only									
$[0.5, 0.7]$	$[0.99, 1.21]$	0.23(0.05)	2.07(0.55)	3.41(0.15)	7.26	3.29(0.18)	1.07	2	0.54
$(V-I_C)_0$, using data from all available clusters and the Sun									
$[0.5, 1.0]$	$[0.82, 1.35]$	0.63(0.11)	4.55(0.99)	3.56(0.34)	6.97	2.85(0.16)	2.96	6	0.24
$[1.0, 1.5]$	$[0.67, 0.82]$	0.26(0.06)	5.16(1.24)	4.25(0.48)	5.83	3.11(0.44)	6.59	2	2.08
$[1.5, 2.0]$	$[0.56, 0.67]$	0.58(0.16)	4.39(0.47)	12.02(2.08)	2.06	8.20(2.37)	68.21	4	7.52
$[2.0, 2.5]$	$[0.24, 0.56]$	0.29(0.05)	7.28(1.06)	15.67(3.20)	1.58	3.16(1.59)	3.99	2	1.49
$(V-I_C)_0$, using data from M37, the Hyades, and the Sun only									
$[0.5, 1.0]$	$[0.82, 1.35]$	0.42(0.18)	4.09(1.32)	3.22(0.40)	7.69	2.89(0.17)	2.35	2	1.02

[a]The rough range in masses corresponding to the color range of the bin.

[b]Estimates of the $1-\sigma$ uncertainties on the parameters are given in parentheses. These uncertainties are determined by conducting an MCMC simulation.

[c]Number of degrees of freedom in the fit.

[d]The formal confidence level in σ at which the null hypothesis that the model fits the data can be rejected.

[e]We exclude clusters with fewer than 4 points in the color bin from the fit. The Sun is only included for the bluest color bin.